NTNU
Norwegian University of
Science and Technology

Investigate Techniques for Low-Volume Injection Molding Production

Øystein Bjelland

Master of Science in Mechanical Engineering
Submission date: June 2016
Supervisor: Martin Steinert, IPM

Norwegian University of Science and Technology
Department of Engineering Design and Materials

Investigate Techniques for Low-Volume Injection Molding Production

Master’s Thesis
Spring 2016

By Øystein Bjelland

Abstract

Because of expensive tooling, injection molding is only suited for large production volumes. Consequently, this makes it hard to justify making prototypes and small production volumes. In spite of recent advances in additive manufacturing, this technology can still not capture performance properties of injection molded products. This report proposes several ways of prototyping injection molded components by means of direct rapid tooling. By Wayfaring, several techniques could be explored. Molds were built using rapid prototyping techniques such as fused deposition modeling, selective heat sintering, laminated object manufacturing, polymer jetting and CNC-milling. The molds were tested using a desktop injection molding machine, and the molded components were tested using a three point bending setup. Furthermore, a more complex mold was CNC-milled and tested in a full scale injection molding machine with the tool insert method. The tested techniques were evaluated with respect to cost, efficiency and effectiveness. From the study, it was found that polymer jetting could fabricate the molds quickest and with best quality of the tested techniques. Furthermore, it was found that desktop injection molding could be a good way of prototyping small components, while the tool insert method is better suited for larger, more complex geometry, and for low-volume production.

Sammendrag

Grunnet høye verktøykostnader egner sprøytestøping seg kun for store produksjonsvolum. Dette medfører at det er vanskelig å produsere små volum, samt å lage prototyper. Til tross for fremgang i prosesser for additiv tilvirkning, er det fortsatt et stort sprang fra prototyper laget med disse prosessene til sprøytestøpte produkter. Det er derfor ønskelig å komme frem til en prosess hvor man kan lage prototyper av sprøytestøpte produkter på en billig, effektiv og hensiktsmessig måte. Denne oppgaven presenterer ulike måter å prototype sprøytestøpte produkter på, ved å bruke prosesser for rask prototyping for å produsere former. I oppgaven ble former laget med additive tilvirkningsprosesser som filamentekstrudering (eng: fused deposition modeling), selektiv varme-sintring (eng: selective heat sintering), lamineringstilvirkning (eng: laminated object manufacturing) og spraying av fotosensitiv polymer (eng: polymer jetting). I tillegg ble noen former frest. De tilvirkede formene ble deretter testet i en manuell sprøytestøpemaskin, og de støpte komponentene ble testet i en tre punkts bøyetest. I tillegg ble en større og mer kompleks forminnsats frest i en CNC-fres, og testet i et fullskala sprøytestøpeanlegg ved bruk av stamformer. De undersøkte prosessene ble så evaluert med tanke på pris, effektivitet og kvalitet. I studien ble det vist at formtilvirkning ved spraying av en fototsensitiv polymer, var mest effektiv, og ga best kvalitet i det sprøytestøpte produktet. I tillegg ble det vist at manuell sprøytestøping kan være en god prosess for prototyping, mens metoden med forminnsatser egner seg bedre for vanskeligere geometrier og lavvolumproduksjon.

NTNU - NORWEGIAN UNIVERSITY
OF SCIENCE AND TECHNOLOGY
DEPARTMENT OF ENGINEERING DESIGN
AND MATERIALS

MASTER THESIS SPRING 2016
FOR
STUD.TECHN. Øystein Bjelland

Investigate Techniques for Low-Volume Injection Molding Production.

The majority of plastic parts are today manufactured using injection molding. However, due to expensive tooling, injection molding is only suited for large production volumes. Moreover, the high tooling cost makes it difficult both to produce low volume batches (150-300), and to make prototypes. Therefore, it is desirable to find a cheap means of production for injection molding tooling.

This master thesis aims to investigate the applicability of novel manufacturing methods for injection molding tooling. Prototypes will be built and tested in the context of SBS Scandinavian Business Seating.

Utforsking av teknikker for sprøytestøping ved lavt produksjonsvolum

Sprøytestøping er i dag den vanligste metoden for produksjon av plastdeler. En ulempe med sprøytestøping er at produksjonsmetoden i stor grad egner seg kun for store produksjonsvolumer. Årsaken til dette er at verktøyene som benyttes er svært dyre å tilvirke. Dette medfører at det er vanskelig å produsere plastdeler i små volum (150-300), samt å lage prototyper. Det er derfor ønskelig å finne en billigere produksjonsmetode for verktøy til sprøytestøping.

Denne masteroppgaven skal utforske nye tilvirkningsmetoder for verktøy til sprøytestøping, samt deres anvendbarhet. Prototyper vil bli laget og testet, i samarbeid med SBS Scandinavian Business Seating.

Formal requirements:
Three weeks after start of the thesis work, an A3 sheet illustrating the work is to be handed in. A template for this presentation is available on the IPM's web site under the menu "Masteroppgave" (https://www.ntnu.edu/web/ipm/master-thesis). This sheet should be updated one week before the master's thesis is submitted.
Risk assessment of experimental activities shall always be performed. Experimental work defined in the problem description shall be planed and risk assessed up-front and within 3 weeks after receiving the problem text. Any specific experimental activities which are not properly covered by the general risk assessment shall be particularly assessed before performing the experimental work. Risk assessments should be signed by the supervisor and copies shall be included in the appendix of the thesis.
The thesis should include the signed problem text, and be written as a research report with summary both in English and Norwegian, conclusion, literature references, table of contents, etc. During preparation of the text, the candidate should make efforts to create a well arranged and well written report. To ease the evaluation of the thesis, it is important to cross-

reference text, tables and figures. For evaluation of the work a thorough discussion of results is appreciated.

The thesis shall be submitted electronically via DAIM, NTNU's system for Digital Archiving and Submission of Master's theses. The contact person at SBS is Christian Lodgaard and Prof. Martin Steinert and Carlo Kriesi at NTNU.

Torgeir Welo
Head of Division

Martin Steinert
Professor/Supervisor

NTNU
Norges teknisk-naturvitenskapelige universitet
Institutt for produktutvikling og materialer

Preface

This report was written as a part of the master work of Øystein Bjelland, spring 2016. The master thesis is a continuation of the pre-master thesis “Improve The Handover Between 3D-models and Injection Molding Production”. In the pre-master, I looked into how to improve the transition from design and development to production of injection molded components at Scandinavian Business Seating (SBS). The focus was then on diverging, and consequently finding good approaches to solving the needs of SBS on an applied level. In this report, the focus is shifted towards exploration of specific techniques.

In my pre-master and master work, I have employed the Wayfaring methodology (see Chapter 2) for conducting research and development. Some of the experiences made in relation to the Wayfaring model was collected and formalized in “Requirements Exploration Through Iteratively Emerging Critical Functionality From Prototyping”, and will be published in the proceedings of the 26th CIRP Design Conference in Stockholm June 15-17th, 2016. The article in its entire length is attached in appendix A, and forms a part of the master work.

I would like to express my most sincere gratitudes to my mentors Martin Steinert and Carlo Kriesi at TrollLabs for guidance. I would also like to thank Marius Sollie and Christian Lodgaard at SBS for support, Knut Richard Kviserud at OM BE Plast for help with full scale testing, and Per-Erik Heksem, Bjarne Stolpnessæter and Robert Schistad for assistance on prototyping.

Øystein Bjelland

NTNU Gløshaugen, June 2016

Contents

9 Preface

13 Introduction

15 Chapter One: Methodology

19 Chapter Two: Background

27 Chapter Three: Techniques for Direct Rapid Tooling

39 Chapter Four: Rapid Prototyping Machinery

45 Chapter Five: Probing

59 Chapter Six: Three Point Bending Test

65 Chapter Seven: Full Scale Testing

75 Chapter Eight: Evaluation

81 Chapter Nine: Discussion

91 Chapter Ten: Concluding Remarks and Further Work

96 References

99 Appendices

Introduction

During the last few decades, globalization have opened up the international marketplace for novel players, and made competition fiercer than ever. In order to obtain a competitive advantage, or rather keep up with competitors, it is necessary for companies to come up with newer, better and cheaper solutions for their customers in a shorter amount of time. Consequently is reducing the time-to-market, by utilizing rapid prototyping in product development, of increasing importance.

One company that feels the heat of the international marketplace is Scandinavian Business Seating (SBS). SBS designs, manufactures and sells office seating worldwide. More than 244 000 chairs are produced annually at one of SBS' production facilities in Røros, Norway. Because of these large production volumes, injection molding is a beneficial means of production for many components. However, injection molding poses several challenges in relation to rapid prototyping. This report will provide an introduction to some of these challenges, as well as proposing several techniques for prototyping injection molded components.

Chapter two is dedicated to introducing the reader to the topic, while chapter three introduces techniques for direct rapid tooling. Chapters four to seven are dedicated to experiments and testing the different techniques, while chapters eight and beyond evaluates, discusses and concludes on the findings.

Chapter One

Methodology

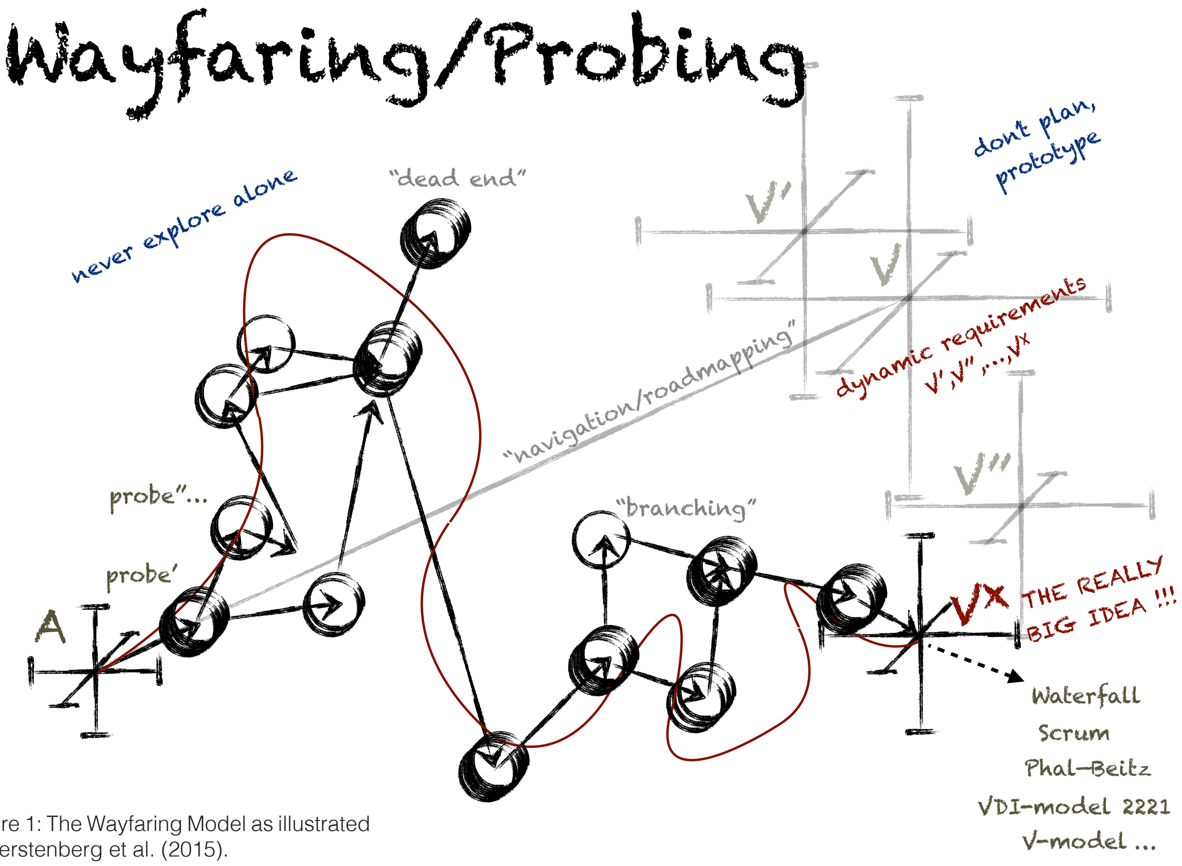

Figure 1: The Wayfaring Model as illustrated in Gerstenberg et al. (2015).

The Wayfaring Model

The wayfaring model is based on "The Hunter-Gatherer Model" by Steinert and Leifer (2012). Instead of following a fixed plan, analogous to following a map, wayfaring allows for finding one's way on the go. The idea of the Hunter-Gatherer Model is to aim for the last known location of the prey (or an idea), and from there go wayfaring (see figure 1). Successively, the Wayfaring Model has been refined into a methodology for early concept creation in high risk, high innovation product development projects in the Fuzzy Front End (Gerstenberg et al., 2015). One argument for employing the Wayfaring model in these projects instead of more traditional product development models, such as Pahl and Beitz (1968) or Ulrich and Eppinger (2012), is that one can not possibly know and target an optimum solution beforehand, because one do not have empirical evidence of something that has not previously been done. Kittilsen et al. (2016) explain that the Wayfaring methodology include four main elements. These are:

- Probing ideas - through short sprints of design-build-test, by using low-resolution prototypes to fail early and enable abductive learning.
- Merging multidisciplinarity - by including all knowledge domains from the beginning, in order to reveal interdependencies and build interlaced knowledge.
- Speed - by having sprints in a short timeframe, allowing for more iterations.
- Agility - by adapting the direction of the project as new information is revealed, allowing for serendipity findings.

The Wayfaring is divided into short sprints of probing, or design-build-test (see figure 2). The probing is split between divergent and convergent thinking. When diverging, the goal is to come up with as many solutions to the problem as possible. These solutions are then rapidly prototyped using low resolution prototypes, with focus on critical functionality. After the ideas have been tested, some are eliminated, and convergent thinking is employed. The probing allows for testing many ideas early in the product development process, which again enables the team to maximize learning. The high degree of learning early in the process contributes to minimizing the risk of developing the project into a disadvantageous direction.

Another element of the wayfaring model is merging multidisciplinarity. If all knowledge domains are included from the very beginning of the development process, dependencies between the different knowledge domains can be revealed. More specifically should the technical solutions that do not belong in the same knowledge domains be prototyped simultaneously, and furthermore tested together. This will allow for building knowledge in several knowledge domains as the project progress.

By maintaining speed, the team can maximize the number of iterations of design-build-test, while minimizing the amount of resources spent on each iteration. This is especially important early in the project, as the team is prone to design fixations such as sunk cost decision traps (Hammond et al., 1998, Viswanathan and Linsey, 2011).

Instead of prefixing the desired outcome of a project, being agile allows for adapting to change. Because each probing will increase the understanding of the problem, these new discoveries will alter the initial perception of what the product or outcome should be. The wayfaring model embraces this ambiguity, and furthermore allows for opportunistically choosing the next step of the project according to the updated knowledge database.

Although the Wayfaring model is best suited for high innovation product development projects, with many degrees of freedom and a high degree of uncertainty, Kittilsen et al. (2016) have demonstrated the use of the Wayfaring model in the design of an experiment setup. For additional information on the Wayfaring model in a prototyping setting, please see appendix A.

Prototypes

Prototypes are a crucial element of the Wayfaring model. There are many proposed definitions of what a prototype can be. Ulrich and Eppinger (2012) define a prototype as "An approximation of the product along one or more dimensions of interest". Therefore, their definition of a prototype includes both non-physical and physical models, and includes sketches, mathematical models, simulations, test components, and fully functional preproduction versions of the product (Elverum & Welo, 2015). On the contrary, Beaudouin-Lafon and Mackay (2003) define a prototype as "(...) a tangible artifact, not an abstract description that requires interpretation." In this report, prototyping is regarded as transferring ideas from the mind and into the physical world, and a prototype can therefore be anything that takes a physical form (Stanford Bootcamp Bootleg, 2015).

Furthermore, this report embraces that there exist both high- and low resolution (or fidelity) prototypes and a transition in between. Fidelity and resolution are sometimes used interchangeably for describing the level of details in a prototype, or how close the prototype resembles the final product (Elverum & Welo, 2015). However, McCurdy et al. (2006) use fidelity to describe the level of richness and functionality of the prototype. In this case, resolution will refer more to the appearance rather than the functionality. Furthermore, McGurdy et al. demonstrate the use of a mixed-fidelity approach, namely combining low- and high fidelity on various dimensions of the design.

Both low- and high fidelity prototypes are valuable for different use. Ulrich and Eppinger (2012) explain that all prototypes should answer questions. For example, "will it work?" or "how well does it meet customer needs?". Furthermore, this report distinguishes between prototypes used for exploration or learning, and prototypes used for verification or validation. Ullman (2010) defines four types of prototypes that falls within the category of verification or validation, namely proof-of-concept, proof-of-product, proof-of-process and proof-of-production. Conversely, Lim and Stoltermann (2008) suggest that the strength of a prototype is its incompleteness. The incompleteness of the prototype makes it possible to examine the strengths and weaknesses of an idea, without building a copy. Hartmann et al. (2006) takes it further, by explaining that the threshold for prototyping should be minimized, because it is through prototyping that designers learn about the problems they are trying to solve. Ultimately, the prototyping resolution should be increased throughout a project (Stanford Bootcamp Bootleg, 2015).

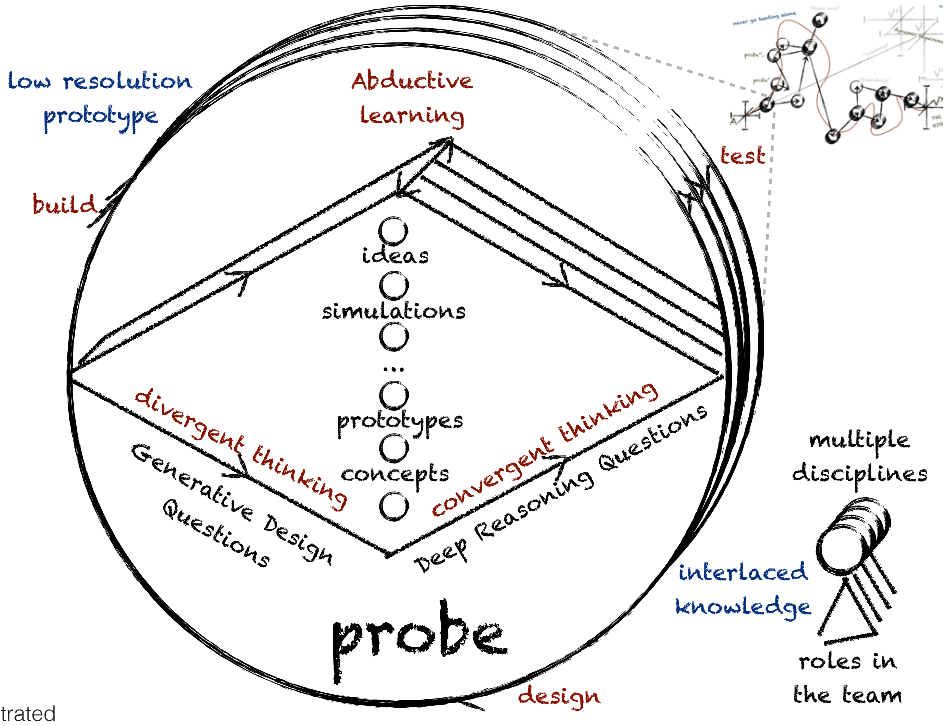

Figure 2: Probing as illustrated in Gerstenberg et al. (2015).

Chapter Two

Background

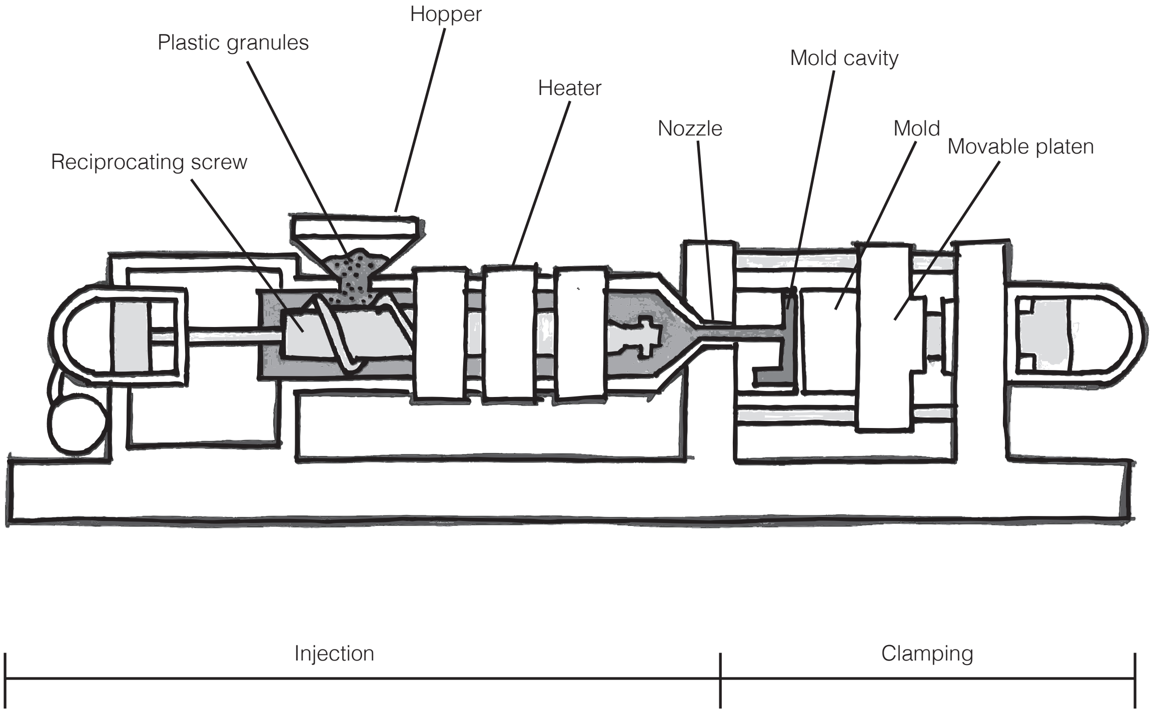

Figure 3: Modern injection molding machinery.
Figure adapted from Rogers (2015).

Injection Molding

Injection molding is a process where a thermoplastic polymer is melted into a resin, and further injected into a cavity using high pressure. First plastic granules are poured into a heated cylinder containing a reciprocating screw. When the reciprocating screw is rotating, the plastic granulate is melted and mixed, and pressure is built up. When enough pressure is built up, an hydraulic cylinder pushes the reciprocating screw forward, and the resin is forced through a nozzle and into a cavity (see figure 3). Here, the resin freezes into a solid part. After the part has cooled, it is ejected using ejector pins. Typical cycle times for this process is 10 to 30 seconds, while it is not uncommon to have cycle times of one minute or longer for larger components (Groover, 2011).

The mold itself is often referred to as tooling, and can contain a nozzle, sprue, runners and gates, depending on the inlet design. A sprue is a distribution channel that leads the resin from the nozzle and into the mold. Where the sprue ends, runners lead the resin into the cavity. If multiple parts are made in one shot, each cavity must have its own runner. Finally, the gate constricts the flow of resin into the cavity. According to Groover (2011) will this constriction increase the shear rate, and also reduce the viscosity of the resin. The various inlet designs, such as sprue gate, edge gate, ring gate and reverse taper sprue gate, are beneficial for different components. For example is a sprue gate normally used for large components. Here, no runner is required (Gate Types, 2016).

According to Ståle Rian at injection molding company Lycro, the pressure during injection molding is typically 400 - 600 bars (personal communication, September, 2015). The pressure first evacuates the air that is trapped inside the cavity. Normally, the trapped air escapes through the clearance between the mold and the ejector pins. Sometimes, additional air vents are machined into the parting surface. The air vents are only 0.03 mm deep and 12 to 25 mm wide. This makes them large enough for the air to escape, but small enough to permit the resin from flowing through.

The tooling can consist of two or three plates, depending on the geometry of the molded component. The two plate design consist of an inlet side and an ejector side. In addition to the inlet and ejector sides, the three plate mold designs have an extra plate that allows for the use of hot runners. Additionally, extra cores can be used to provide geometry features.

Design for Injection molding

Because the manufacturing process of injection molding poses significant constraints on the design, the manufacturability of the product must be considered already in the design phase. Some constraints include draft angles, undercuts, sink marks, weld lines, rounded corners and ejector pin marks. Firstly, draft angles must be included so that the component does not stick permanently to the mold. Plastic design features, such as ribs, must therefore be thickest at the root, and thinner further out. Typical draft angles are from two to five degrees (Injection-Molding Part Radiusing and Draft Guidelines, 2015). Because of the partition of the mold, the component cannot include undercuts, as these will prevent the component from releasing from the mold. However, in some cases, small undercuts are acceptable.

Another major concern regarding design for injection molding is sink marks. As the polymer melt freeze in the cavity, areas with higher thickness will contract more than areas with lower thickness. This can lead to sink marks in the component. In addition to being a visual defect, sink marks also represent notches that will give stress concentrations under load. A rule of thumb for avoiding sink marks in ribs is that the width of the rib should be from 40 - 60 % of the thickness of the flange. Likewise can full warping occur if there exist sections of non-uniform wall thickness (Design Guidelines: Injection Molding, 2016).

When the resin flows into the mold around a core, friction causes the temperature to increase where the flow reunites. The place of which the flow reunites is called a weld line. At the weld line, the temperature becomes so high that soot particles are formed from burning of the polymer. The soot particles represent a type of contamination that can reduce the mechanical properties of the component (Groover, 2011). Also, poor bonding decreases the mechanical properties significantly (Wu & Lang, 2005).

Corners are usually rounded in plastic components. This is foremost to allow the resin to flow easily inside the cavity. In addition, generous radii on corners will reduce stress concentrations significantly. A common measure is the corner radius divided by wall thickness, or R/T. For R/T values less than 0.5, the stress concentration can be more than 1.5. It is therefore recommended that the inside radius is at least one times the thickness (Design Guidelines: Injection Molding, 2016).

In addition to the above mentioned design considerations, multiple process parameters such as inlet location, input pressure, mold temperature and flow rate significantly affect the quality of the component.

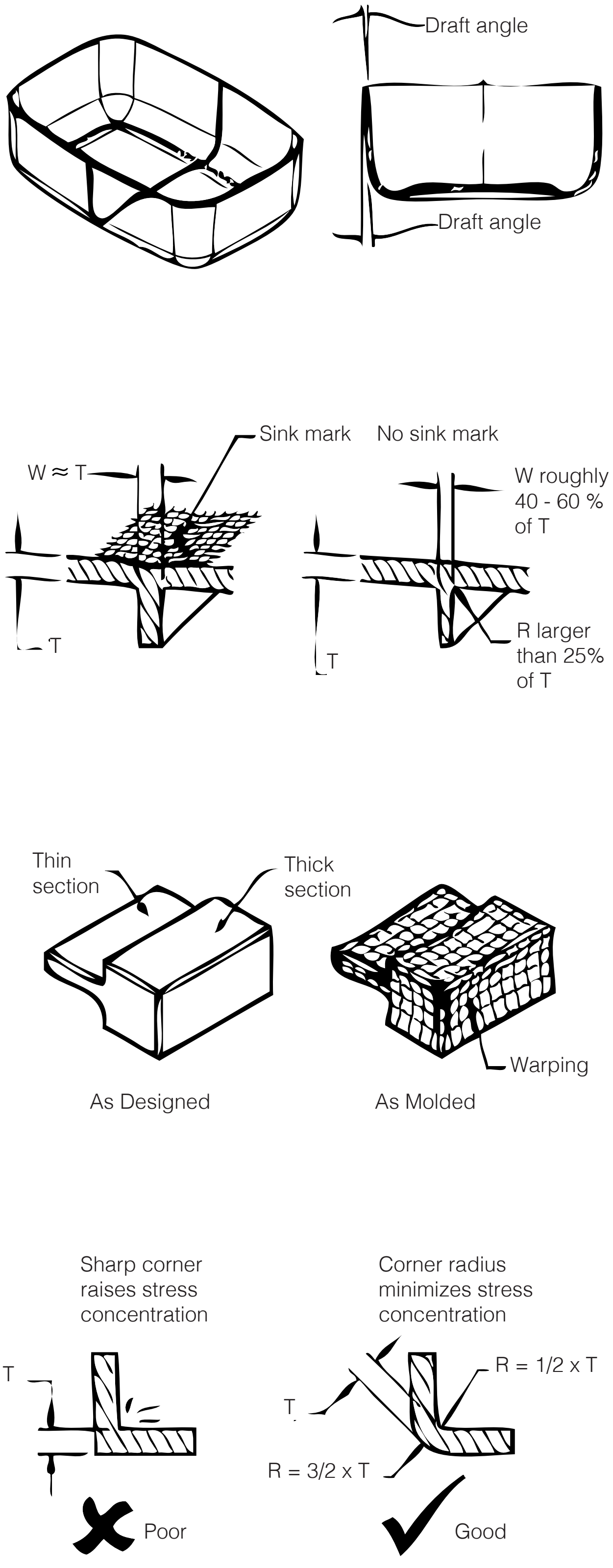

Figure 4: Draft angles, sink marks, warping and rounded corners must all be considered when designing for injection molding. Figures adapted from Design Guidelines: Injection Molding (2016).

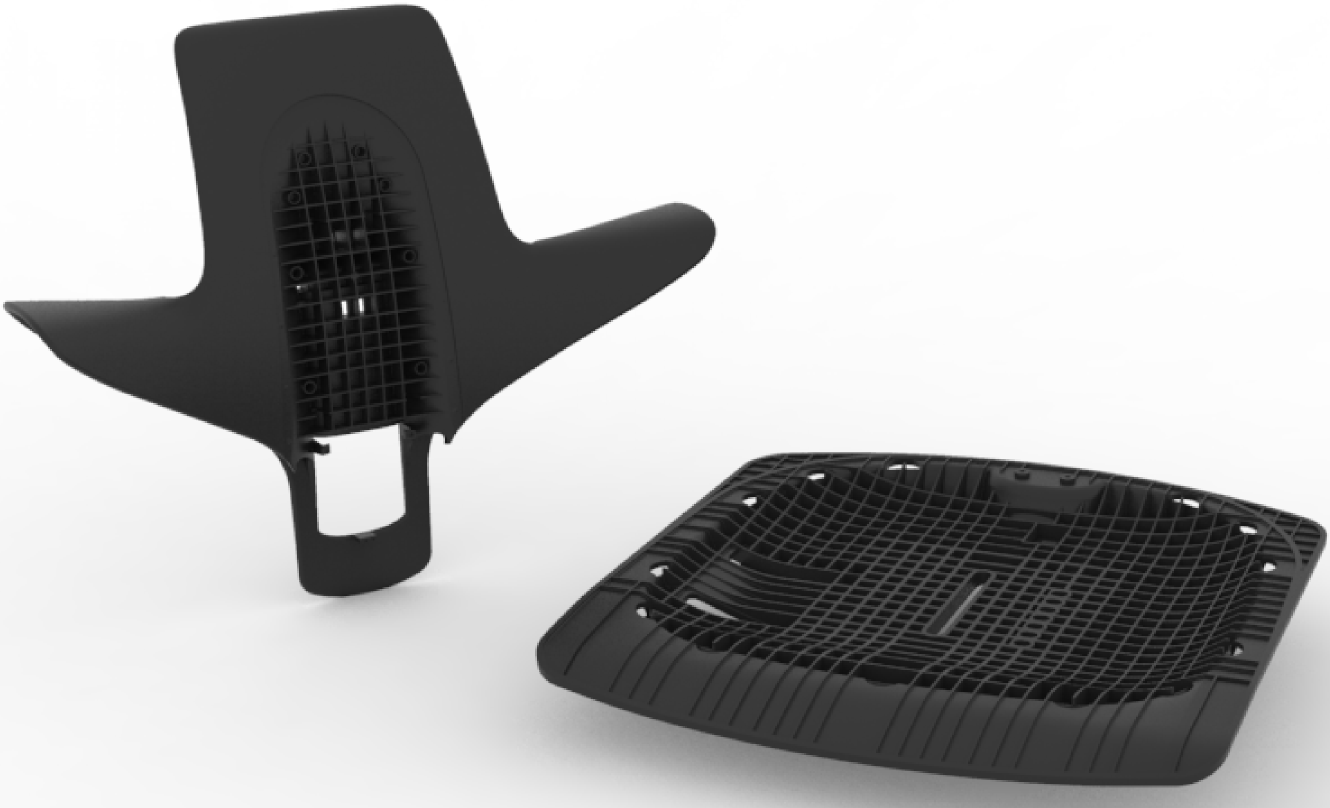

Figure 5: The Håg Capisco Pulse backrest (left) and Håg H09 seat (right). Illustration rendered in KeyShot.

The Case of Scandinavian Business Seating

Scandinavian Business Seating (SBS) is a company that designs, manufactures and sells office seating worldwide. Because of the size, shape and production volumes of SBS-chairs, injection molding is a beneficial means of production for many components (see figure 5). However, because of expensive tooling, the design phase of injection molded components is critical. Tooling for a large and complicated part can cost more than a million norwegian kroner to manufacture. If a design-fault is overlooked, or the component fails to bear the required loads, changes have to be made on the design. This implies that the tooling must be shipped back to China where it was originally manufactured to have additional machining performed. Not only is this extremely costly in terms of shipping and machining work, it also causes a design re-loop that sets back the project significantly, and further delays the product launch. For SBS, reducing the time-to-market would imply great savings. As for today, the time-to-market for a new office chair is roughly three years. A one year reduction, would mean millions of kroner saved.

In the preceding work, “Improving the Handover Between 3D-models and Injection Molding Production”, it was suggested to focus more on the mechanical integrity of injection molded components, before expensive tooling is made. There are at least two approaches that can provide this information, namely predicting the strength using finite element simulations, and to build prototypes and test them accordingly. A brief summary of some the findings from the pre-master is restated in the following paragraphs.

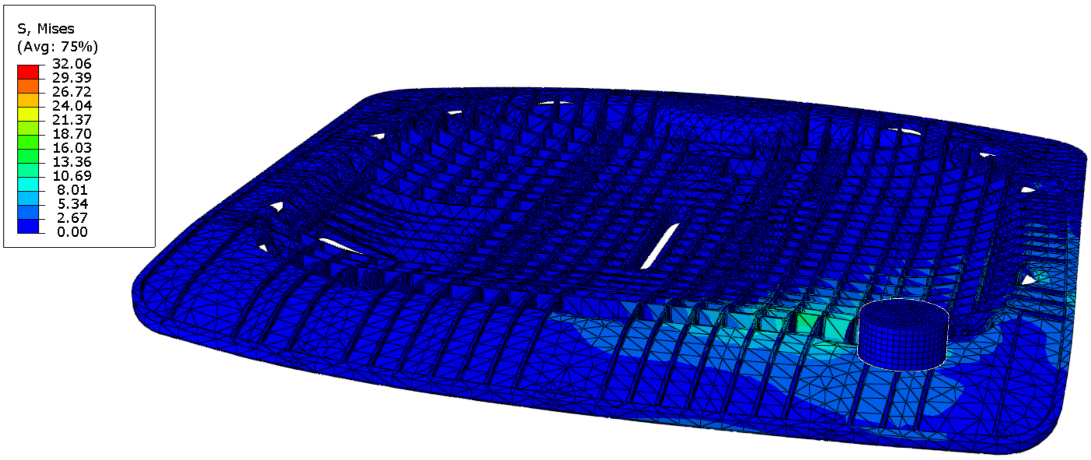

Figure 6: A nonlinear FEA analysis of the Håg H09 seat performed in ABAQUS during the pre-master work.

Structural Finite Element Analysis

The first approach was to simulate the mechanical behaviour of injection molded plastics using finite element analysis. Although finite element simulations is a common way of obtaining knowledge when designing with metal, plastics, and especially injection molded plastics, are more difficult to predict. Polypropylene (PP), which is a common injection molding plastic, has a nonlinear stress-strain response. The reason for this is that PP is a semicrystalline thermoplastic polymer. A thermoplastic polymer consists of long molecular chains that sometimes can be covalently cross-linked. Furthermore, a semicrystalline thermoplastic polymer, such as PP, has a mix of crystalline and amorphous regions (Røstum, 2014). When subjected to loading, the amorphous regions are first uncoiled, and then crystalline areas are rotated and separated. Because the molecular chains can slide relative to each other, these polymers can take large plastic deformations (Sælen, 2012). Additionally, PP has a higher yield stress in compression than in tension.

In “Improving the Handover Between 3D-models and Injection Molding Production”, four different approaches of simulating PP, in simulations softwares Siemens NX and ABAQUS, were looked into. These were:

- Linear elastic FEA.
- Piecewise linear FEA, using metal plasticity curves.
- Hyperelastic, viscoelastic and viscoplastic approaches.
- A hyperelastic-viscoplastic material model proposed by NTNU Simlab.

It was found that the linear elastic approach gave an imprecise but conservative estimation. However, the linear elastic approach gave a quick insight into problematic areas of stress concentrations. The piecewise linear FEA, using metal plasticity curves, gave a more precise result, but was not suited for unloading conditions. The hyperelastic, viscoelastic and viscoplastic approaches were more accurate, but indeed more time consuming than the previous ones, and less suited for the tetrahedral mesh of the complex test geometry. An excerpt from “Improving the Handover from 3D-models to Injection Molding Production” describing FEA is attached in appendix B, and provides a more thorough introduction to the topic. Examples of a nonlinear FEA is shown in figure 6.

Furthermore, it was found that although numerical errors can be mitigated, a finite element analysis is an approximation to reality. In all the different approaches, it was assumed that PP is a homogeneous, isotropic material. However, much of Røstums work (2012) revolved around mapping the skin/core behavior of PP, which implies that PP is not homogeneous. This is supported by the findings of Fitchmun and Mencik (1973) who found that the density varies throughout a sample as a function of temperature and time. Also, some anisotropy will be introduced due to the flow of the polymer during injection (Fujiyama & Awaya, 1977). Moreover, defects associated with injection molding, such as weld lines, can reduce mechanical properties significantly (Wu & Lang, 2005).

Significant efforts of providing a realistic material model for simulating PP have been made at NTNU SimLab by Arild Clausen (Polanco Loria et. al, 2010) and his master students Kristin Sælen (2012) and Heine H. Røstum (2014) (See appendix B). In spite of its importance, this topic is beyond the scope of this report. For further reading, master’s theses of Røstum and Sælen are recommended.

Prototyping Plastic Components

The second approach on obtaining knowledge the mechanical behavior of PP was to build prototypes and test them under loading (see figure 10). As mentioned previously is the main issue with injection molding the tooling cost. It hard to justify making an injection molded prototype when it requires the same expensive tooling as production parts. Although advances in additive manufacturing have opened up for faster prototyping of plastic parts, several challenges still arise.

Cleveland (2008) explain that a plastic prototype must address the four F’s, namely form, fit, function and feasibility. Form is the looks and feels of the product, and concerns properties such as weight and surface finish. Fit is the shape and dimensions of the product, and hence also the interaction with other components. Generally are the form and fit only dependent on the design. Function concerns performance characteristics like the mechanical response, as well as chemical resistance. The function is dependent on the design and material as well as the manufacturing process. Finally, feasibility is how cost-effectively and successfully the production method can produce the part. The four F’s are illustrated in figure 7.

In the early stages of product development, the form and fit can be prototyped using various rapid prototyping methods. Some of these include polymer additive manufacturing, CNC-milling the part from a workpiece of plastic, or using indirect rapid tooling techniques such as vacuum casting, spray metal tooling or aluminum-filled epoxy tooling Malloy (2011). However, none of these techniques will provide material properties that resemble the final product, and consequently not covering the function. Although some novel additive manufacturing techniques such as continuous liquid interface production (CLIP) claim to make fully isotropic parts, they will not represent the anisotropy, inhomogeneity and weld lines imposed by the injection molding process (Rosochowski and Matuszak, 2000).

One way to include function characteristics in prototyping is to perform low-volume production by employing direct rapid tooling techniques. Direct rapid tooling when the rapidly prototyped geometry is used directly as a mold. Although a few solutions exist on the market today, there is much ongoing research in the field. This will be discussed more thoroughly later.

After the product design is verified, it can be useful to run a pilot series to verify feasibility or market testing. For this purpose, bridge tooling can be made from aluminum. Bridge tooling is the tooling that bridges the gap between low-volume production and high-volume steel tooling. The aluminum tooling can manufacture from 1000 to 10000 components, and is usually machined on a CNC-mill (Cleveland, 2008). Because there already exist good solutions for bridge tooling, this topic will not be discussed further.

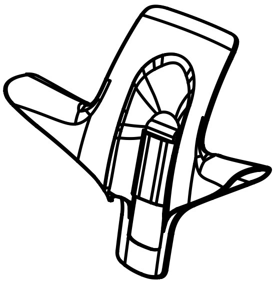

Form

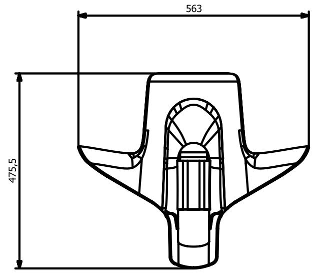

Fit

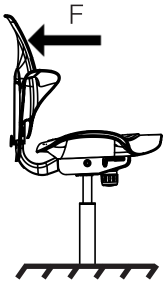

Function

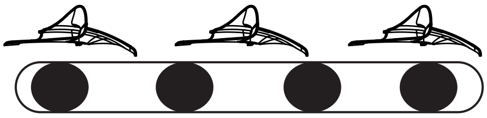

Feasibility

Figure 7: The four F’s illustrated.

Scope of the Work

Theoretically can the four F's be considered using a mixed fidelity approach. The form and fit can be prototyped using high resolution rapid prototyping. If combined with some of the FEA-techniques listed previously, the mechanical response, or function, can also be considered. Finally, the feasibility can be simulated using software such as Autodesk Moldflow or Solidworks Plastics. Here the effect of injection time, inlet location and weld lines can be considered.

However, simulation tools fails to include several aspects of function and feasibility, and nor were they intended to. Product developer at SBS, Marius Sollie, explain that they design chairs to flex during use, and further that the deformation behavior of the chair is an important design feature (personal communication, August 2015). Although finite element simulations can give a good impression of how much load a component can take before it breaks, it will not provide a haptic feeling of the stiffness of the component. Likewise will a flow simulation of the manufacturing process give an idea of where it is clever to place the inlet, and how much pressure should be utilized. However, the flow simulation will not include important design factors such as draft angles, ejector pin marks and sink marks.

By utilizing direct rapid tooling techniques, where the mold is manufactured directly by rapid prototyping, can the manufacturing process of injection molding, and the form, fit and function of the product be prototyped simultaneously. This may provide sufficient information on the various dimensions of the product to avoid design re-loops. Ultimately, this may reduce the time-to-market.

This thesis will investigate direct rapid tooling techniques for low volume injection molding production, by employing the Wayfaring model and using prototypes for learning. The ultimate goal of the work is to find a cheap, efficient and effective way of prototyping injection molded components.

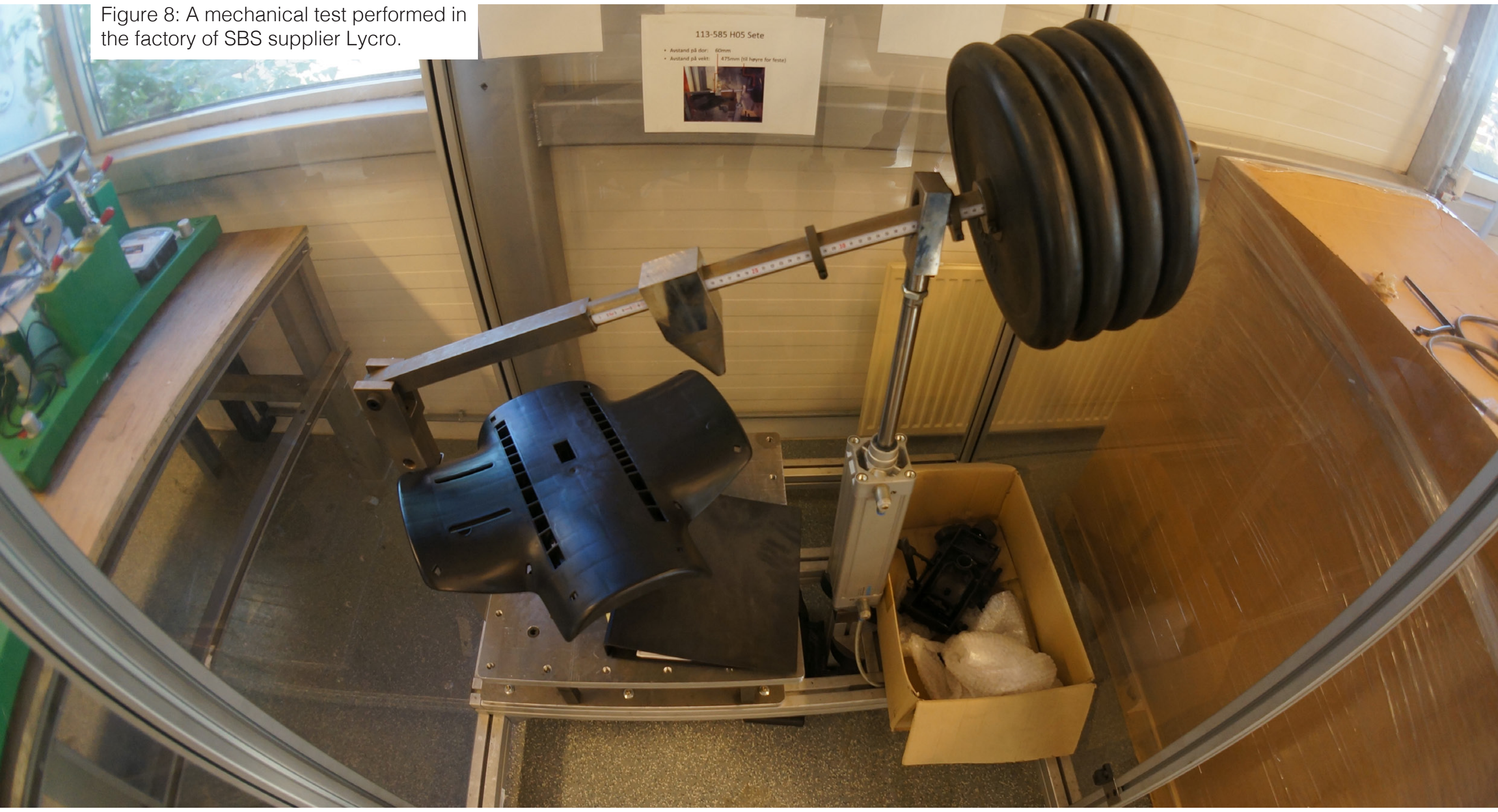

Figure 8: A mechanical test performed in the factory of SBS supplier Lycro.

Chapter Three

Techniques for Direct Rapid Tooling

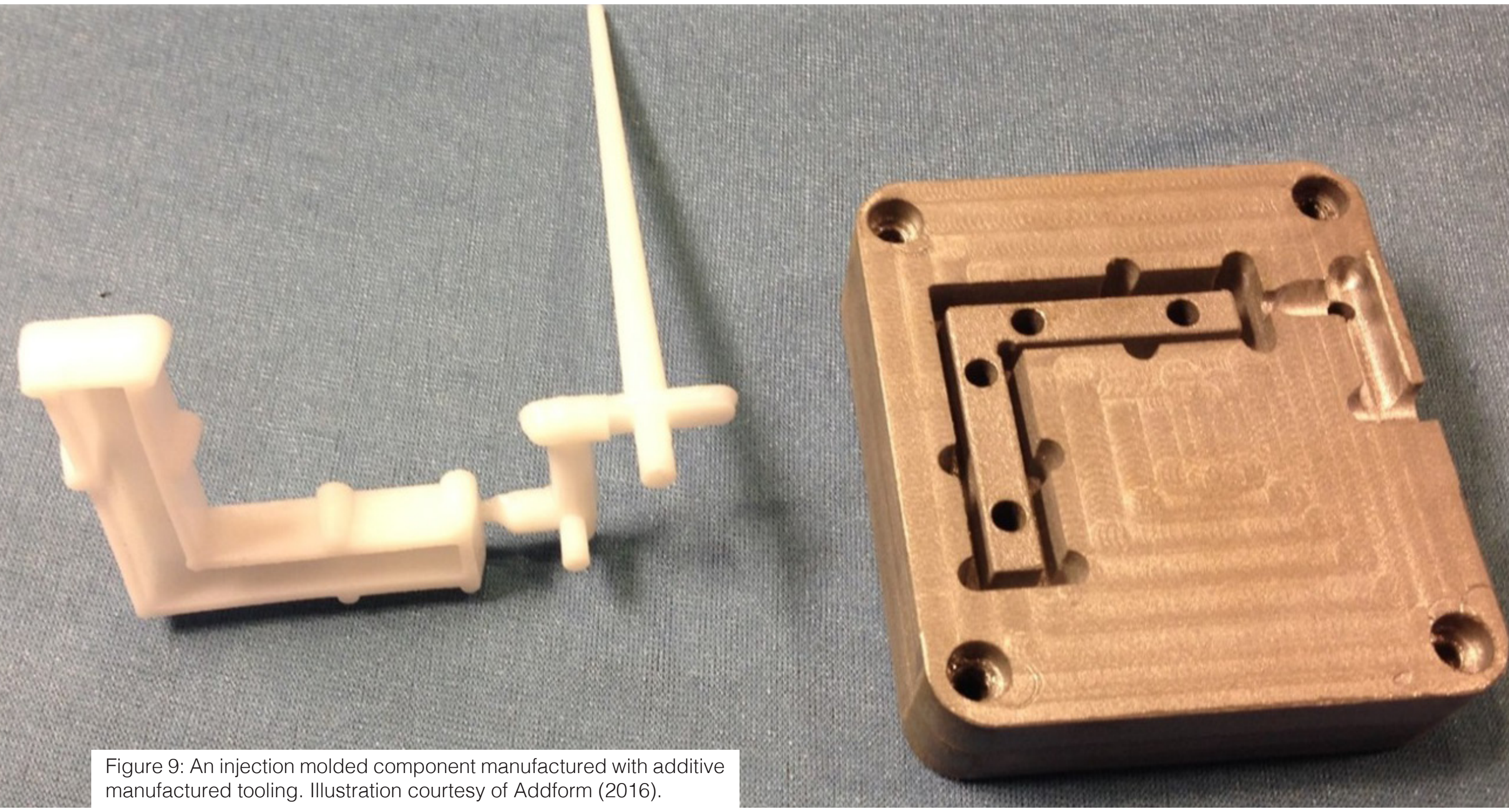

Figure 9: An injection molded component manufactured with additive manufactured tooling. Illustration courtesy of Addform (2016).

Introduction

Rapid tooling is the process of using rapid prototyping to manufacture the tooling. From a manufacturing perspective is rapid prototyping the process of quickly fabricating a model using three dimensional computer aided design (CAD)-techniques. Although many consider rapid prototyping to be synonymous with additive manufacturing, rapid prototyping is also considered, in this context, to include CNC-milling. Furthermore can rapid tooling be divided into direct- and indirect rapid tooling. In “Direct rapid tooling: a review of current research” (1998), the following definition of direct rapid tooling is suggested:

> *Direct rapid tooling (DRT) is an industrial concept aimed at the realization of production tooling directly from CAD data files, with the smallest possible process chain (number of operations). Its purpose is the manufacture of tools that can be used under normal production conditions, in terms of durability, accuracy and surface quality.*

What ultimately separates indirect- from direct rapid tooling is the need for a pattern. In indirect rapid tooling, a rapid prototyped shape, also referred to as a pattern, is used to fabricate the tool. In direct rapid tooling however, the tooling is made directly using rapid prototyping. Indirect rapid tooling techniques will not be covered in this report.

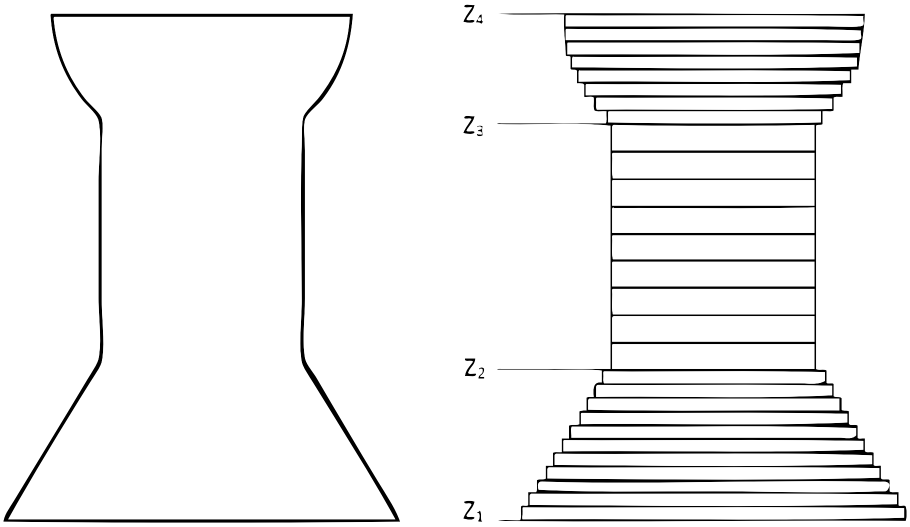

CAD model

Part geometry after slicing

Figure 10: The slicing process can result in a stair stepped finish for the additive manufactured part.

Additive Manufacturing

Although it is nothing new, most research in the field of direct rapid tooling concerns the use of additive manufacturing (Karapatis et al., 1998). For example discusses King and Tansey (2002) the use of SLS-technology in combination with polyamide (PA) and steel materials. Furthermore have Masood and Song (2004) presented new metal/polymer materials for rapid tooling using fused deposition modelling (FDM). Boparai et. al (2016) also discusses the potential of using FDM, in combination with new materials and post processing, for rapid tooling. Colton et. al (2007) reported on the failure of rapid prototyped stereolithography molds during injection molding, while Rosochowski and Matuszak (2000) also include laminated object manufacturing and sintering with metal and ceramics in their discussion of the topic. Because there is a significant cost gap between cheap materials such as polymers, and high-end materials such as metals and ceramics, the more expensive alternatives will not be discussed any further.

In Norway, the ongoing research project AddForm, with several partners in Norwegian industry, including SBS, have shown good results (see figure 9). In the project, tool inserts were made successfully using a nylon composite material, namely a PA12 matrix reinforced with aluminum particles. According to main partner OM BE Plast's website (Addform, 2016), as many as 9000 parts have been injection molded using one single mold. Although no publications have come out yet, this method seem very promising.

Preparing the File

When performing additive manufacturing, a three-dimensional geometry is first created using computer aided design (CAD) software. From the CAD-software, an STL-file is exported. An STL-file is a faceted body, which only represents the surface of the geometry through triangles. Therefore, the resolution must be fine enough to capture all necessary details.

After the STL-file is generated, it is imported into a slicer program. The slicer program slices the faceted geometry into layers, and simulates the additive process. It is here important to evaluate the part's orientation in the 3D-space, as the layering will cause a stair stepping effect (see figure 10). For overhanging geometry, it can be necessary to add support materials. The type of support materials varies throughout the different technologies: for polymer jetting it is a gel, for selective laser sintering, it is powder and for fused deposition modeling it is simply the extruded material. The support material can normally be generated automatically in the slicer program. However, in some cases, especially concerning fused deposition modeling, it can be useful to design the support in the CAD-software.

Fused Deposition Modeling

Fused deposition modeling (FDM) is the simplest and cheapest of the AM-technologies. In FDM, a filament of thermoplastic material is extruded through a heated nozzle and onto a build plate (see figure 11). The position of the nozzle relative to the build plate is controlled using computer numerical control (CNC). In order to provide good traction to the build plate, the build plate can be heated. Also, glue is sometimes added to provide extra traction.

Materials capable with FDM printers are thermoplastics such as acrylonitrile butadiene styrene (ABS), polylactic acid (PLA) and polyamide (PA). The latter is also known as nylon. An important factor to consider when dealing with FDM is the warping efect. As the material cools after manufacturing, it contracts, depending on the coefficient of thermal expansion of the material. Warping can cause the geometry to fail ultimately, even though it appears to be fine during manufacturing. To prevent warping, a decrease in density can be introduced. Because a fully solid material will contract more, it can be beneficial to utilize an internal build structure with a covering shell. However, as the outer layer is only a few millimeters thin, the geometry is more susceptible to melting when used for direct rapid tooling.

Several novel materials have been introduced for FDM. Masood and Song (2004) utilized a composite filament consisting of iron particles in a PA matrix, for direct rapid tooling. Several other variants are commercially available, including copper, bronze, aluminum and wood particles in different thermoplastic matrices.

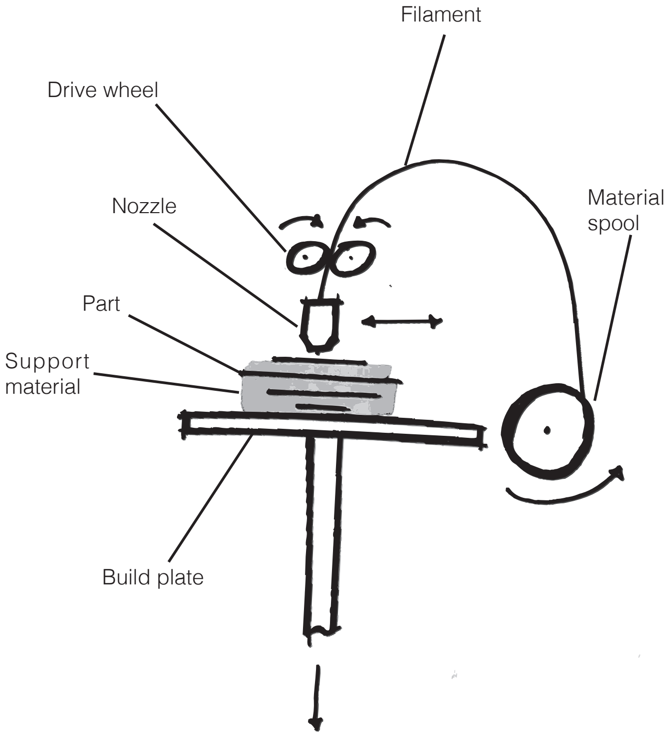

Figure 11: Illustration of the FDM process.

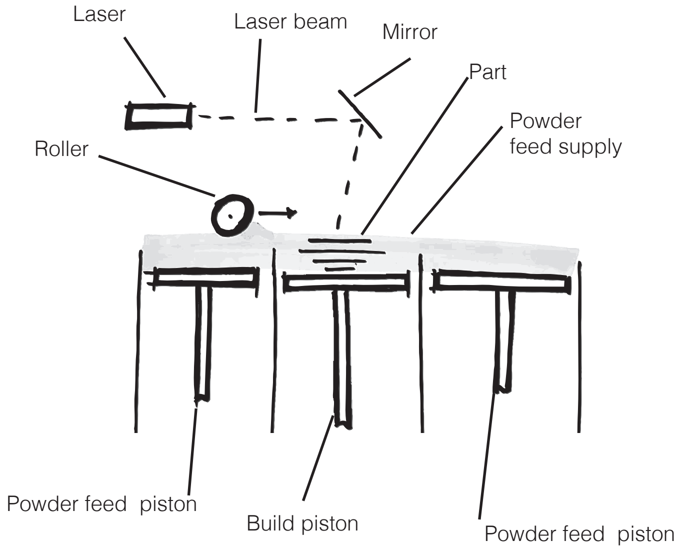

Figure 12: Illustration of the SLS process. Note that this is not the same as SHS, although it is very similar.

Selective Heat Sintering

Selective heat sintering (SHS) is a process in the family of powder techniques. Similar to selective laser sintering (SLS), SHS deposits a thermoplastic polymer powder layer by layer. Instead of sintering powder particles together using a laser (such as SLS), SHS utilizes a thermal printhead. The powder that is not sintered works as support material, and can be reused (Bogue, 2013). An illustration of an SLS process is shown in figure 12.

Polymer Jetting

Polymer jetting is a technique in the family of photopolymerization. In this family, photosensitive polymers are cured using UV-light. Unlike the other members of the family, namely stereolithography and solid ground curing, polymer jetting sprays the polymer onto a build plate, where it is cured (see figure 13). For support, a gel like structure is jetted and cured where needed. The clear benefit of this technique is that fully isotropic and homogeneous components can be made. Although some stair stepping is present on the surface, this layering effect can be removed afterwards by polishing. However, materials and machinery are fairly expensive.

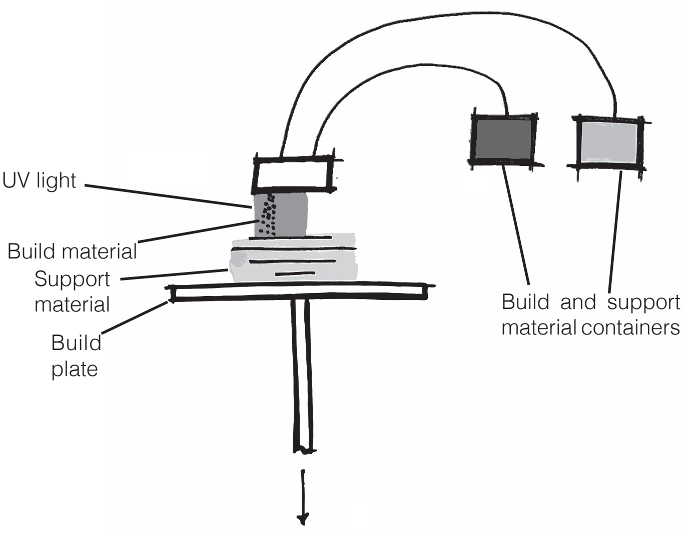
UV light
Build material
Support material
Build plate
Build and support material containers

Figure 13: Illustration of the polymer jetting process.

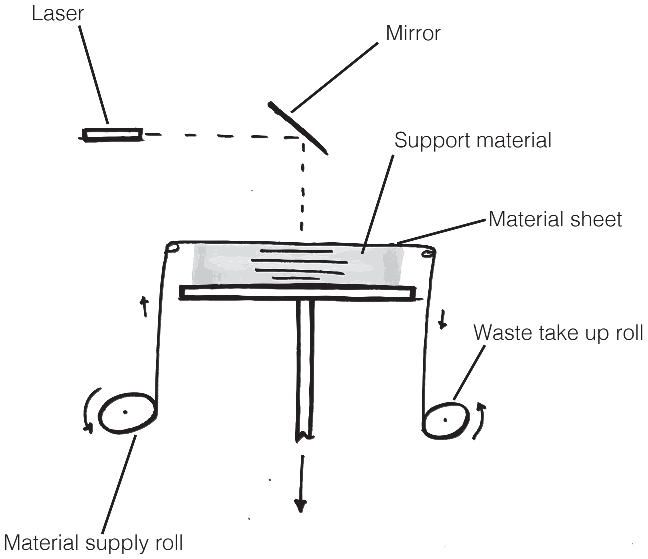
Laser
Mirror
Support material
Material sheet
Waste take up roll
Material supply roll

Figure 14: Illustration of the LOM process.

Laminated Object Manufacturing

Laminated object manufacturing (LOM) is a technique where sheets are stacked and cut one by one. The sheets are adhered to each other using glue. For the top layer, a profile in the XY-plane is cut using a knife or a laser (see figure 14). The next sheet is then glued onto the previous cut sheet, and the process is repeated. Because the sheets are larger than the manufactured geometry, this technique normally require some post processing for freeing the geometry. However, the excess material also serves very well as support. LOM is normally used in combination with materials such as metal, polymers and paper. The benefit of this technique is that parts are of full density, and that larger parts in the XY-plane can be as fast as smaller parts.

Subtractive Rapid Prototyping

In “Alternative materials for rapid tooling”, King and Tansey (2002) present another approach than additive manufacturing, namely machining the mold from fibreboards especially designed for tool building applications. This resembles techniques more common in the composite material industry. Here, milling molds from softer materials such as high density polyurethane (HDPU) foam and medium density fiberboards (MDF) is a common way for making one offs (Dang, 2013).

Preparing the FIle

When preparing for CNC-milling, a CAD-file is first generated in a suited software. After this, a computer aided manufacturing (CAM) software generates a tool path according to specified inputs. This process is normally far more complicated than for additive manufacturing, and requires good knowledge in the field. Many product lifecycle management (PLM) softwares, such as Siemens NX, PTC/Creo and Catia, offers both CAD and CAM modules within the same program (see figure 16). Alternatively, a separate CAM program can be utilized. Although machining is a field of its own, a brief introduction will be covered here. For further reading Efunda’s milling guide[1] is recommended.

According to Groover (2011) are parameters that must be considered when milling cut depth, feed rate, spindle speed, number of teeth on the cutter, the width of the tool engaging in the workpiece, and the chip load. The cut depth, d, is the depth, in the direction of the tool axis, of which the mill engage in the workpiece. The cut depth is normally given in millimeters. The spindle speed, N, is given in revolutions per minute, and is the number of rotations around the tool axis. The chip load, f, is given as the feed per cutter tooth, and can be converted into feed rate, f_r, using the following expression (1):

$$f_r = N \cdot n_t \cdot f \tag{1}$$

Where n_t is the number of teeth. Furthermore, the material removal rate is determined using the product of the feed rate and the cross sectional area of the cut. The material removal rate, R_{MR} can therefore be calculated using the following expression (2):

$$R_{MR} = w \cdot d \cdot f_r \tag{2}$$

The best values of the different parameters are dependent on the material being machined as well as the cutting tool material. For reference, please see Uddeholms recommendations[2]. Some cutting parameters are illustrated in figure 15.

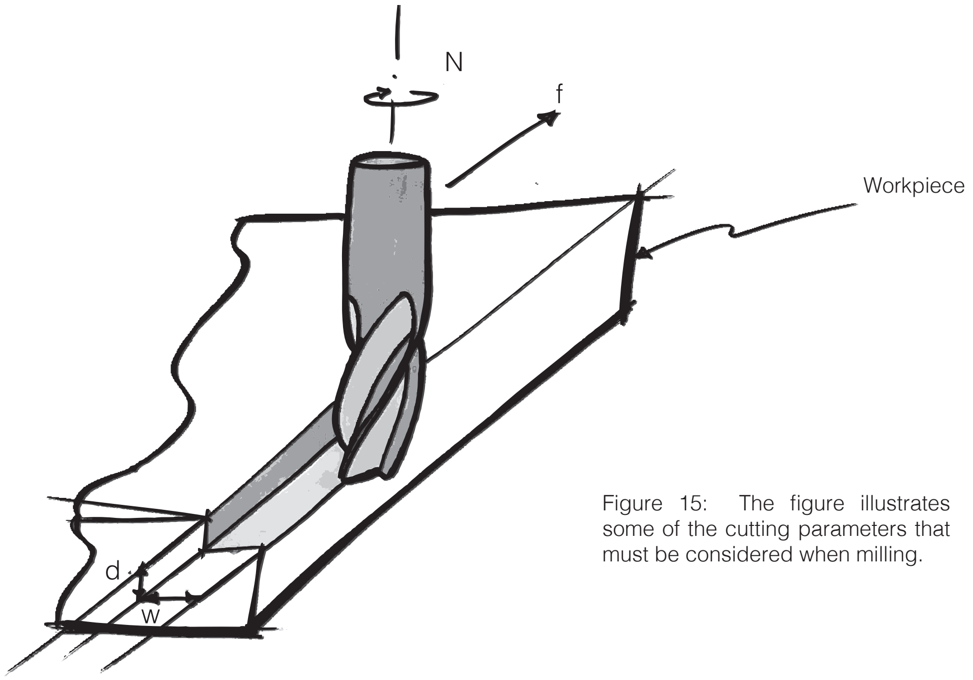

Figure 15: The figure illustrates some of the cutting parameters that must be considered when milling.

---

[1] http://www.efunda.com/processes/machining/mill.cfm

[2] http://www.uddeholm.com/files/Cutting_Data_Corrax_eng.pdf

When generating the tool path, the program is commonly separated into roughing and finishing. The roughing is usually performed with a large flat end mill, enabling the possibility to do large cut depths and high feed rates. The roughing leaves a coarse, stair stepped finish. After roughing, one or more finishing operations can be performed. For curved surfaces, as is common in injection molding tooling, a ball pin mill usually gives best results. Because injection molded parts often contain ribs, small mill heads sometimes have to be employed. In this case, it is important to be aware that there are restrictions to the maximum possible depth of the design feature, depending on what material is being milled.

The tool path is communicated from the CAM-software to the CNC-mill through a G-code. Each CNC-mill have its own list of expressions that is supported. The G-code must therefore be exported through a post-processor, tailored for the specific CNC-machine.

Subtractive Prototyping Materials

Several machinable rapid prototyping materials for CNC-milling exist on the market today. Examples are high density foams, woods and tooling boards (Kucklick, 2013). Criterias for the materials include ease of machining, dimensional stability, temperature resistance, easy surface finishing and large block sizes available. The most popular and inexpensive high density foam is urethane, also known as surfboard foam. Another popular variation is extruded polystyrene foam. Suited wood materials include medium density fiber boards, plank pine and chemical wood. Tooling boards are composite boards especially designed for tooling applications. An example is the Cibatool Express 2000 board, which is an aluminum reinforced epoxy board (Vantico, 2000).

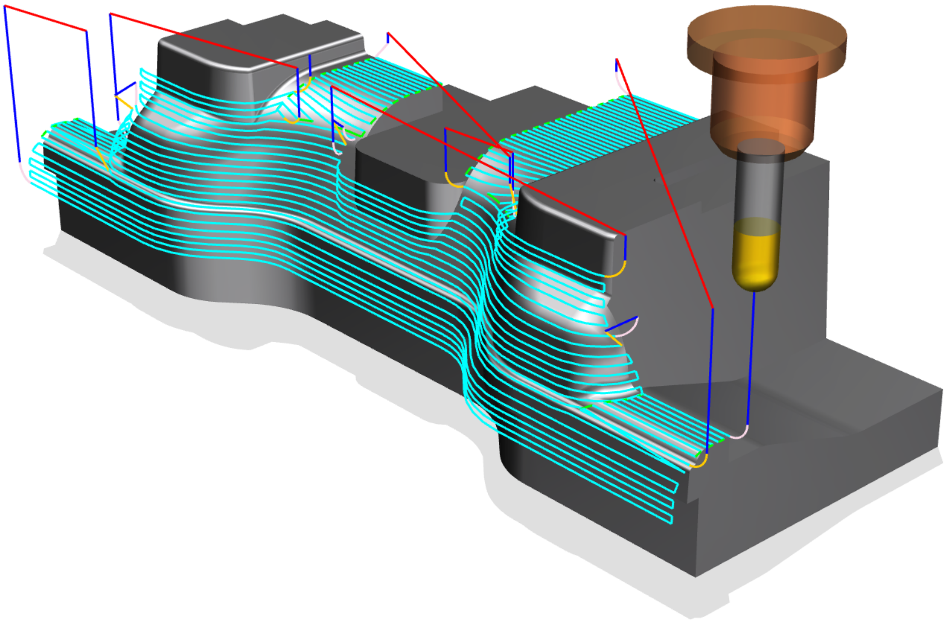

Figure 16:
Visualization of tool path in NX 9 CAM (Cards PLM Solutions, 2016).

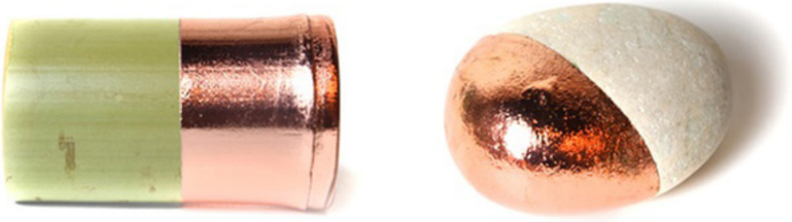

Figure 17: Electroplated 3D-printed polymers. Photo courtesy of Monolith Studio (Kickstarter, 2015)

Coating Techniques

The main challenge with rapid prototyping, whether it is additive manufacturing or CNC-milling, is that the cheap materials that can be processed quickly are often soft. It is very important in injection molding to ensure a hard and smooth surface finish, and accurate dimensions in the tool. This is to ensure easy ejection and to reduce post processing of the injection molded part. One way to address this issue is to apply a coating of a harder material onto the rapid prototyped geometry.

Surface Sealing

A simple way of applying a hard surface to a rapid prototyped geometry is to seal the surface with paint, lacquer or a thermoset material. A versatile medium for this purpose is epoxy, as described by Dang (2013). Other suited thermosets include polyurethane.

Release Agent

In order to allow for easy ejection of the injection molded geometry, it is desirable to ensure as little friction on the mold surface as possible. This can be done by applying a coat of release agent onto the mold. The release agent can be wax or aerosol sprays. In addition to minimizing friction, the release agent will absorb some energy as the hot resin is injected into the mold, thus limiting the immediate heat exchange from the resin to the mold. It is important to consider whether or not the release agent will cause unwanted chemical reactions with the resin. Also, health, safety and environmental aspects should be considered.

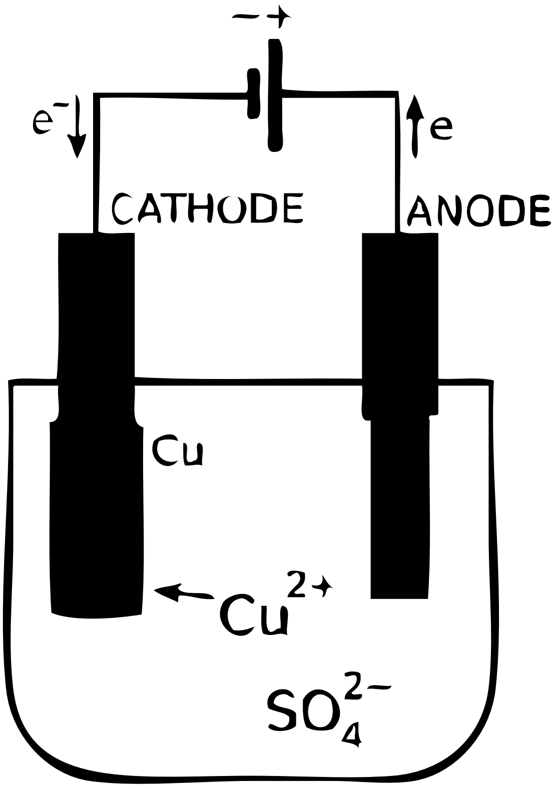

Figure 18: The chemistry of electroplating. Figure adapted from Wikipedia (2016).

Electroplating

A far more advanced technique for coating rapid prototyped geometry is through electroplating. A US-patent from 1997 (US5641448 A) describes a process of which a tool for low volume injection molded production is produced in a rapid prototyped system, such as stereolithography, and further electroplated with a 75-150 μm layer of nickel. Electroplating is where the process of electrolysis is utilized to reduce a layer of metal onto a cathode. An anode is the place of which oxidation occur, whereas a cathode is the place of which reduction occur. In order to make this process work, an anode and a cathode must both be submerged in an electrolytic bath. An electrolyte is an electrically conductive liquid, and contains a dissolved metal salt as well as other ions, and permits the flow of electricity. A direct current (DC) power source is connected to the anode and cathode (see figure 18). This causes the anode to become positive, and consequently, the metal atoms of the anode are oxidized and dissolved into the electrolytic solution (3). The cathode, on the other hand, becomes negative, and attracts the positive ions in the solution. This causes a reduction process (4) of which a layer of anode material is coated onto the cathode.

Anode: $$Cu(s) \rightarrow Cu^{2+}(aq) + 2e^{-} \tag{3}$$

Cathode: $$Cu^{2+}(aq) + 2e^{-} \rightarrow Cu(s) \tag{4}$$

The challenge with electrolysis is that most rapid prototyped materials are not electrically conductive (except metals), as is a requirement for a cathode. However, electroplating of plastics is nothing new. In fact, a patent for electroplating plastic components can be dated as far back as 1967 (US3305460 A). One method for making a plastic component electrically conductive is to spray the component with an electrically conductive spray. This method was attempted to be commercialized by Monolith Studios in 2014 (see figure 17). Unfortunately, their Kickstarter campaign was cancelled in 2015 for unknown reasons (Kickstarter, 2015). Another method, described by Cera on his website (2014), works for polymers dissolvable by acetone, such as ABS. This method includes mixing a fine graphite powder with acetone to create a conductive paint. The conductive paint is then painted onto the ABS-part.

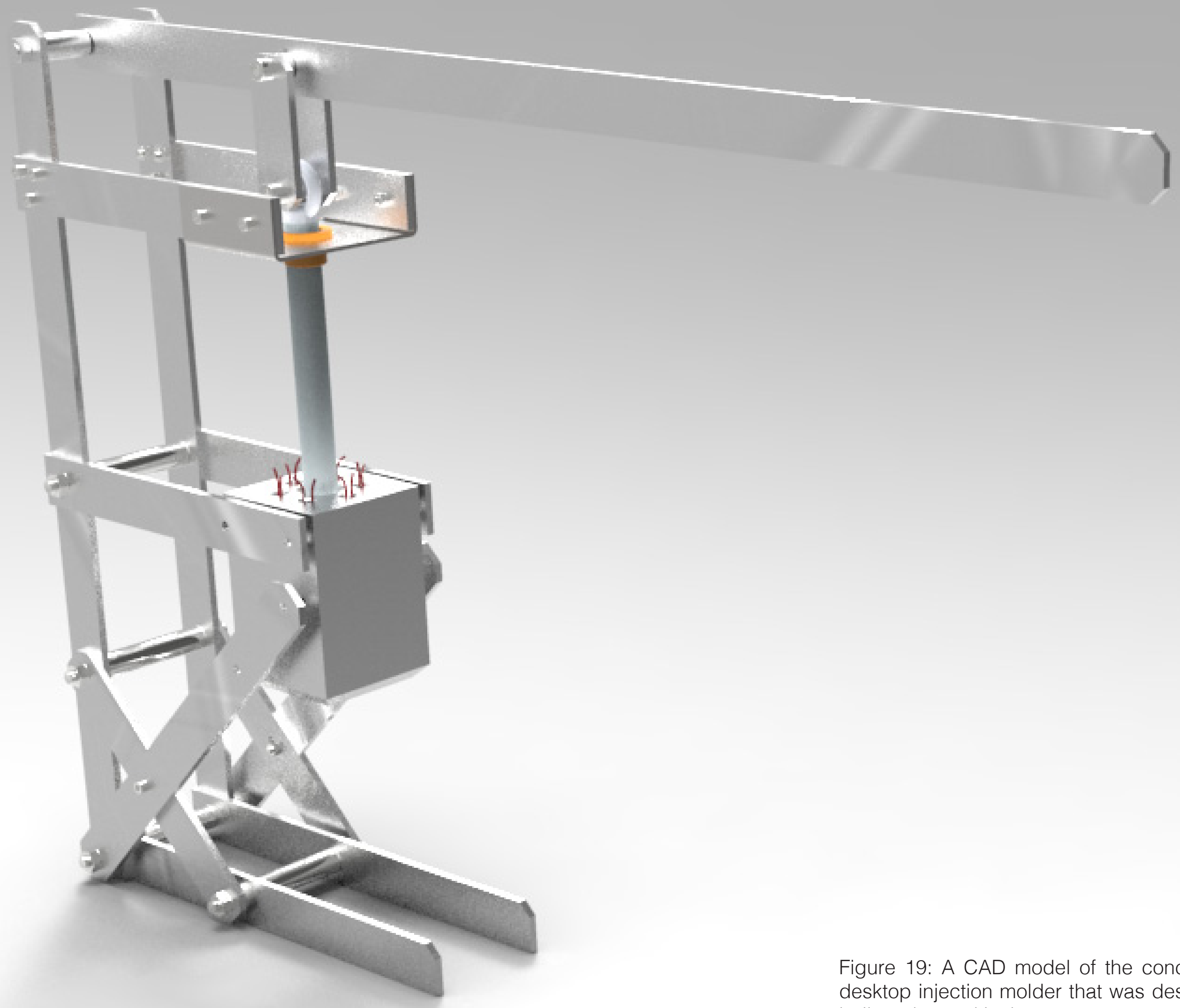

Figure 19: A CAD model of the conceptual desktop injection molder that was designed, built and tested in the pre-master.

Methods for Performing Injection Molding with Rapid Tooling

Desktop Injection Molding

Performing injection molding normally requires full scale injection molding machinery. Although some companies have this machinery in-house, it is more common to outsource injection molding production. For the designer or engineer, this means that if he or she wants to utilize direct rapid tooling techniques for prototyping, an appointment must be scheduled in a factory. This increases probing cycle times significantly, and furthermore sets a higher threshold for prototyping (Hartman et al., 2006).

Consequently, the need for a way of performing injection molding in a near office situation was discovered, and a conceptual desktop injection molding machine was designed, built and tested (see figure 19). The design process is described in Appendix A: “Requirements Exploration Through Iteratively Emerging Critical Functionality From Prototyping”. Essentially, the desktop injection molding machine enables low pressure injection molding prototyping, by manually controlling the injection process. The desktop injection molding machine is described in more detail in Chapter Four, and some technical drawings are attached in Appendix C.

Although a desktop injection molding machine will not be able to achieve the same pressure and volume as its full scale relatives, it can be used to injection mold small geometry, at a lower resolution.

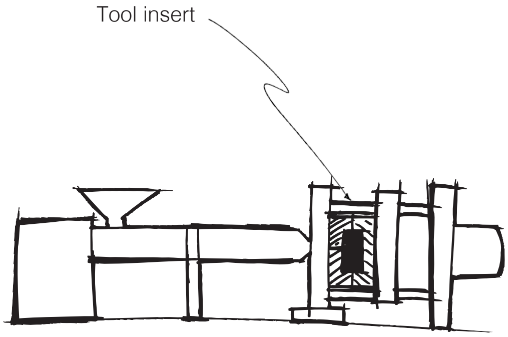

Tool Inserts

A challenge concerning rapid prototyped molds is that they have inferior mechanical properties compared to those made from tool steel or aluminum. In order to deal with the high injection pressure of a full scale injection molding process, a tool insert can be made using rapid prototyping, and be placed into a family mold (see figure 20). The family mold is made from steel, and takes up most of the internal pressure, leaving the tool inserts to take mostly compressive stresses. Additionally, this enables the use of smaller rapid prototyping machinery that only offers limited build sizes (Addform, 2016).

Figure 20: A simplified CAD model of a tool insert in a family mold (below) and where to place it (above). The four screws coming up from the mold are attachment point the the movable plate. The middle cylinder is the nozzle.

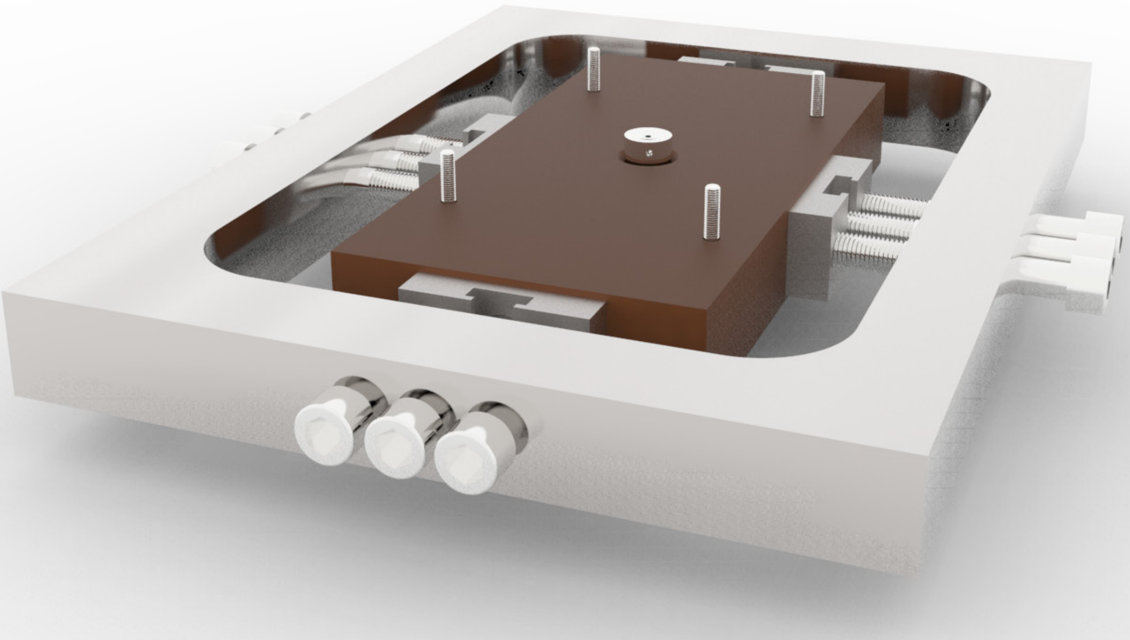

Chapter Four

Rapid Prototyping Machinery

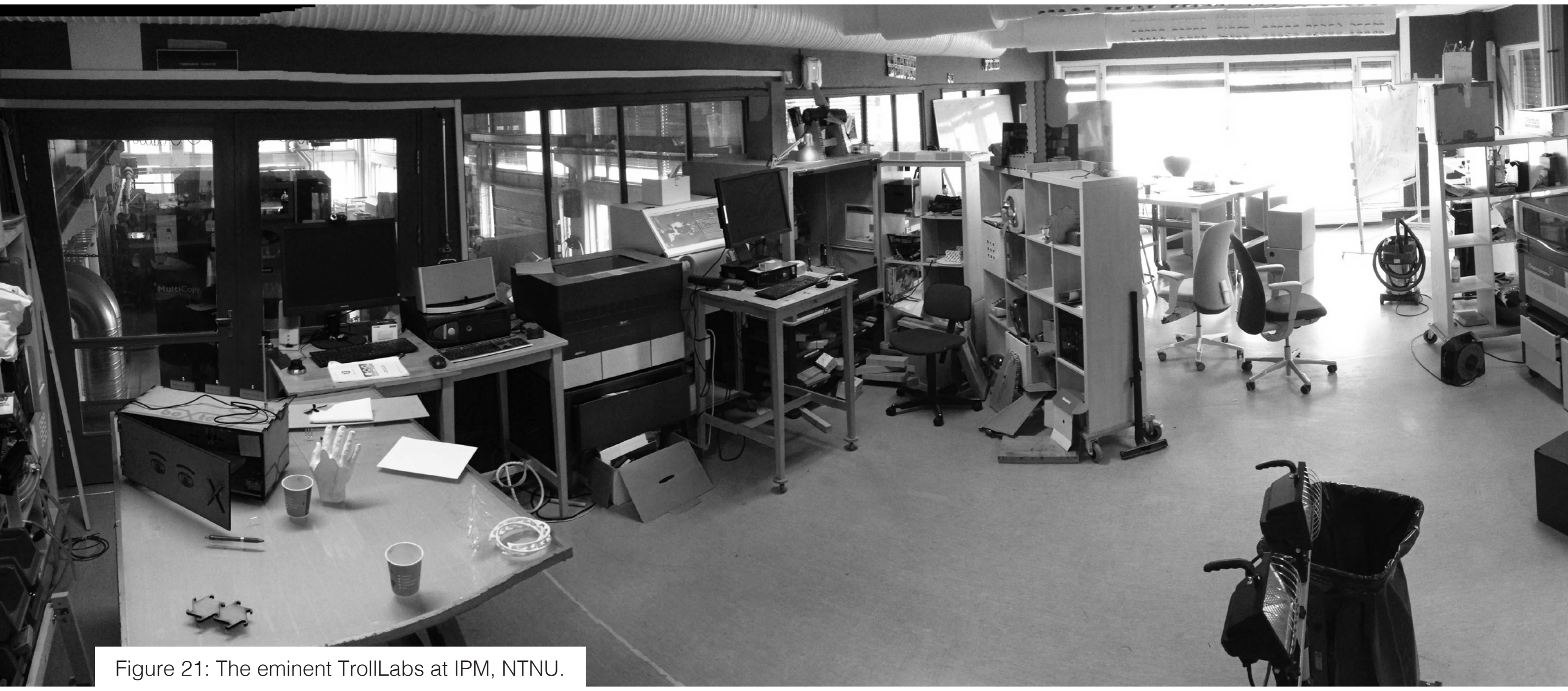

Figure 21: The eminent TrollLabs at IPM, NTNU.

Introduction

The experimental work was performed mainly within the walls of TrollLabs at IPM, NTNU, as depicted in figure 21. Here, tools, materials and machinery were readily available at all times, including several rapid prototyping machines. In this chapter, a brief introduction to each machine is given.

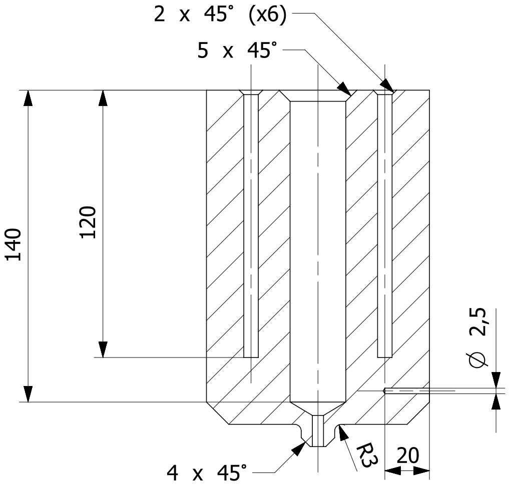

Figure 22: A detailed drawing of the injection chamber of the TrollLabs Rapid Prototyping Injection Molder.

MECHATRONICS
ASK ACHMIMI
LABEL MAKER

TrollLabs Rapid Prototyping Injection Molder

The TrollLabs Rapid Prototyping Injection Molder is capable of performing low pressure, low volume injection molding of small parts. A lever transfers the applied force to a piston, which in turn pushes the resin out through a nozzle, as indicated in figure 19. A heater block fits multiple heater cartridges (see figure 22), which heats the polymer to a desired temperature. The temperature of the heater block is controlled using an Arduino Uno, a k-type thermocouple, a solid state relay and a PID-controller algorithm. The Arduino code is attached in appendix D. MDF protector plates were laser cut and installed to protect from burning hazard. A photography is shown in figure 23.

The maximum volume of injected resin is 68 000 mm^3. With five 220 V, 120 W heater cartridges installed, the maximum temperature is approximately 250 °C.

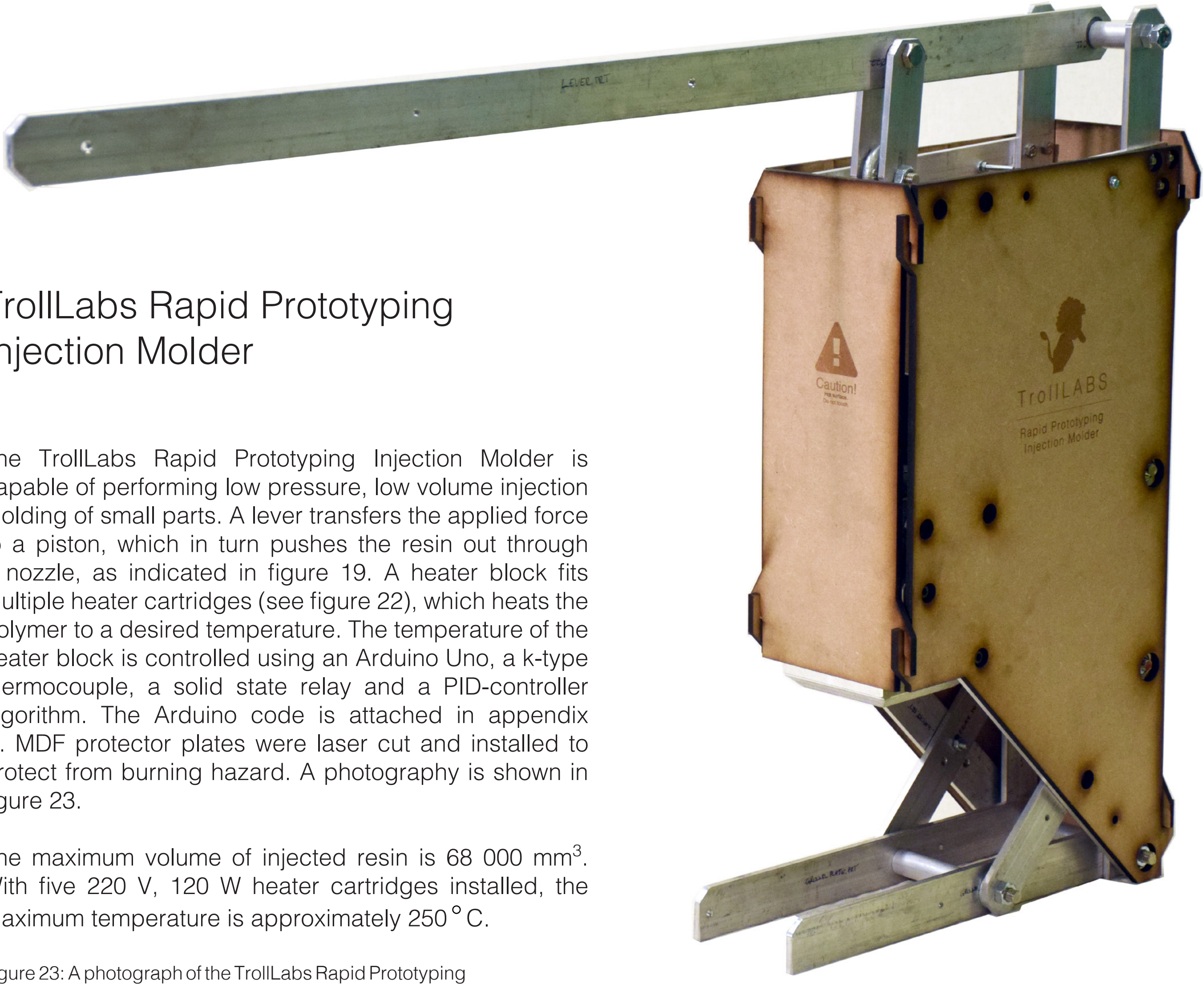

Figure 23: A photograph of the TrollLabs Rapid Prototyping Injection Molder, including MDF safety covers.

Blueprinter SHS 3D-printer

The Blueprinter is a benchtop sized selective heat sintering additive manufacturing system. It utilizes a thermal printhead to sinter particles of thermoplastic powder. After one layer is sintered, a thin layer of plastic powder is deposited on top of the old layer. The process is then repeated. In contrast to other systems, the slicing software is web based, meaning that the printer can be accessed from anywhere in the world. The Blueprinter is displayed in figure 24.

The build size of the Blueprinter is 200x157x150 mm (XYZ), and the layer thickness is 0.1 mm. The printing speed is 2-3 mm/hour.

After the print is finished, excess powder must be cleaned away in a dedicated compartment. Here, pressurized air blows away the excess powder, which in turn can be reused. For now, the only material compatible with the Blueprinter is Monochrome White, which is a thermoplastic nylon material optimized for the machine.

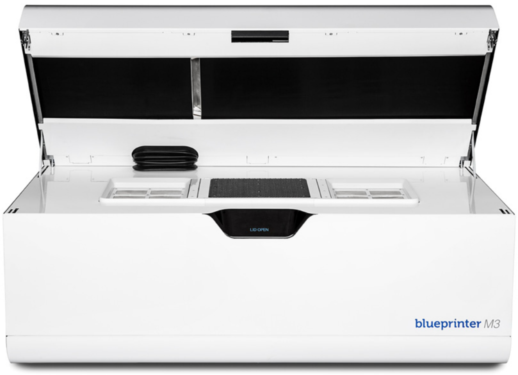

Figure 24: The Blueprinter SHS 3D-printer. Photo courtesy of Blueprinter.

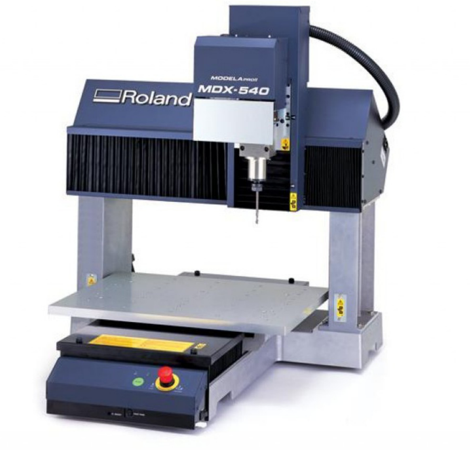

Figure 25: The Roland MDX-540 CNC mill. Photo courtesy of Roland.

Objet Eden 250 3D-printer

Objet Eden 250, from 3D-printing giant Stratasys (previously Objet), is a polymer jetting additive manufacturing system, intended for professional use. Being several times more expensive than the other machinery, it also offers superb quality. A dedicated slicer software named Objet Studio is provided. The Objet Eden 250 is displayed in figure 26. Because of the malfunctioning of a similar machine at TrollLabs, an Objet Eden 250 at CMR Prototech (Bergen, Norway) was used instead.

The build size is 250x250x200 mm (XYZ), and the layer thickness is 0.016 mm. The resolution is less than 0.1 mm. The Eden 250 utilizes a gel-like support material that must be removed manually. This can be done with cutting tools, a water jet or with dissolvable solutions.

Compatible materials are Stratasys photosensitive polymers such as VeroBlackPlus.

Roland MDX-540 Benchtop CNC Milling Machine

The Roland MDX-540 is a subtractive rapid prototyping machine (see figure 25). It is small enough to fit in a makerspace, and relatively cheap compared to large CNC-mills. It is compatible with normal NC-code generated from any CAM-software, but also includes an easier-to-use CAM software interface, namely SRP-player.

The MDX-540 can be set up with either 3-axis or 4-axis milling. When utilizing only 3-axes, the work area is restricted to 400x400x155mm. For the 4-axis setup, constraints are roughly 65mm radius x 370mm length. The MDX also offers automatic tool change, and is compatible with mill heads up to 10 mm in diameter. The maximum spindle speed is 12,000 rpm.

Compatible materials are plastic, resin, wood, foams and non-ferrous metals such as aluminum and copper.

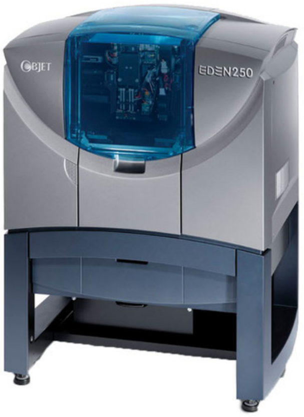

Figure 26: Objet Eden 250 3D-printer. Photo courtesy of Stratasys.

Ultimaker 2 3D-printer

The ultimaker 2 is a desktop sized fused deposition modelling additive manufacturing system (or 3D-printer). It comes with a dedicated slicing software named Cura, which is easy to use. Different from many other cheap systems, the Ultimaker operates independently without having to be connected to an external computer. A variant of the Ultimaker 2 is shown in figure 27.

The Ultimaker 2 utilizes 2.75 mm thermoplastic filament, and has a build size of 223x223x205 mm (XYZ). It offers interchangeable nozzles, making it compatible with different materials. The standard nozzle diameter is 0.4 mm, and the layer resolution is 0.02 mm. The Ultimaker 2 also includes a heated glass build plate (or hot bed), for better traction. The hot bed can be heated up to 90°C, while the nozzle can be heated up to 260°C. This makes it compatible with PLA, ABS, XT and PA thermoplastic materials, as well as some polymer matrix composite filaments.

A benefit of the Ultimaker 2 system, is that there exist an associated open source maker community. The community provides valuable input on hacks, materials, error sourcing and improvements.

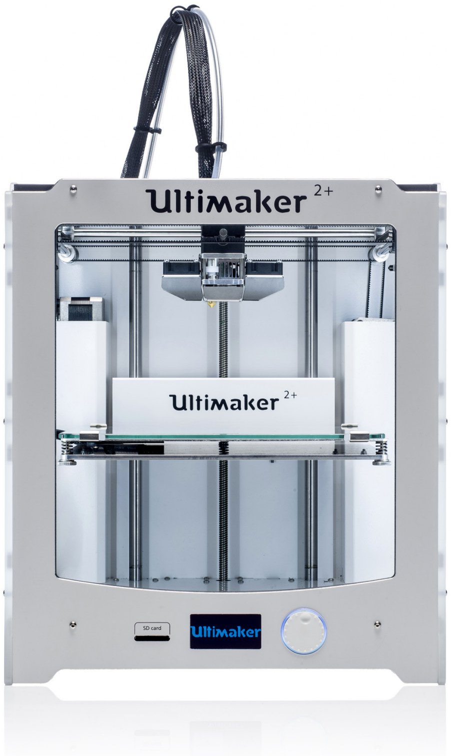

Figure 27: The Ultimaker 2+ 3D printer. Photo courtesy of Ultimaker.

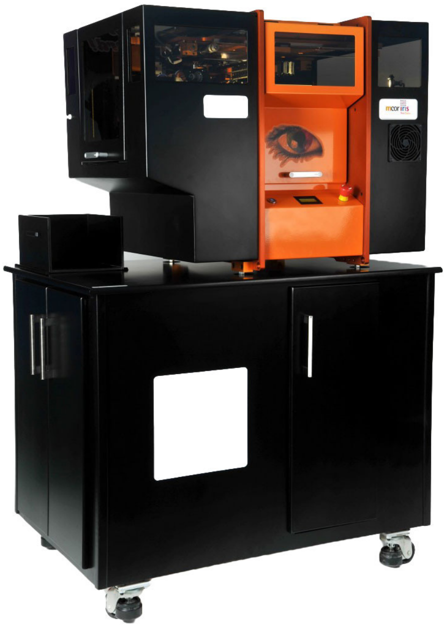

Figure 28: The MCOR Iris 3D-printer. Photo courtesy of MCOR Technologies.

MCOR Iris paper 3D-printer

The MCOR Iris is a laminated object manufacturing system, and utilizes normal office paper (A4-sheets) as print material. The sheets of paper are first pulled in from a stack, and then glued together automatically using a water based, biodegradable glue. The layer cross section is cut using a CNC-controlled knife. In addition to being untraditional in terms of build material, it offers three-dimensional color printing. The MCOR Iris also comes with a dedicated slicer software called SliceIT. The MCOR Iris 3D-printer is shown in figure 28.

The build size is slightly less than a standard A4-sheet, namely 256x169x150mm. It has a resolution of 0.012 mm in the X- and Y-directions, and 0.1 mm in Z-direction (which is also the layer thickness).

The parts produced at the MCOR Iris normally require some post processing. First, the geometry must be freed from its body of support material manually. After this, some finishing like sanding or painting is usually required for a good finish.

Chapter Five

Probing

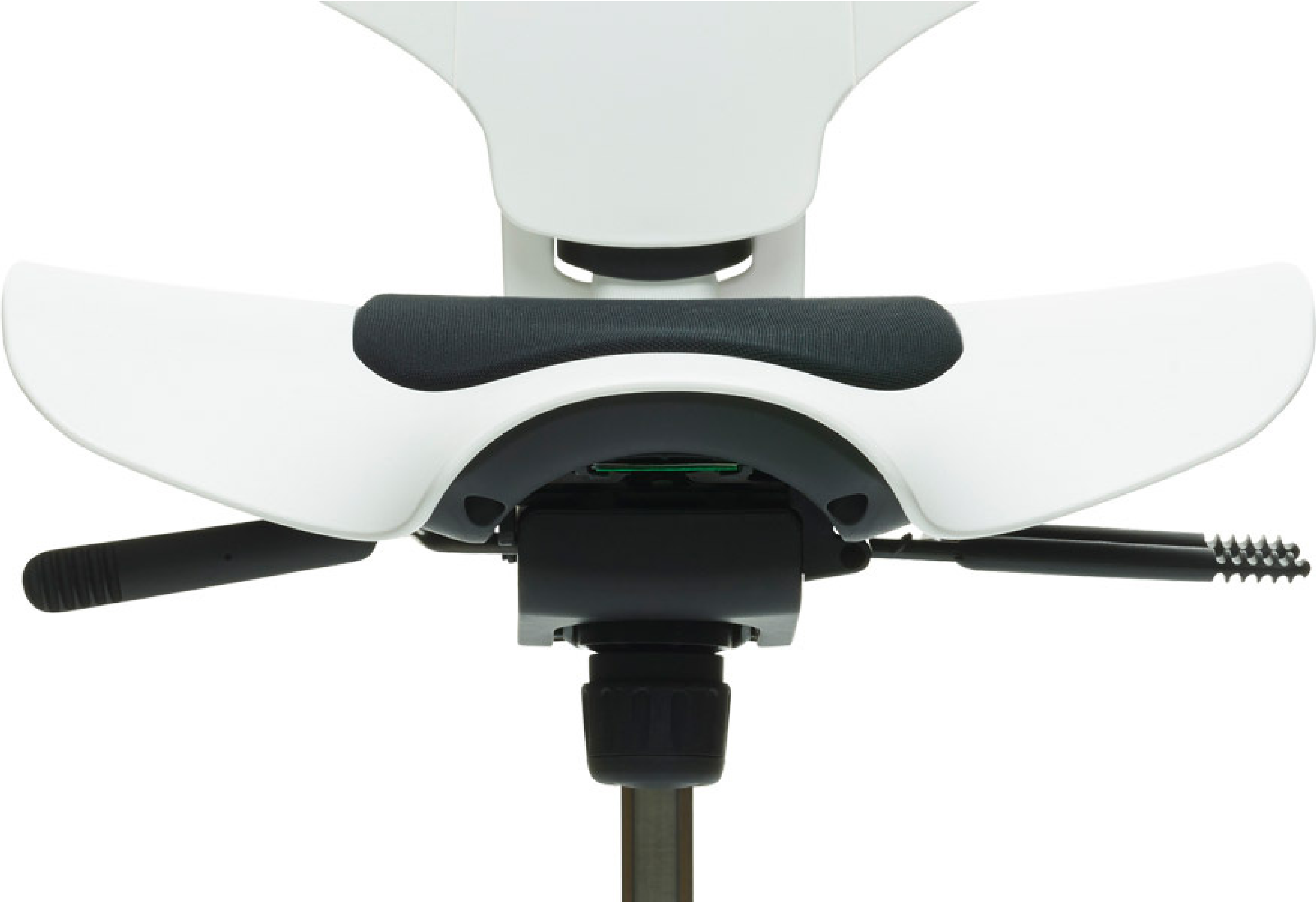

Figure 29: The test component was a handle from the Håg Capisco Pulse chair, as displayed above. Photo courtesy of SBS.

Introduction

In order to test which mold materials that would be suited for direct rapid tooling, several experiments were conducted. The experimental work was done in probes, or rounds of design-build-test. The learnings from each round contributed to the set up for the next round. The intention was to test many molds quick and cheap.

The Test Component

A handle from the Håg Capisco Pulse was selected as a suitable test component due to its small size and semi-complex geometry. A simple mold was modelled in Siemens NX 9. Figure 29 shows the test component, while figure 30 shows the mold.

The Set Up

For the set up, the TrollLabs Rapid Prototyping Injection Molder was utilized to inject a polymer melt. The mold was placed inside a mechanical clamp, and pushed up towards the nozzle to provide good mating. A table fan was utilized to provide cooling for the electronics of the injection molder. The set up is shown in figure 31.

Materials

Table 1 gives an overview over the materials included in the experiments and some of their properties. Please note that the given values are approximate.

Material	Youngs Modulus [MPa]	Ultimate Tensile Strength [MPa]	Compressive Yield Strength [MPa]	Melting temperature [°C]	Glass transition temperature [°C]	Hardness*	Deflection temp at 0.45 MPa [°C]	Source
Polylactic Acid (PLA)	3500	50	94**	160	60	59-77 D	65	http://www.makeitfrom.com/material-properties/Polylactic-Acid-PLA-Polylactide/ Feb 22nd 2016.
Red Oak	12549	-	46	-	-	5738 J	.	http://www.sonoking.com/american-hardwoods-redoak.php Feb 24th 2016
Paper	-	25 - 30	-	-	-	-	-	http://www.paperonweb.com/paperpro.htm Feb 24th 2016
AA 6082-T6 Aluminum	70000	310	-	591 - 638	-	95 V	-	http://www.matweb.com/search/DataSheet.aspx?MatGUID=fad29be6e64d4e95a241690f1f6e1eb7 Mar 29th 2016
VeroBlackPlus (RGD875)	2500	58	-	-	52 - 54	85 D	48	http://usglobalimages.stratasys.com/Main/Files/Material_Spec_Sheets/MSS_PJ_ May 12th 2016 PJMaterialsDataSheet.pdf?v=635785205440671440
Monochrome White	-	-	-	-	-	-	-	No data available
High density polyurethane (HDPU) foam (density: 650 kg/m^3)	614	16	28	-	85	63 D	-	http://www.axson-technologies.com/sites/default/files/TDS%20-%20Prolab%2065%20-%20Rev%20US-04_0.pdf Feb 24th 2016
West Systems 105 epoxy	3200	50	80	-	52	83 D	50	http://www.westsystem.com/ss/assets/Product-Data-PDFs/TDS%20105_206.pdf Feb 24th 2016
Polypropylene	1600	32	45	160***		40 - 83 D	100***	Sælen (2012)
Alloy 910	503	56	-	210	82	-	-	http://www.taulman3d.com/alloy-910-spec.html May 12th 2016
Acrylonitrile butadiene styrene (ABS)	2000	40	49**	252	108	107 R	95	https://static.webshopapp.com/shops/021593/files/045088826/tds-abspro.pdf?_ga=1.95978524.1421237610.1464348636

Table 1: Materials used in the experiments and associated material properties.
*Hardness tests: “D - Shore Hardness”, “V - Vicker’s Hardness”, “J - Newtons in Janka Hardness”, “R - Rockwell Hardness”.
** http://2015.igem.org/wiki/images/2/24/CamJIC-Specs-Strength.pdf
*** http://www.matweb.com/reference/deflection-temperature

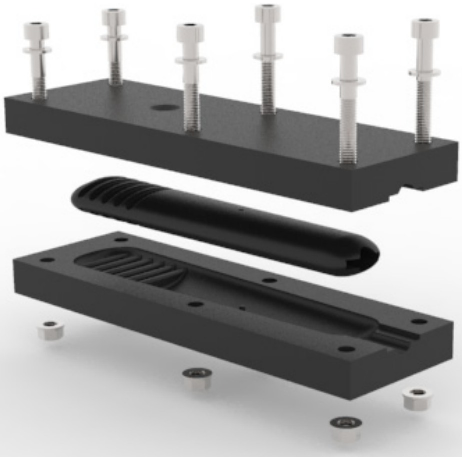

Figure 30: The test component and the mold.

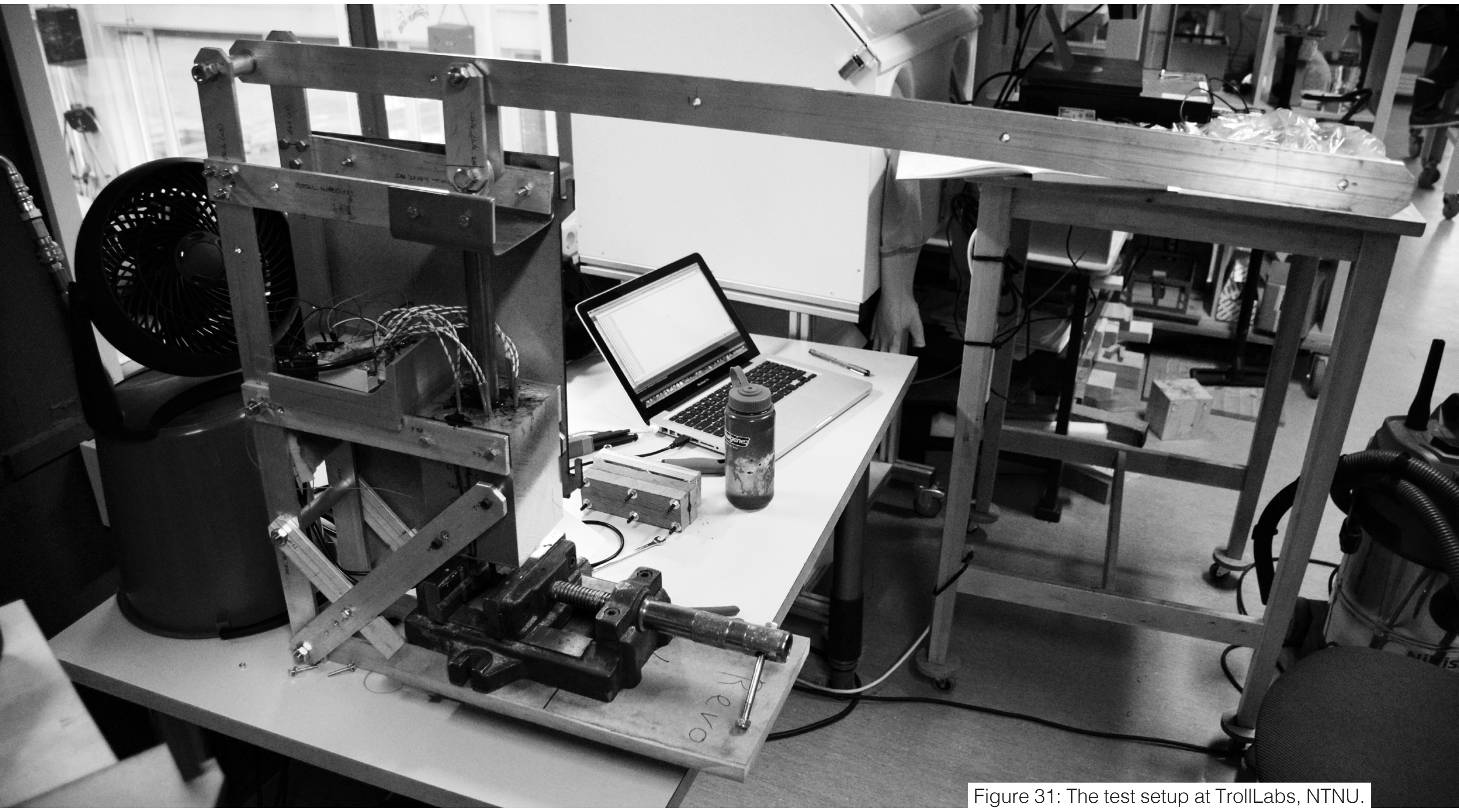

Figure 31: The test setup at TrollLabs, NTNU.

Round One: Getting Started

Design

The first probe included four different molds. They were Green PLA, Wood, Epoxy-Wood and Aluminum filled PLA. A chopped up black PLA FDM 3D-printer filament was used as the injection molding material. PLA has a melting temperature of 160 ° C (see table 1).

Build

Mold Name	Material	Rapid Prototyping Machine	Coating
Green PLA	PLA	Ultimaker 2	No
Wood	Red Oak	Roland MDX-540	No
Epoxy-Wood	Red Oak	Roland MDX-540	West Systems 105 Epoxy
Aluminum Filled PLA	PLA-aluminum	Ultimaker 2	No

Table 2: The techniques tested in round one.

The first batch of molds were built using the rapid prototyping machinery listed in table 2. The Green PLA-mold and the Aluminum Filled PLA mold were manufactured on the Ultimaker 2, using a fill density of 20%, a layer height of 0.06 mm, shell thickness of 0.8 mm and a print speed of 50 mm/s. A brim was used to ensure good adhesion to the build plate. The build plate temperature was 40 ° C, and the nozzle temperature 220 ° C.

Two wood molds were milled on the Roland MDX-540, with “hard wood” cutting settings. One of the wooden molds were coated with West systems 105 epoxy system, including a 105 resin and a 206 slow hardener. The mixing ratio was five parts resin to one part hardener. The mixed epoxy was then left in a degassing chamber for 10 minutes to extract bubbles. Finally, the epoxy was distributed over the mold surface using a paintbrush and a glove. The epoxy was left to cure in room temperature for 24 hours.

Mold Name	Injection Material	Injection Temperature [°C]	Result
Green PLA	Black PLA	230	Did not fill cavity. Mold is reusable.
Wood	Black PLA	230	First attempt: Core was included. Did not fill cavity. Second attempt: Removed core. Cavity was filled good. OK finish.
Epoxy-Wood	Black PLA	230	Did not fill cavity. Mold is reusable.
Aluminum filled PLA	Black PLA	210	Resin adhered to the mold. Mold is not reusable.

Table 3: Results from round one.

Test

The chopped up black PLA plastic was inserted into the injection molder and melted for two minutes at an injection temperature. The temperature for each mold is given in table 3. The resin was then injected into the cavity. A core was initially included for all molds except the Aluminum Filled PLA. In a second attempt, the core was removed for the Wood mold.

For the first attempt, the resin failed to fill any of the molds. In the Green PLA mold, the resin stopped at the inlet. In the Wood and Wood-Epoxy molds, the resin stopped where the core started. The Aluminum Filled PLA mold was filled roughly 70%, but the resin adhered completely to the mold, and the part was unable to be ejected. For the second attempt, the core was removed for the wood mold. This time, the resin filled the cavity fine. Upon ejection, some fibers from the mold adhered to the part. However, most dimensions were preserved. The Wood and Aluminum Filled PLA molds are shown in figure 32.

Learnings

After preparing the first batch of molds, some learnings were made. Firstly, a thinner, less viscous, epoxy was better suited for coating. The thick Loctite Power epoxy would sometimes fill details in the mold, altering the shape of the molded component. Other learnings included that the Ultimaker 2 was slow and provided poor dimensional quality, whereas the Roland MDX-540 was robust and provided good dimensional quality.

Testing the first batch of molds revealed that one major principle of injection molding had been missed. The pressure must first push out the air that is trapped inside the cavity, before the resin can be injected. Because neither air channels nor ejector pins had been included in the design of the mold, the mold cavity now worked as an air spring. The initial idea was that the trapped air should be able to escape through the partitioning of the two mold halves. However, as the pressure supplied by the rapid prototyping injection molder was not sufficient for this purpose, the air ended up being trapped inside. After noticing this mistake, the core was removed, leaving an open end for the air to escape. In spite the fact that this would alter the initially planned geometry, it was deemed good enough for the purpose of testing mold materials.

On the material side, it was learned that a PLA resin in combination with a PLA mold was not a good combination. Not surprisingly will two materials with the same melting temperature adhere when exposed to temperatures above the melting point. Furthermore, it became obvious that the porous structure and low density of the Green PLA and Aluminum Filled PLA molds were less suited, as the covering shell was easily melted.

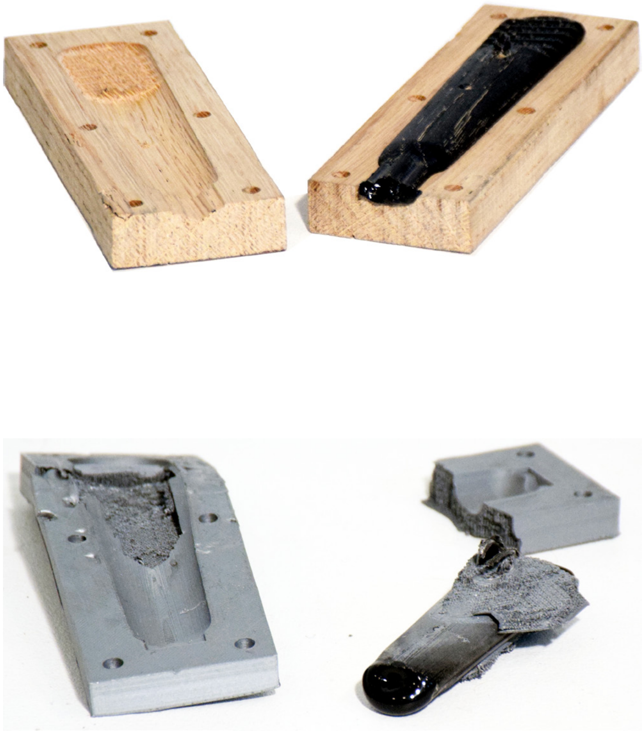

Figure 32: The results from the Wood mold (top) and Aluminum Filled PLA mold (bottom).

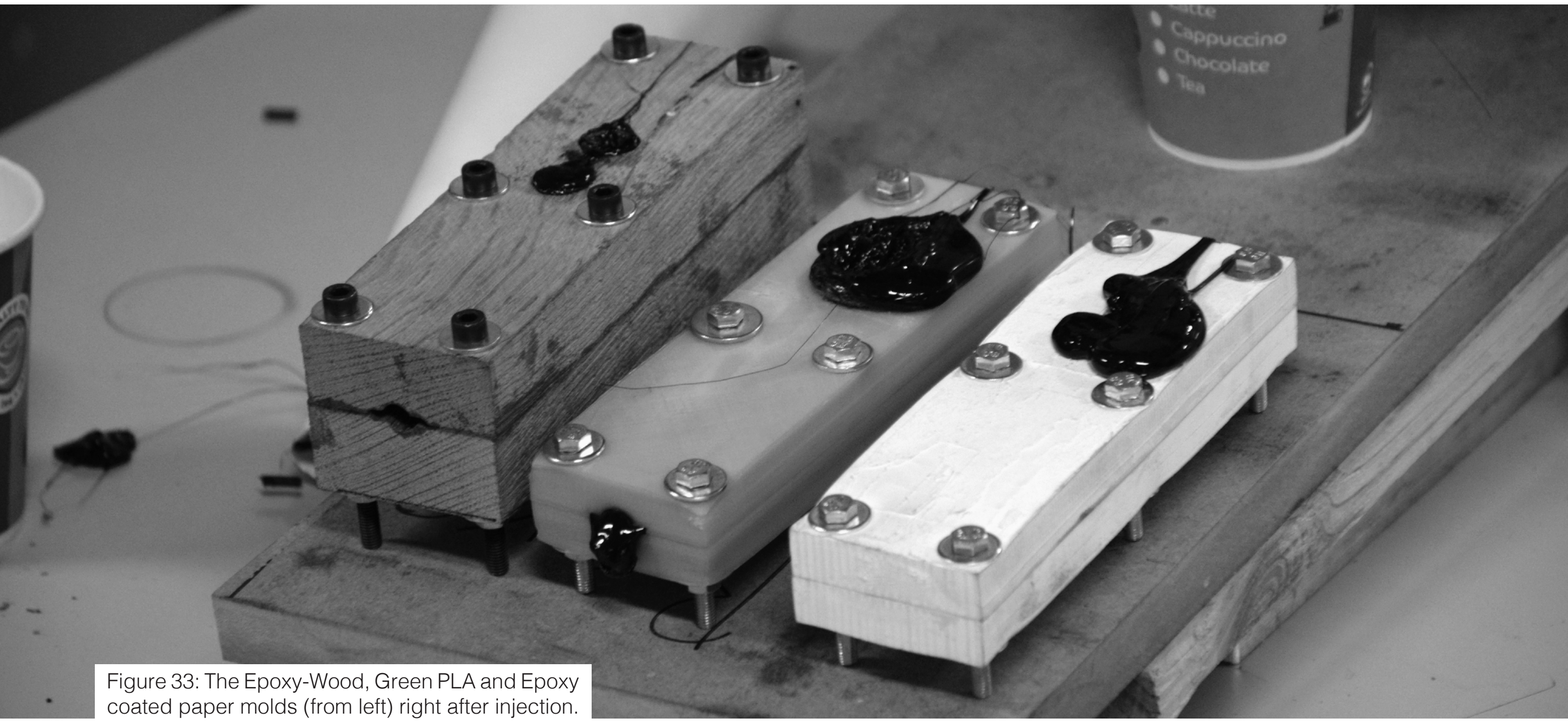

Figure 33: The Epoxy-Wood, Green PLA and Epoxy coated paper molds (from left) right after injection.

Round Two: Learning

Design

The second probe included three molds. The Wood-Epoxy and Green PLA molds from round one were reused. Additionally, an epoxy coated paper mold was included. The injection material was still chopped up black PLA 3D-printer filament with a melting temperature of 160 °C.

Build

Mold Name	Material	Rapid Prototyping Machine	Coating
Green PLA	PLA	Ultimaker 2	No
Epoxy-Wood	Red Oak	Roland MDX-540	West Systems 105 Epoxy
Epoxy Coated paper	Paper	Mcor IRIS	Loctite Power Epoxy (extra time)

Table 4: The techniques tested in round two.

The Green PLA and Epoxy-Wood molds were made as described in round one. The paper mold was manufactured on the Mcor IRIS machine. The part was raised 1 mm from the build plate. All other settings were default. The part was then freed from the support material manually. The mold was finally coated with Loctite Power Epoxy Extra Time. The mixing ratio was 1:1, and the part was left to cure in room temperature for 24 hours.

Test

The chopped up black PLA material was inserted into the injection molder and melted at 230 °C for two minutes. On the fourth try of the epoxy-wood mold, the PLA material was melted at 230 °C for 10 minutes. No cores were used. In figure 33, the tested molds are shown right after injection.

For the Green PLA mold, the resin adhered completely to the mold. Consequently, the resin did not fill the cavity, nor was it possible to eject the part. For the Epoxy Coated Paper mold, the resin was successfully injected into the cavity on the second attempt. However, the part broke as it was ejected. Several voids were observed on the surface of the molded geometry. For the Epoxy-Wood mold, neither of the first three attempts succeeded on injecting material. On the fourth attempt, the melting time was increased to ten minutes. This time, the resin filled 90% of the cavity. Similar to the part from the epoxy coated paper mold, this part also broke upon ejection. Many voids were observed on the surface. The results from round two are displayed in figure 34.

Mold Name	Injection Material	Injection Temperature [°C]	Result
Green PLA	Black PLA	230	Resin adhered to the mold. Ejection was impossible.
Epoxy-Wood	Black PLA	230	First three attempts: cavity was not filled. Fourth try: cavity was filled to some degree.
Epoxy Coated Paper	Black PLA	230	First try: cavity was not filled. Second try: cavity was filled fine. The molded part broke upon ejection.

Table 5: Results from round two.

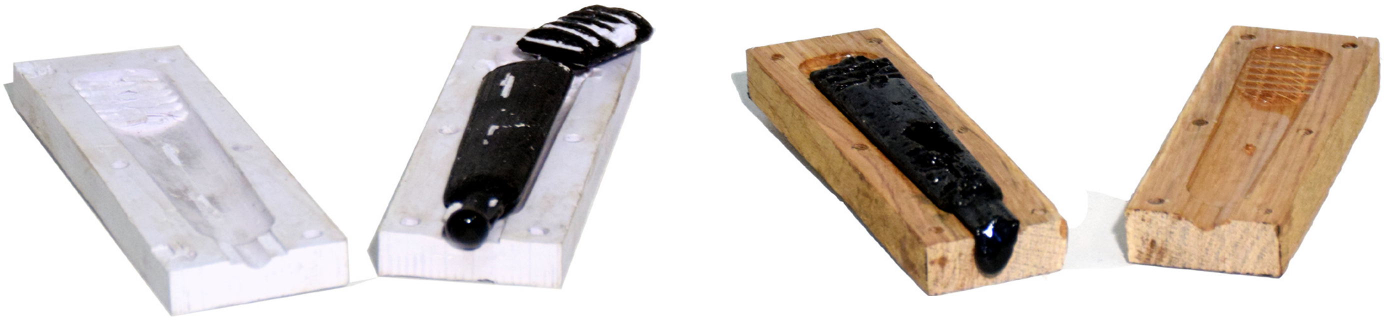

Figure 34: Results from the Epoxy coated paper (top left), Epoxy-Wood (top right) and Green PLA (below) molds.

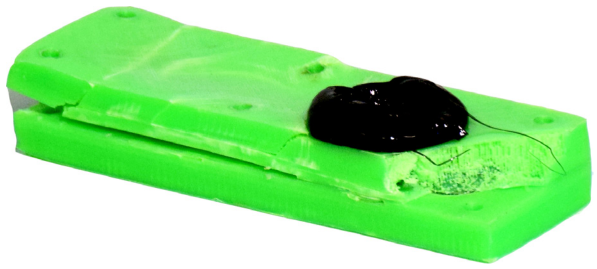

Learnings

Because expectations were high for the epoxy-wood mold, it was found strange that it did not fill the cavity at all. It was therefore suspected that the resin was not fully melted as it was injected into the cavity. As a countermeasure, the melting time of the resin was increased from two to ten minutes. After this, the injection of the resin was easier, and roughly 90% of the cavity was filled.

Furthermore, it was learned from the Epoxy Coated Paper and Epoxy-Wood molds that easy ejection of the molded part is critical. In order to reduce friction, it was decided that some sort of release agent should be applied as a next move. Additionally, it was desirable to test the epoxy coated paper mold with a thinner epoxy, as this would provide a smoother surface.

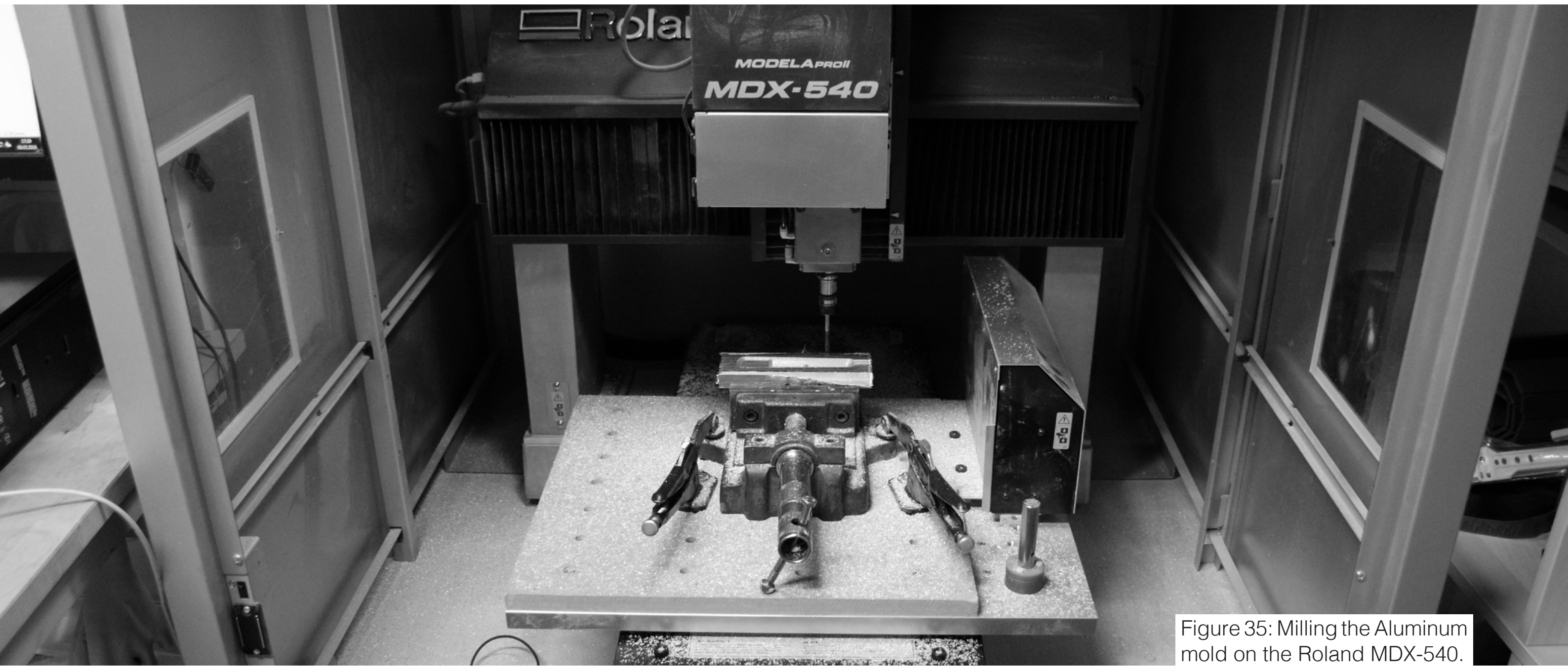

Figure 35: Milling the Aluminum mold on the Roland MDX-540.

Round Three: Succeeding

Design

In the third probing, a new batch of molds was made. The batch consisted of epoxy coated wood, epoxy coated paper, epoxy coated high density polyurethane (HDPU) foam and aluminum. The Aluminum mold was included as a reference. In this round, pellets of black polypropylene were used as injection molding material. Polypropylene has a melting temperature of 160 °C (see table 1). Also, a release wax, Renlease QV5110, was applied to reduce friction.

Build

Mold Name	Material	Rapid Prototyping Machine	Coating
HDPU foam	HDPU foam	Roland MDX-540	West systems 105 epoxy. Renlease QV5110 release agent.
Epoxy-Wood	Red Oak	Roland MDX-540	West systems 105 epoxy. Renlease QV5110 release agent.
Aluminum	AA 6082-T6	Roland MDX-540	Renlease QV5110 release agent.
Epoxy Coated Paper	Paper	Mcor IRIS	West systems 105 epoxy.

Table 6: The techniques tested in round three.

The HDPU foam mold was milled on the Roland MDX-540 CNC-mill. The cutting settings were “foam”, except from the roughing cut depth which was modified to 2 mm. A West systems epoxy was made using 105 resin, and 205 slow hardener. The resin to hardener ratio was 5:1. After mixing, the epoxy was left in a degassing chamber for ten minutes to extract bubbles. The surface of the mold was sealed with the mixed epoxy, and left to cure for 24 hours in room temperature. Finally, a Renlease QV5110 release agent was applied.

The Epoxy-Wood mold was manufactured as described in round one. Additionally, the surface of the mold was coated with Renlease QV5110 release agent.

The Aluminum mold was milled on the Roland MDX-540 using “aluminum” cutting settings (see figure 35). Renlease QV5110 release agent was applied.

The Epoxy Coated Paper mold was manufactured on the Mcor Iris 3D-printer. The surface was coated with the West Systems 105 epoxy system, using the same approach as for HDPU foam. No release agent was applied.

Mold Name	Injection Material	Injection Temperature [°C]	Result
HDPU foam	Polypropylene	230	Filled cavity great. Some shrinkage after freezing. Easy to eject. Some pores on surface.
Epoxy-Wood	Polypropylene	230	Filled cavity great. Good surface finish. Easy to eject.
Aluminum	Polypropylene	230	First try did not fill cavity. Second and third attempts filled cavity well. For these, a smooth, but wavy surface finish was achieved. Easy to eject.
Epoxy Coated Paper	Polypropylene	220	Filled cavity great. Some flash present. Slightly porous surface. Ok to eject. Mold was not reusable.

Table 7: Results from round three.

Test

The polypropylene pellets were poured into the injection molder and heated for ten minutes at 230 °C, before it was injected into the cavity. Additionally, the Aluminum mold was heated with a heat gun prior to injection on the second and third attempts.

All tests finally provided good results. The HDPU foam filled the cavity great and was easy to eject. Although some shrinkage and pores were present, the surface finish was generally good. This time, the Epoxy-Wood mold was completely filled and was easy to eject. The surface quality was good. The Epoxy Coated Paper mold was also completely filled. However, it was slightly more difficult to eject, and some paper residue was present on the surface of the molded geometry. The mold could not be reused. For the first attempt of the aluminum mold, the resin was injected into a room tempered aluminum mold. This time, the resin did not fill the cavity, as it froze soon after it was injected. For the second and third attempts, the aluminum mold was pre-heated with a heat gun. This time, the resin filled the cavity great. The parts were easy to eject. Although some patterns were present on the surface of the molded geometry, the finish was generally good. The results are displayed in table 7 and figure 36.

Learnings

Finally, all test provided good results. Some critical elements for achieving this were:

- A high enough injection temperature, of 230 °C.
- A long enough melting time, of at least ten minutes.
- A hard and smooth mold surface coated with a release agent.
- Air channels to allow the air to escape.

The Aluminum mold was included in this round as a reference. Although injection went smoothly after some testing, the surface was not perfect, as some flow lines were present. It is therefore likely that the injection pressure or mold temperature was not constant during the molding. In order to further improve the quality of the molded parts, it is reasonable to believe improvements should be made to the injection molder.

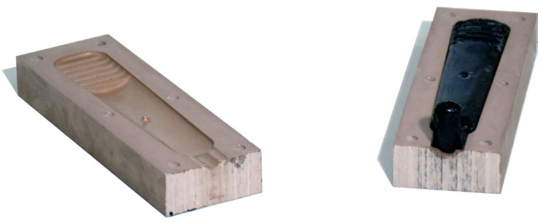

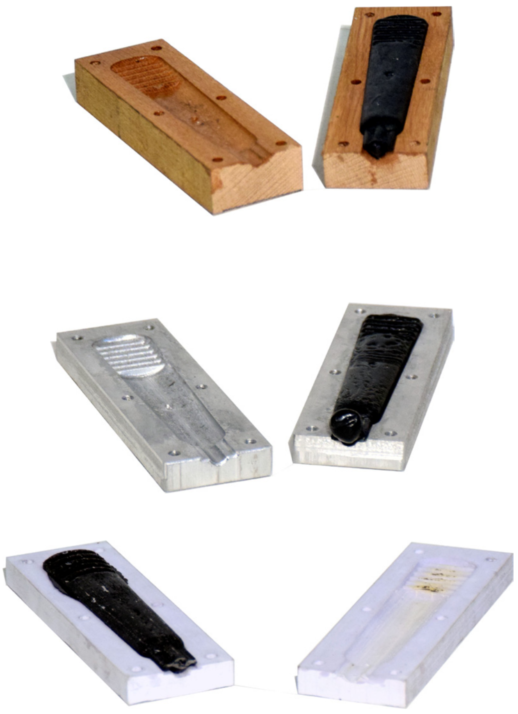

Figure 36: Results from round three. Above: HDPU foam. Right top: Epoxy-Wood. Right middle: Aluminum. Right bottom: Epoxy coated paper.

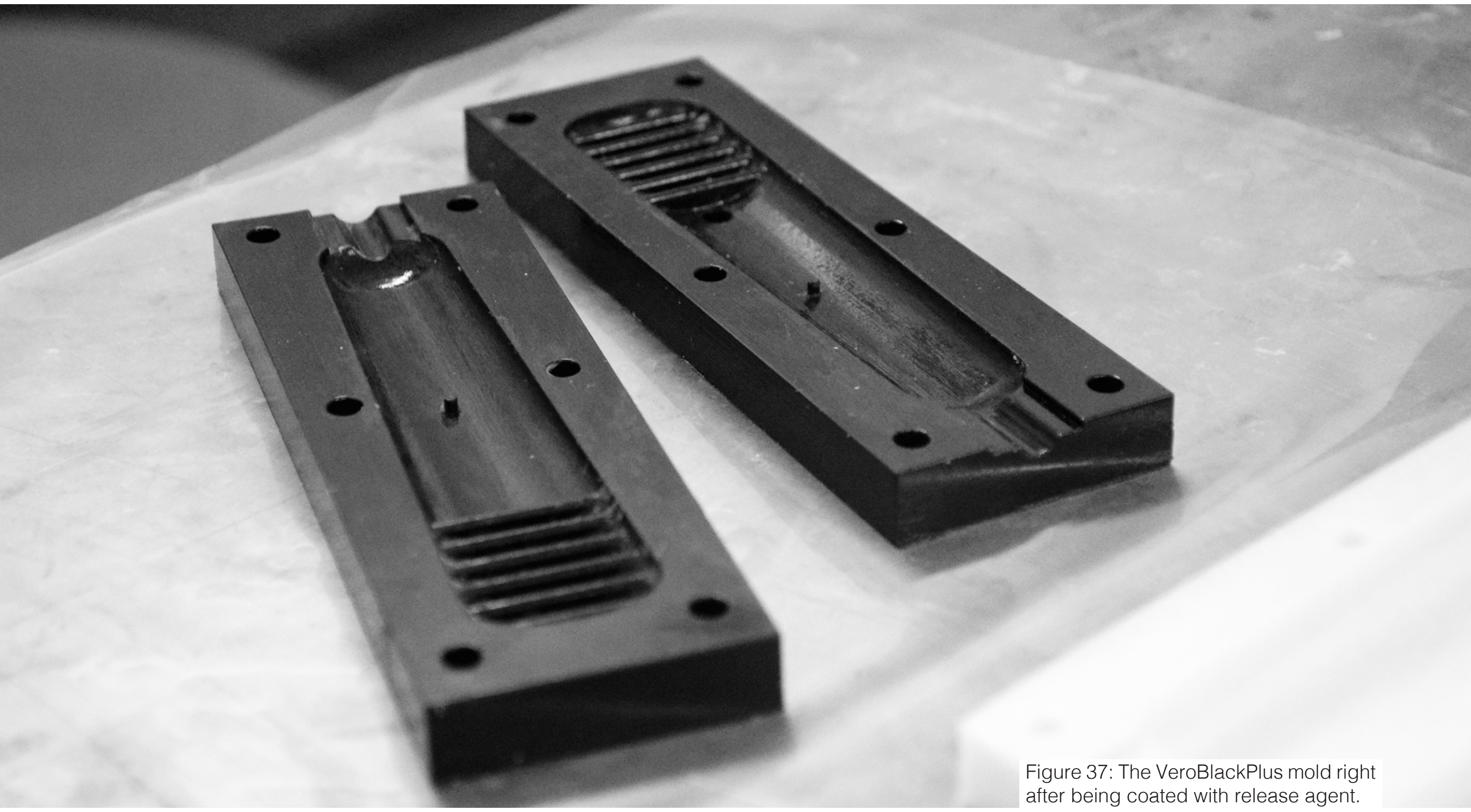

Figure 37: The VeroBlackPlus mold right after being coated with release agent.

Round Four: Additive Manufacturing

Design

Because the CNC-milled molds had dominated the probing so far, the focus was now on 3D-printed molds. In the fourth probing, three new mold materials were tested. These were Alloy 910, VeroBlackPlus and Monochrome White. Additionally, the HDPU foam mold was re-tested. The injection molding material was black polypropylene pellets. The molds were coated with Renlease QV5110 release agent (see figure 37).

Build

Mold Name	Material	Rapid Prototyping Machine	Coating
Alloy 910	Alloy 910	Ultimaker 2	Renlease QV5110 release agent.
Monochrome White	Monochrome White	Blueprinter	Renlease QV5110 release agent.
VeroBlackPlus	VeroBlackPlus	Objet 250	Renlease QV5110 release agent.
HDPU foam	HDPU foam	Roland MDX-540	West systems 105 epoxy. Renlease QV5110 release agent.

Table 8: The techniques tested in round four.

The Alloy 910 mold was manufactured on the Ultimaker 2 3D-printer. The layer height was 0.06 mm, the shell thickness 0.8 mm, the bottom and top thicknesses 0.6 mm, and the fill density 20%. The print speed was 50 mm/s. A brim was used in combination with glue to provide adhesion. The build plate temperature was 90 ° C, and the nozzle temperature 245 ° C. After printing, the part was coated with Renlease QV5110 release agent.

The Monochrome White mold was manufactured on the Blueprinter with standard settings. The VeroBlackPlus mold was manufactured at CMR Prototech on the Objet 250 with high quality glossy finish settings. It was oriented in the 3D-space so that the cavity surface was facing upwards. No support material was needed. The HDPU foam mold from round three was re-used.

Mold Name	Injection Material	Injection Temperature [^{o}C]	Result
Alloy 910	Polypropylene	230	Filled cavity great. Some shrinkage after freezing. Easy to eject. Some pores on surface.
Monochrome White	Polypropylene	230	Did not fill cavity completely due to too little resin in the molder. Mold melted.
VeroBLackPlus	Polypropylene	230	First attempt: Did not fill. Second attempt: Filled cavity great. Superb surface finish.
HDPU foam	Polypropylene	220	Filled cavity great. Some pores present, but otherwise good finish. Some shrinkage. Ok to eject. Mold is reusable.

Table 9: Results from round four.

Test

The black polypropylene was poured into the injection molder and melted at 230 ° C. For the first attempt of the VeroBlackPlus-mold, the melting time was five minutes. For the remaining moldings, the melting time was ten minutes.

For the Alloy 910 mold, the cavity was filled great and the part was easy to eject. Because the surface of the mold cavity was not smooth, neither was the surface of the molded part. However, few pores were present. Some shrinkage was observed. The mold was reusable, although some marks from the nozzle were present. The testing of the Monochrome White mold partly failed due to too little resin in the injection chamber. However, 50 % of the cavity was filled. Unfortunately, the mold melted as the hot resin made contact. The VeroBlackPlus-mold gave by far the best surface finish of the test. For the first attempt, the cavity was not filled. On the second attempt, the cavity was filled easy, and the part was easy to eject. The mold showed little wear and was reusable. The molded part had a great surface finish and good dimensions. The HDPU foam mold provided roughly the same result as in round three. The cavity was filled easily, and the part was easy to eject. The mold showed little wear, and was reusable. The part had some shrinkage, and some pores, but otherwise good quality. Results from round four are shown in table 9 and figure 38.

Learnings

Because of the poor results from round one, expectations were not very high for the additive manufactured molds. However, this round showed that these molds indeed could provide good quality. From testing the Alloy 910 mold, it is likely that a mold material with a slightly higher melting point than the resin is enough to provide a successful molding. The Alloy 910 has a melting temperature of 210 ° C, while polypropylene has a melting temperature of only 160 ° C. The molding was successful even though the fill density of the Alloy 910 mold was only 20 %. However, the shell thickness was increased slightly compared to the PLA molds tested in round one.

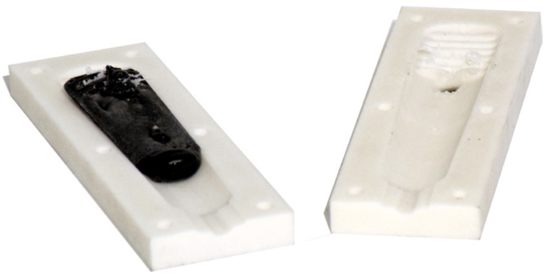

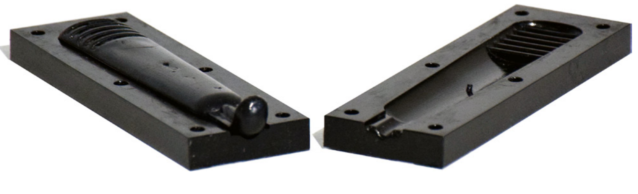

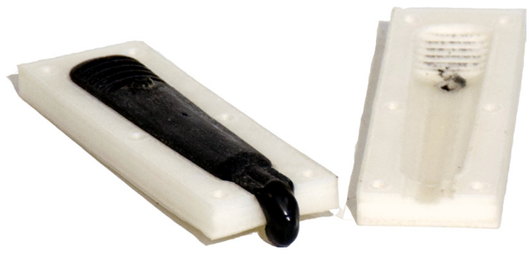

Figure 38: The VeroBlackPlus mold (left) provided good results. The Monochrome White mold (top right) melted upon injection. The Alloy 910 mold (bottom right) also provided satisfactory results.

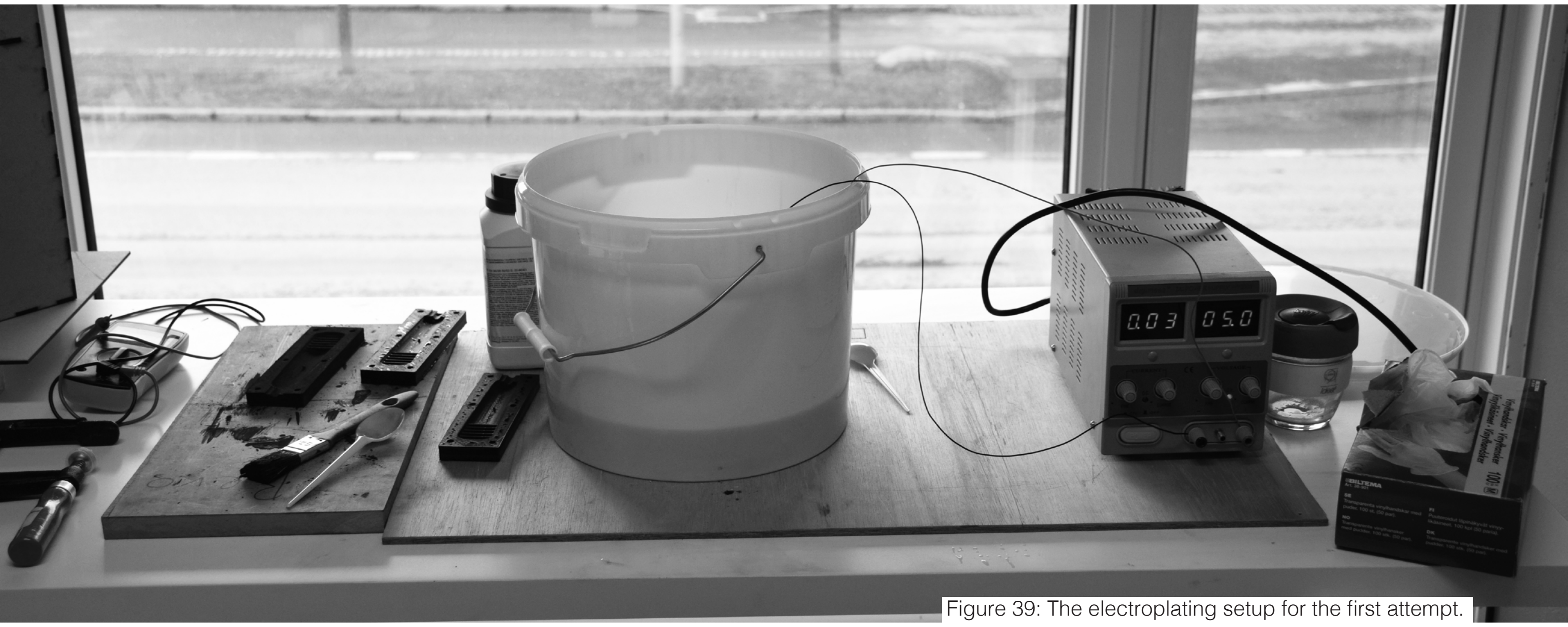

Figure 39: The electroplating setup for the first attempt.

Round Five: Failing at Electroplating

Design

For the fifth round of probing, the challenge was to electroplate plastic components. An experimental test setup was built for electrolysis, and four mold halves were attempted to be electroplated. Three mold halves were made from ABS-plastic, and one from conductive PLA filament. Conductive PLA is an electrically conductive PLA filament for fused deposition modeling. According to the supplier (Proto-pasta, 2016), a printed part will have a volume resistivity of 30 ohm-cm perpendicular to the layers, and 115 ohm-cm through the layers (along z-axis).

Build

Mold Name	Material	Rapid Prototyping Machine	Coating
ABS-copper	ABS plastic	Ultimaker 2	Copper plating
Conductive PLA	Conductive PLA from Proto-pasta	Ultimaker 2	Copper plating

Table 8: The techniques tested in round four.

The ABS- and Conductive PLA molds were manufactured on the Ultimaker 2, using a fill density of 20%, a layer height of 0.06 mm, shell thickness of 0.8 mm and a print speed of 50 mm/s. A brim was used to ensure good adhesion to the build plate. For the ABS mold, the build plate temperature was 90 degrees celsius, and the nozzle temperature 260 degrees celsius. For the Conductive PLA mold, the build plate temperature was 40 degrees celsius, and the nozzle temperature 220 degrees celsius.

In order to make the surface of the ABS-molds electrically conductive, a blend of West Systems Graphite Powder and VWR Chemicals technical acetone (UN1090) was mixed. The blend was mixed so that it had a watery consistency. The mix was then painted onto the ABS molds using a brush and left to dry for a few minutes. The electrical conductivity was checked with a multimeter, and was measured to 1.5 ohms.

For the first attempt, two tablespoons of $CuSO_4 \bullet 5 H_20$ were mixed in 1 liter of water in a plastic bucket. The negative pole of a direct current (DC) source was attached with alligator clips to the painted ABS mold half, and submerged in the $CuSO_4$-solution. The positive pole was attached to a piece of copper and submerged. The setup is shown in figure 39. The DC power source was set to 5 V, and left to run for eight hours.

For the second attempt, the concentration of $CuSO_4 \bullet 5 H_20$ was increased to ten tablespoons per one liter of water. Furthermore, the plastic bucket was changed to a chemically inert glass bowl (see figure 41). The piece of copper was replaced by a copper pipe with a larger surface area. The voltage was set to 1.5 V and left for eight hours.

For the third attempt, the alligator clips were raised above the water line.

For the fourth attempt, the conductive PLA-mold was tested using a concentration of 10 tablespoons per liter water, a voltage of 5V and left for six hours.

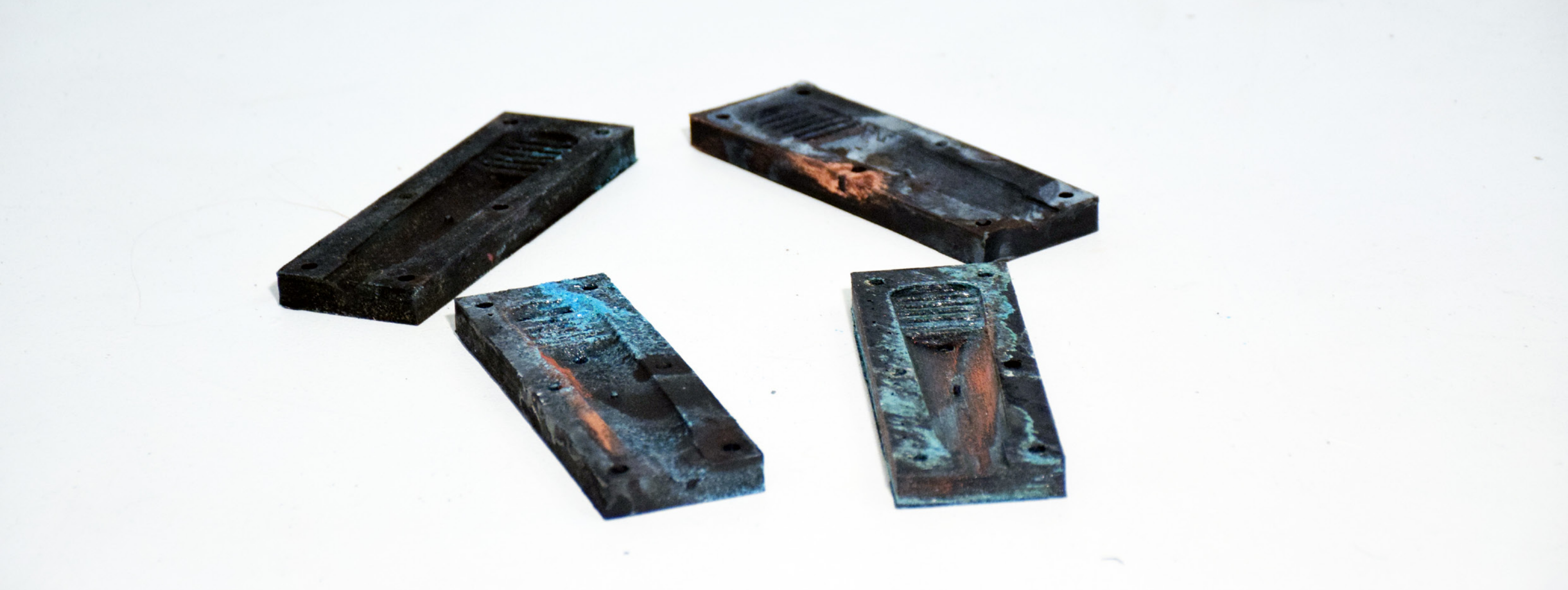

Figure 40: Results from the electroplating.

Test

Unfortunately, none of the plating attempts provided any useful molds (see figure 40). For all molds, some electrodeposition was observed on the cathode, especially around the alligator clip. However, none provided enough plating to alter the hardness of the surface.

For reference, a coin was plated using the exact same setup as in the third attempt, except that the mold half was replaced by a coin. This provided good results, as the coin was fully plated within a matter of minutes.

Learnings

Due to the reference experiment of the coin, it is likely that the 3D-printed mold halves were not electrically conductive enough. This may have been caused by inaccurate coating for the ABS molds. Because of the failed attempts, success of the method using this setup was judged unlikely.

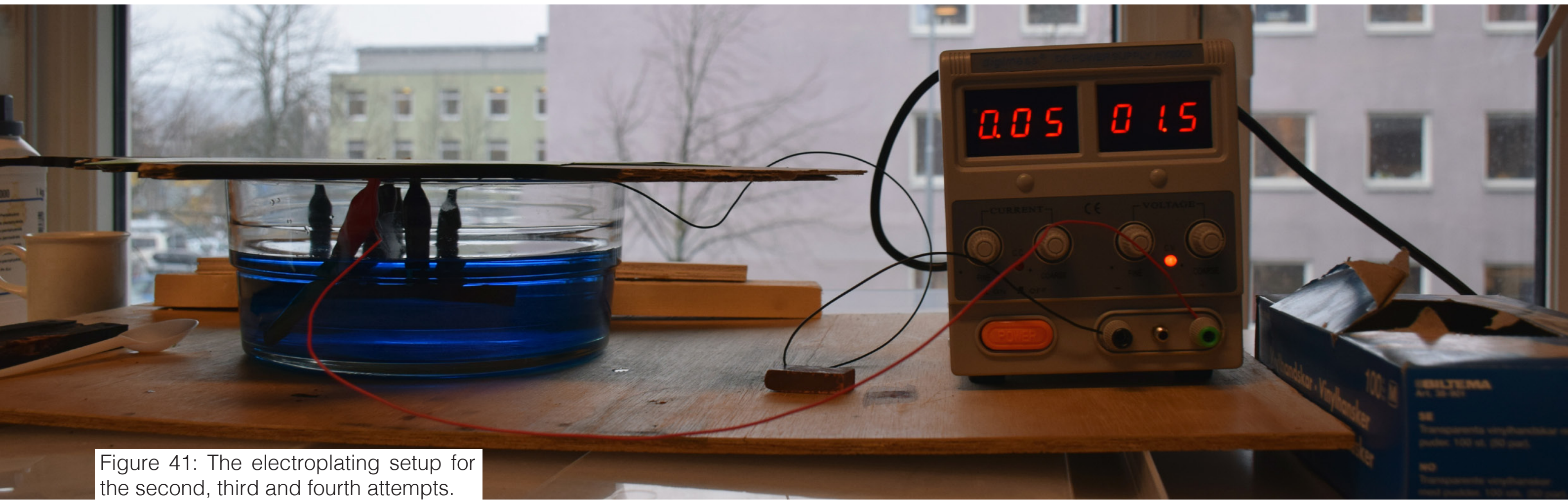

Figure 41: The electroplating setup for the second, third and fourth attempts.

Chapter Six

Three Point Bending Test

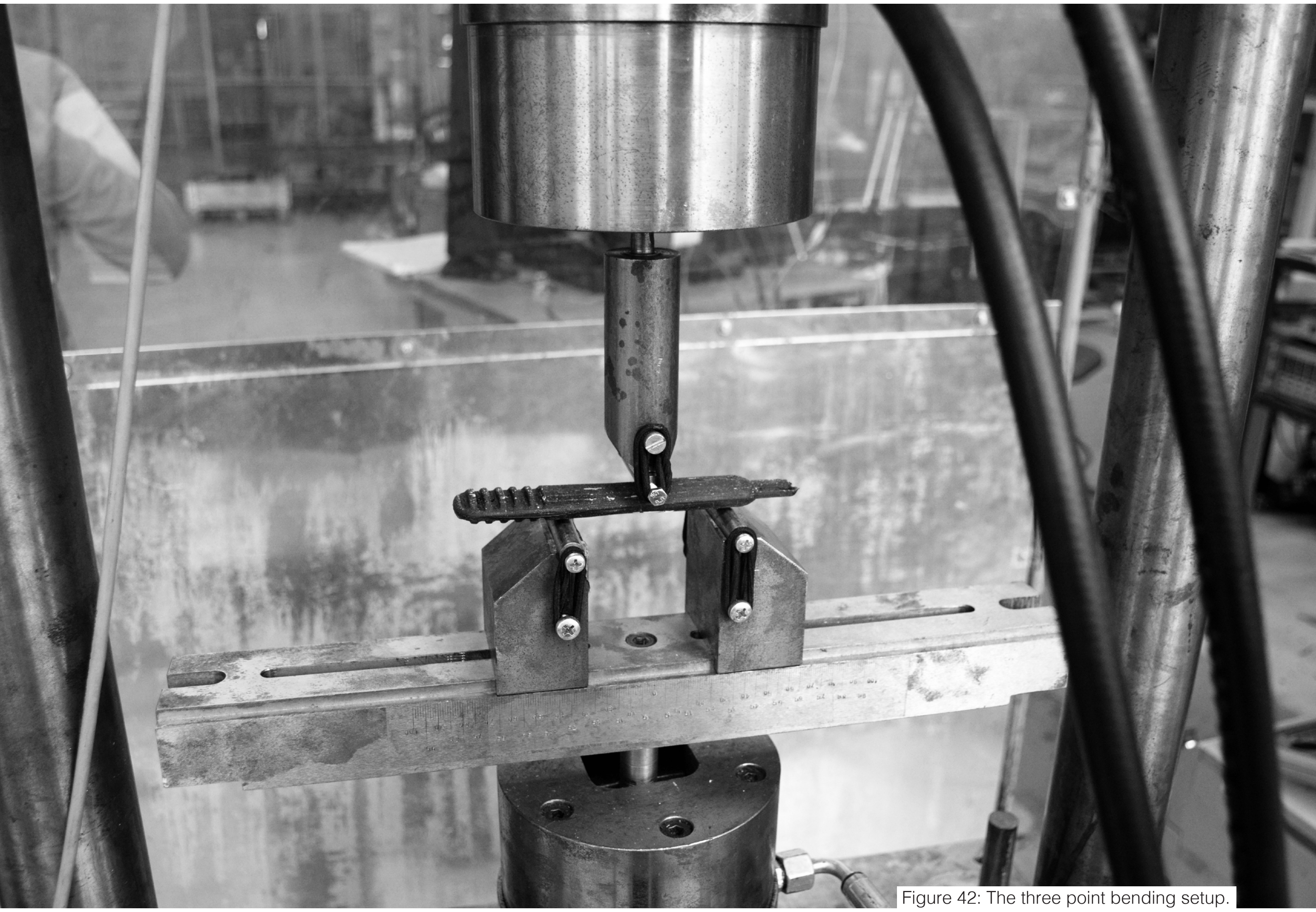

Figure 42: The three point bending setup.

Introduction

The initial motivation behind prototyping injection molded components using direct rapid tooling was to obtain data on their mechanical behavior. A mechanical test was therefore included to give a quantitative measure of the structural quality of the molded components, as well as demonstrating how a mechanical test can be used in prototyping. In this chapter, the mechanical strength of the molded test components was tested in a three point bending setup. Additionally, a nonlinear structural finite element simulation was included to provide a benchmark of theoretical versus real performance.

Three Point Bending

Three point bending is a common materials test for testing flexural strength and stiffness of many materials. Procedures for testing flexural properties of plastic materials are described in ISO170 and ASTM D790. The setup is also commonly used to obtain data on fracture toughness of different materials, using crack tip opening displacement methods. However, because of the somewhat specialized geometry of the test specimens, the standard procedures are not applicable. The test setup for this specific test is shown in figure 42. The distance between the two lower supports was 70mm, and the diameter of the rods was 10 mm.

Predicting Results using FEA in ABAQUS CAE

Model

A standard explicit model was created in ABAQUS computer aided engineering (CAE). The test geometry was imported into ABAQUS from NX 9. Additionally, the testing rod was modeled in ABAQUS. The rod and test geometry were placed in an assembly as shown in figure 45.

Mesh

The test geometry was meshed using a tetrahedral mesh type. The pin was meshed with hexahedral mesh of size 0.9 mm. The tetrahedral and hexahedral meshes are shown in figure 43.

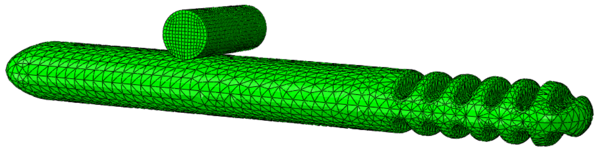

Figure 43: Mesh and assembly.

Materials

The pin was assigned with linear elastic isotropic steel properties. The modulus of elasticity was 210 000 MPa and the Poisson's ratio 0.3. The test geometry was assigned linear elastic and nonlinear plastic isotropic properties, to account for the nonlinear behaviour of polypropylene. The Von Mises yield criterion was utilized. The material data was based on tensile testing of polypropylene specimens performed by Sælen (2012). The Young's modulus was 1600 MPa, and the Poisson's ratio 0.38. Data for the plastic region is found in appendix F.

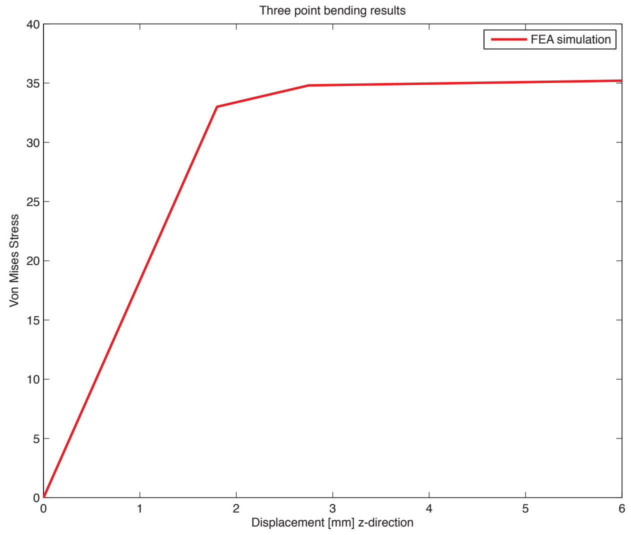

Figure 44: Von Mises stress (along y-axis) versus displacement in Z-direction (along x-axis).

Boundary Conditions

Interaction boundary constraints were given to the contact surfaces between the pin and the test geometry. The contact properties were frictionless tangential behaviour, and "hard" contact for normal behavior. Separation was allowed after contact.

The test geometry was constrained by the mid-plane in the X- and Y-directions. This prevented rigid body motion, and at the same time allowed for the body to expand due to Poisson's ratio effects. To represent the two lower pins, the lines shown in figure 45 were constrained in the Z-direction. The distance between the lines was 70 mm.

For the pin, one side was fixed in the X- and Y-directions. Additionally, an enforced displacement of 5.5 mm in the negative Z-direction was added. The enforced displacement was added to a general, static step. This loading does not account for viscoelastic or viscoplastic behavior.

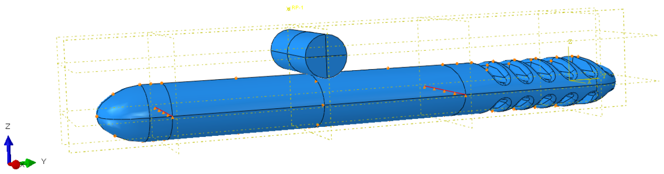

Figure 45: Boundary conditions in Z-direction.

Results

The nonlinear simulation showed that the test geometry should reach the ultimate tensile stress of 32 MPa (see table 1) after the pin have displaced about 2 mm (see figure 47). This was found by tracking the stress in a node on the opposite side of the rod throughout the loading. After this, the plastic region spreads throughout the top and bottom of the test geometry (see figure 46). There are compressive stresses at the top, and tensile stresses at the bottom. Figure 44 shows the load-displacement curve in the Z-direction. Please note that the finite element model does not account for failure modes such as fracture, and therefore showed theoretical results throughout the entire enforced displacement.

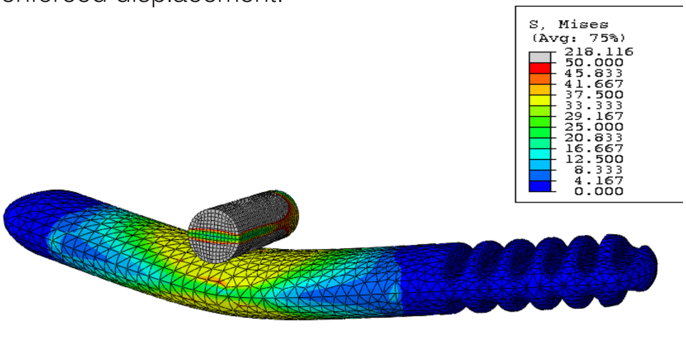

Figure 46: Results from the FEA.

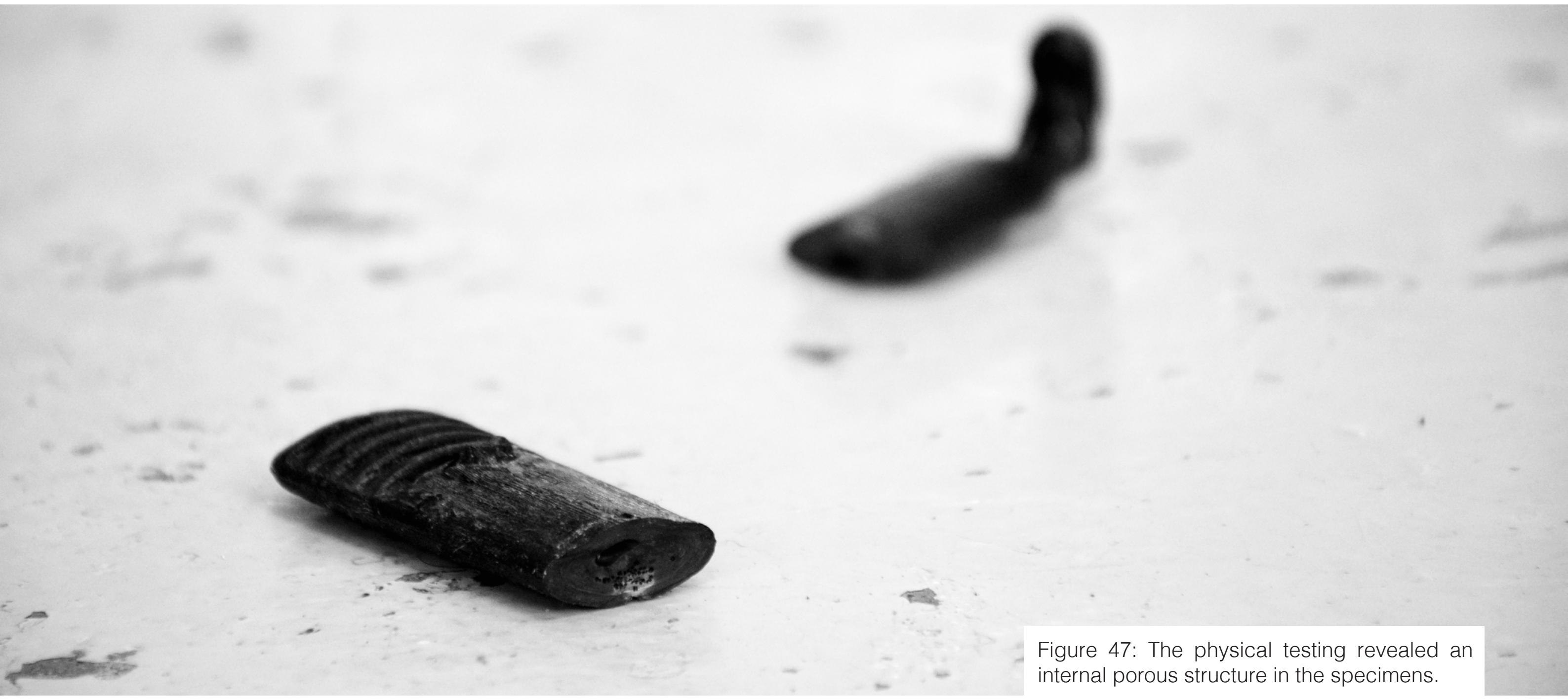

Figure 47: The physical testing revealed an internal porous structure in the specimens.

Physical Testing

The test geometry was tested in a Schenk 10kN tensile/compressive test machine. The setup is shown in figure 42. The diameter of the testing rods were 10 mm, and the distance 70 mm. A displacement of 30 mm in the axial direction was enforced at a rate of 3 mm/s. The sample was placed on the two lower rods, and the machine was started. The applied force and displacement were logged using the built-in sensors of the machine. The sampling frequency was 25 Hz.

Results

The three point bending test revealed that almost all molded test geometry had an internal porous structure, with voids of various sizes. Most probably, the voids initiated premature crack growth, which ultimately lead to failure. Furthermore, the result showed a big difference in maximum applied force between the specimens. For polypropylene, specimen #7 took the largest load of 1210 N and largest deformation of 7.58 mm, while specimen #4 took the lowest load of 555 N and smallest deformation of 3.80 mm. Specimen #1, which was the original part, had a different geometry than the remaining specimens, and was therefore left out of further discussion.

Specimen no.	Material	Mold	Maximum applied force [N]	Displacment at fracture [mm]	Comment
1	PA	Steel	1229	-	Specimen did not fracture. Only large deformations.
2	PP	VeroBlackPlus	862	5.24	Cracked in small voids.
3	PP	Alloy 910	889	4.98	Cracked in large void.
4	PP	HDPU	555	3.80	Cracked in porous region.
5	PP	HDPU	701	3.97	Some small pores present.
6	PP	Epoxy-Wood	966	4.44	Ductile fracture. One small void in fracture surface.
7	PP	Aluminium	1210	7.58	Ductile fracture. Cracked in pores.
8	PP	Epoxy-Paper	780	4.37	Cracked at medium sized void. Very brittle.
9	PLA	Wood	2454	3.58	Broke in four pieces. Very brittle. Made strong noise upon failure.
10	PP	Aluminium	831	3.94	Cracked in pores and one medium sized void.

Table 11: Results from three point bending test. Specimen no. 1 (the master model) had a different geometry than the other specimens and was therefore left out of further discussion.

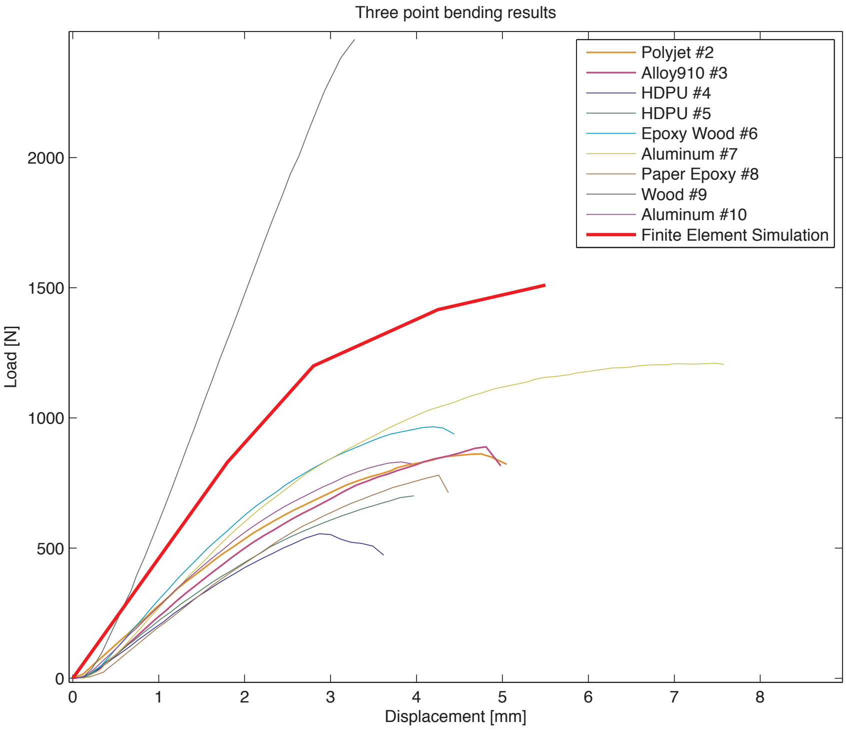

Figure 48: The plot shows the load-displacement curve in the Z-direction from the three point bending test, and FEA. The grey curve to the left was the specimen from the Wood mold, which was made from PLA, and therefore was not comparable to the remaing specimens. Also note that the curve for the FEA does not indicate yield or fracture.

Seing that specimens #4 and #7 were made from the same material, this indicates that the internal porous structure had a large impact on strength. Furthermore, specimen #9, which was made from PLA, showed a much higher stiffness and strength than the polypropylene specimens. This corresponds well to the indications from the values in table 1. The arithmetic average of the maximum applied load of the polypropylene specimens, namely specimens 2, 3, 4, 5, 6, 7, 8 and 10, was 849 N. The fractured specimens are shown in figure 49.

Reflections

Comparing the results from the simulations to the testing, it can be seen from figure 48 that the simulation indicated that the specimen should have reached the ultimate tensile stress of 32 MPa (see table 1) after 2 mm of deformation. This implies that the simulation estimated that the tested specimens should have fractured before they did, and consequently that the simulation was conservative. A calibration of the FEA material model would most likely have provided more accurate results. Likewise would accounting for the viscoelastic and viscoplastic behavior contributed to accuracy. It is however uncertain whether the simulation was too imprecise, as the specimens tested most likely were not comparable to a specimen made in a high-end injection molding machine. Nonetheless, this comparison illustrates that accurate mechanical behavior of injection molded plastics can be difficult to predict, as impurities and design effects will affect mechanical strength.

Looking at the difference in strength across the tested specimens, it is hard to utilize this measure solely as an indication to which direct rapid tooling technique provided best quality. Most likely, the limitations in the TrollLabs Rapid Prototyping Injection Molder contributed to the large distribution in strength. This may have been caused by insufficient pressure, or trapped gas inside the injection chamber, which in turn created inhomogeneity and voids. For further convergence, full scale testing is required.

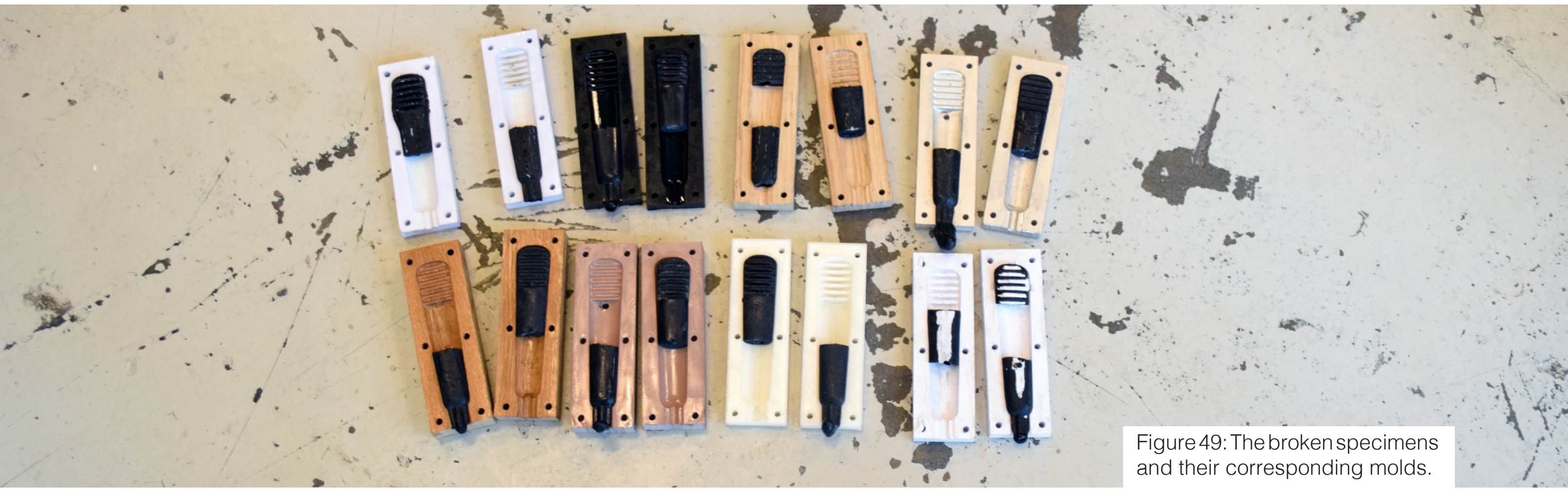

Figure 49: The broken specimens and their corresponding molds.

Chapter Seven

Full Scale Prototype

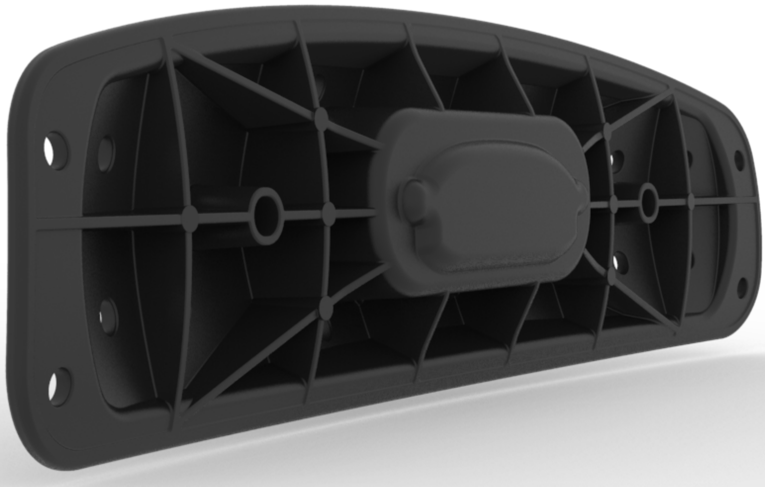

Figure 50: A rendering of the test component (top), and a photo of the Håg Sofi (below).

Introduction

In the probing, several direct tooling techniques showed good results. At this point however, the maximum achievable quality of the molded components was restricted by the TrollLabs Rapid Prototyping Injection Molder, rather than the mold material itself. It was therefore desirable to increase the prototyping resolution, and furthermore to perform a test in a full scale scenario.

The Test Component

The component selected for the full scale testing was a headrest part from the Håg Sofi chair. It was chosen because of its size, and high complexity. Design features include drafted ribs, bosses, radii and holes. The size is roughly 327x90x26 mm. The test component is shown in figure 50.

Requirements

The mold for the test component was to be tested using the tool insert approach, which imposed several constraints on the tooling design. The largest family mold available was 480x340x56 mm. By utilizing additional mechanical clamps could the size be reduced. The mold had to be partitioned into two halves due to the design of the injection molding machine. One mold half served as the ejector side. Here, holes for ejector pins had to be distributed over the component to provide easy ejection. The holes had to be large enough to allow air to escape between the ejector pin and the wall. The other mold half had to serve as the inlet side, and consequently have room for a Ø12 mm nozzle. Additionally, the two mold halves had to be attached with bolts to movable platen on each side. The bolt hole patterns were determined by the injection molding machine.

Because the size of the test component exceeded the maximum build size of any of the available additive manufacturing machinery, it was decided that the tooling should be CNC-milled. From the probing in Chapter Five, it was learned that the tooling should have a smooth and hard surface. Furthermore, it was learned that a release agent should be used to minimize friction, and ease ejection. Both the epoxy coated HDPU-foam and epoxy coated wood molds showed good results during the probings. However, because wood is anisotropic and highly sensitive to moisture, its dimensional stability is not superb. Therefore, it was decided that tooling material should be epoxy coated HDPU-foam, with a layer of release agent applied.

Designing the Tooling in NX 9

A CAD file of the test component was supplied by SBS. The 3D-geometry of the headrest served as a virtual pattern, as the 3D-geometry was subtracted from a blank. The blank, now containing a cavity, was then partitioned into two halves. The remaining design features such as bolt holes, air channels and ejector pin holes were then added. A CAD-model of the tool insert is shown in figure 51.

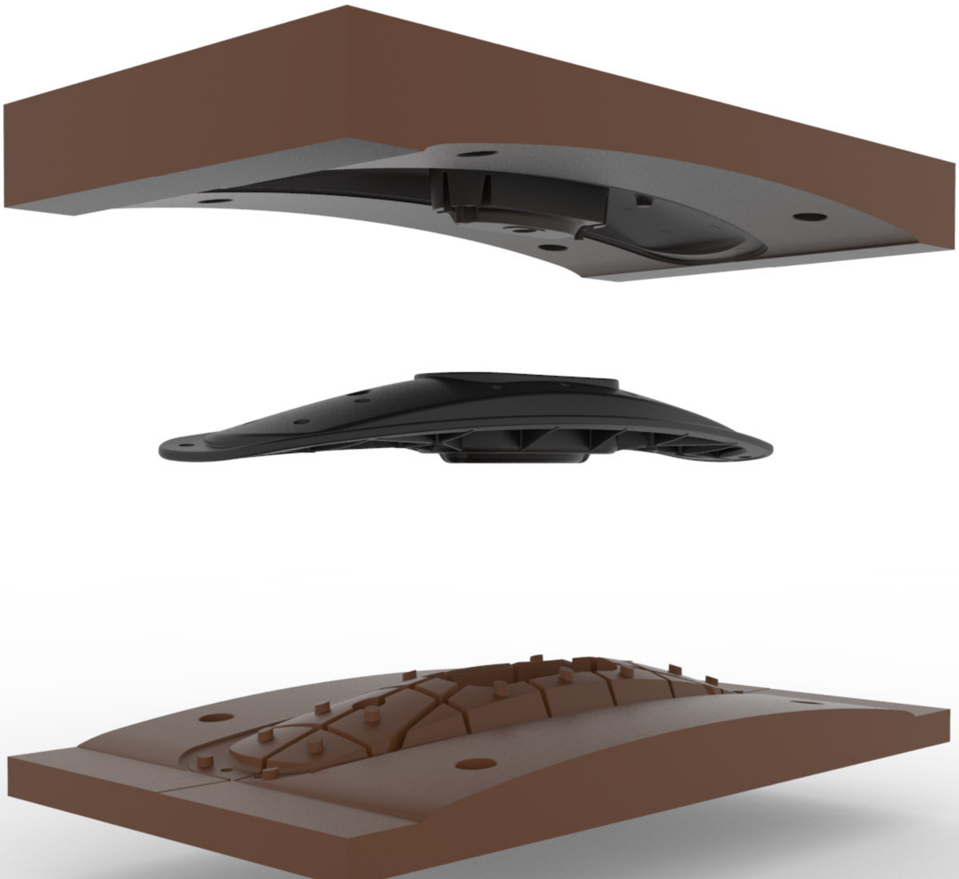

Figure 51: A CAD model of the tool insert and test component.

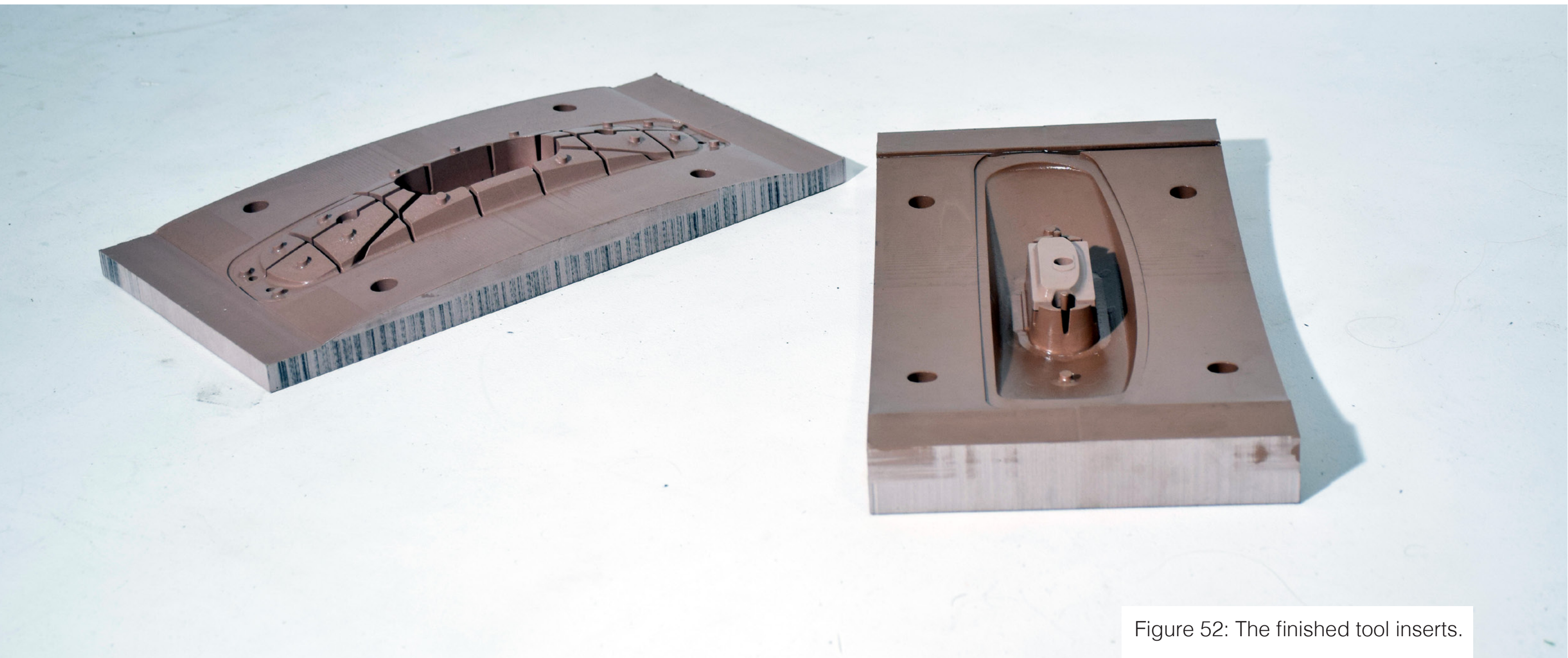

Figure 52: The finished tool inserts.

Building the Tooling

Both mold halves were milled on the Roland MDX-540 CNC mill. The CNC-program was made using SRP-player. The roughing was done with a 6 mm flat end mill, a cut depth of 2 mm and a feed rate of 2700 mm/min. The spindle speed was 12000 rpm. The fine milling of the large surfaces was also done with the 6 mm flat end mill, but with a cut depth of only 0.1 mm. The fine milling of the details was done with an R1 ball pin mill, also with a cut depth of 0.1 mm. For the ejector side, the part had to be milled from both sides due to the through holes for the ejector pins.

After milling, the two mold halves were coated with a very low viscosity epoxy, namely Epikote Resin MGS RIMR135 resin and Epikote MGS RIMH137 curing agent. The mixing ratio was 100 weight units resin to 30 weight units hardener. The mixed solution was placed in a degassing chamber for 10 minutes to extract bubbles. The coated mold halves were then cured in an oven at 60 °C for 8 hours.

Finally, the mold halves were cut free from the support material and coated with Renlease QV5110 release agent. The finished tool inserts are shown in figure 52, and some photos from the building are shown in figure 53.

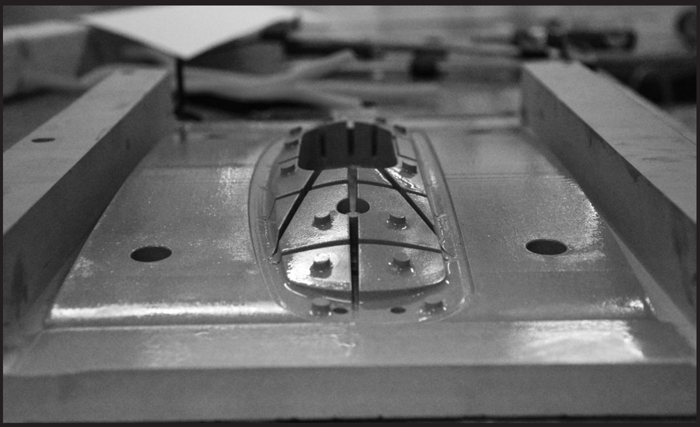

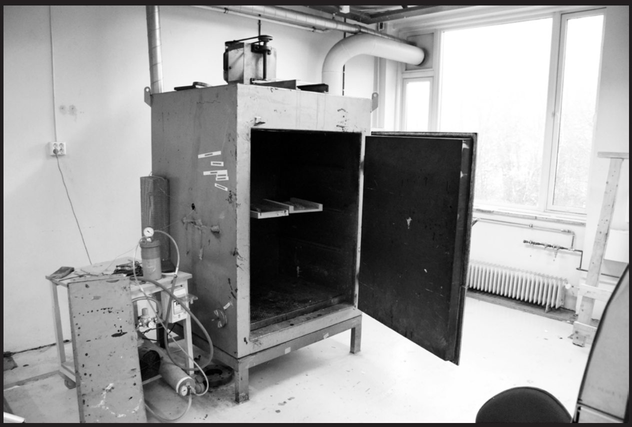

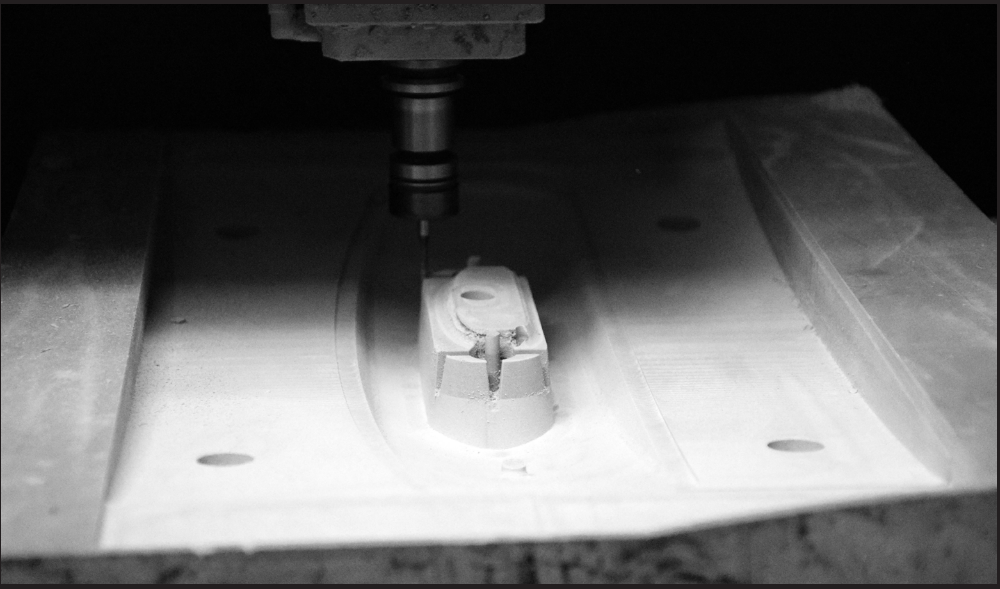

Figure 53:
Top left: The mold halves were just finished coated with epoxy. Top right: the oven used for curing. Left: Many fine details had to be milled. The section shown actually had to be replaced. Lower left: The inserts after milling. Lower right: The ejector side had to be milled from both sides due to ejector pin holes. Bottom left: pipe cleaners were used to coat the fine details with epoxy. Bottom right: A closeup of wet epoxy. Some bubbles were present.

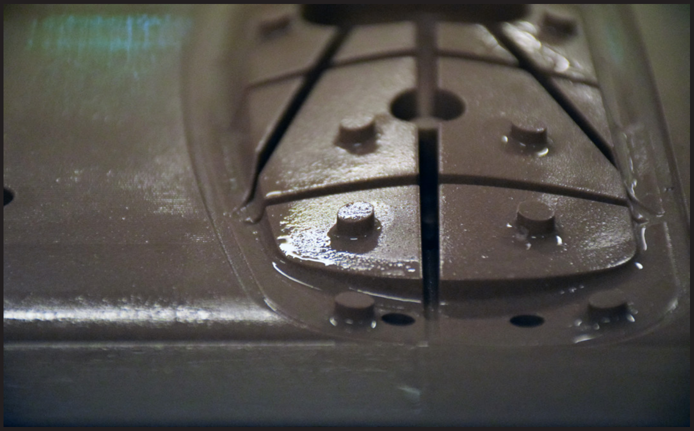

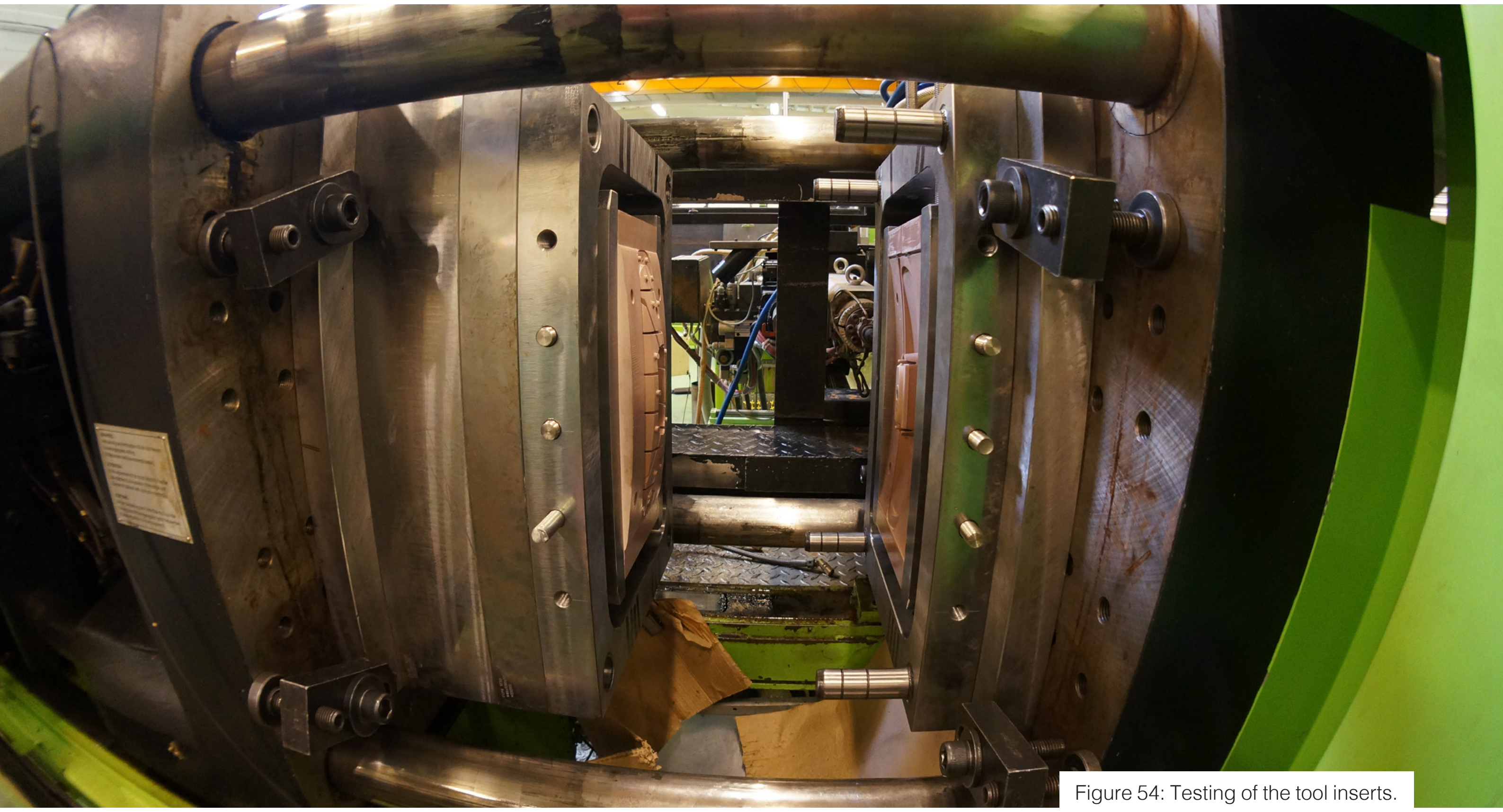

Figure 54: Testing of the tool inserts.

Testing the Tooling

The trial molding was performed at OM BE Plast in Fredrikstad. The tool inserts were mounted in a family mold and placed in an Engel injection molding machine, as shown in figure 54. The injection material was low viscosity polypropylene of type 401-CB50. The test parameters are given in table 12.

Two shots were injected into the mold. For the first shot, the parameters were as given in table 12, and the cooling time was 30 seconds. For the second attempt the volume of injected polymer melt was increased, and the cooling time increased to 120 seconds.

Test Parameter	Value
Cylinder Temperature	190 deg cels
Injection Time	3.55 sec
Post filling time	5 sec
Cooling time	First attempt: 30 sec, Second attempt: 120 sec
Clamping Force	800 kN
Ejector pins	35 mm
Injection Pressure	100 Bar

Table 12: Parameters in the full scale testing.

Results

For the first attempt, too little resin was injected to completely fill the part. However, except for the very outer ends, all geometry features were captured well. Upon ejection, some of the thicker areas had not yet frozen, and consequently was the geometry of these areas affected. Except from these areas, the general surface finish was excellent. The mold was completely intact after the first molding, and was reusable (see figure 55).

For the second attempt, more resin was injected as an attempt to fill the entire part. Unfortunately, the increased volume put too much pressure on the mold, and consequently were some pieces from the mold torn out upon ejection. The increased volume was also shown on the geometry of the second component. For this component, the rib thickness was increased to 5 mm, compared to 2.5 mm in the first component. Both components are shown in figure 56.

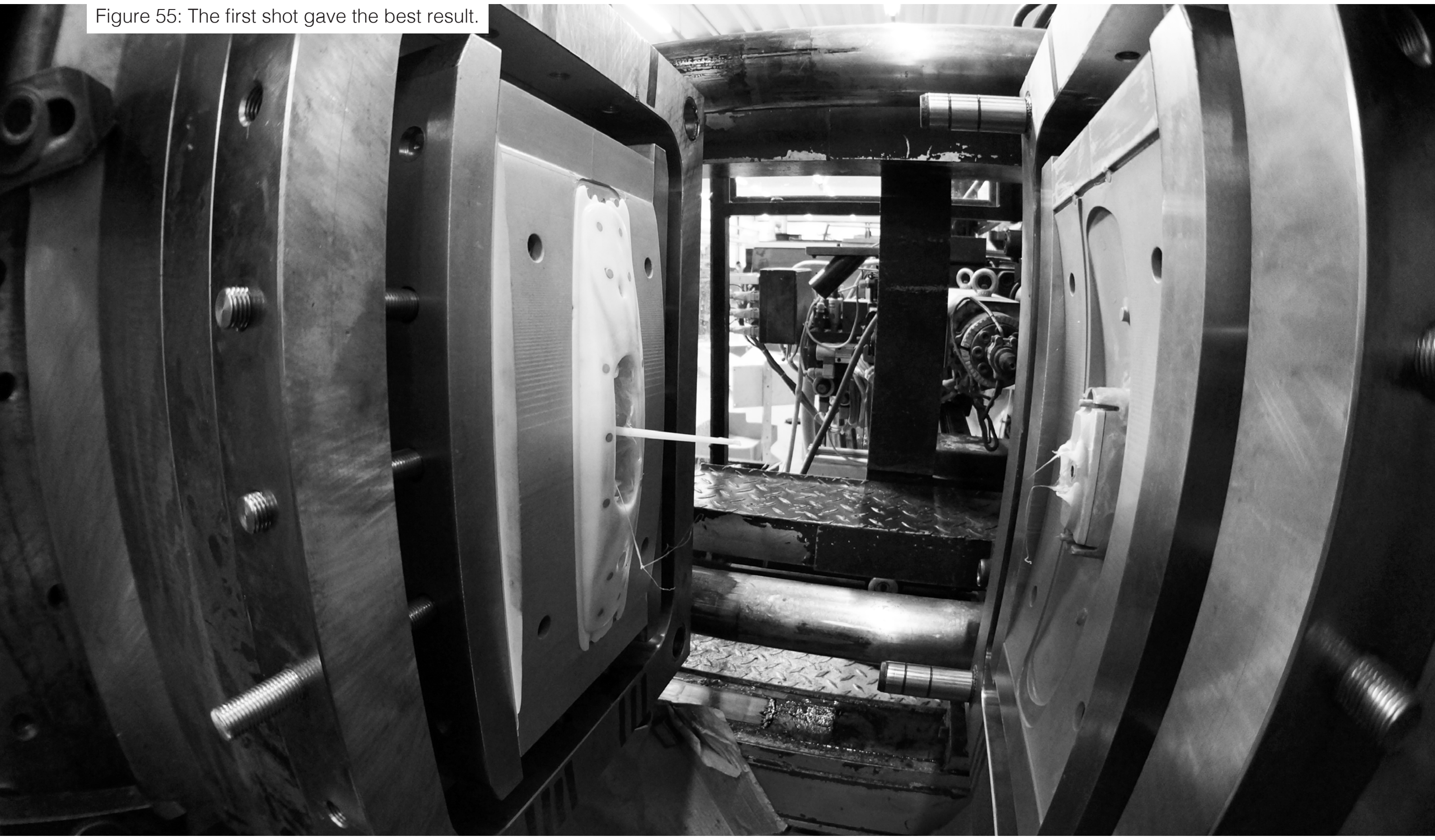

Figure 55: The first shot gave the best result.

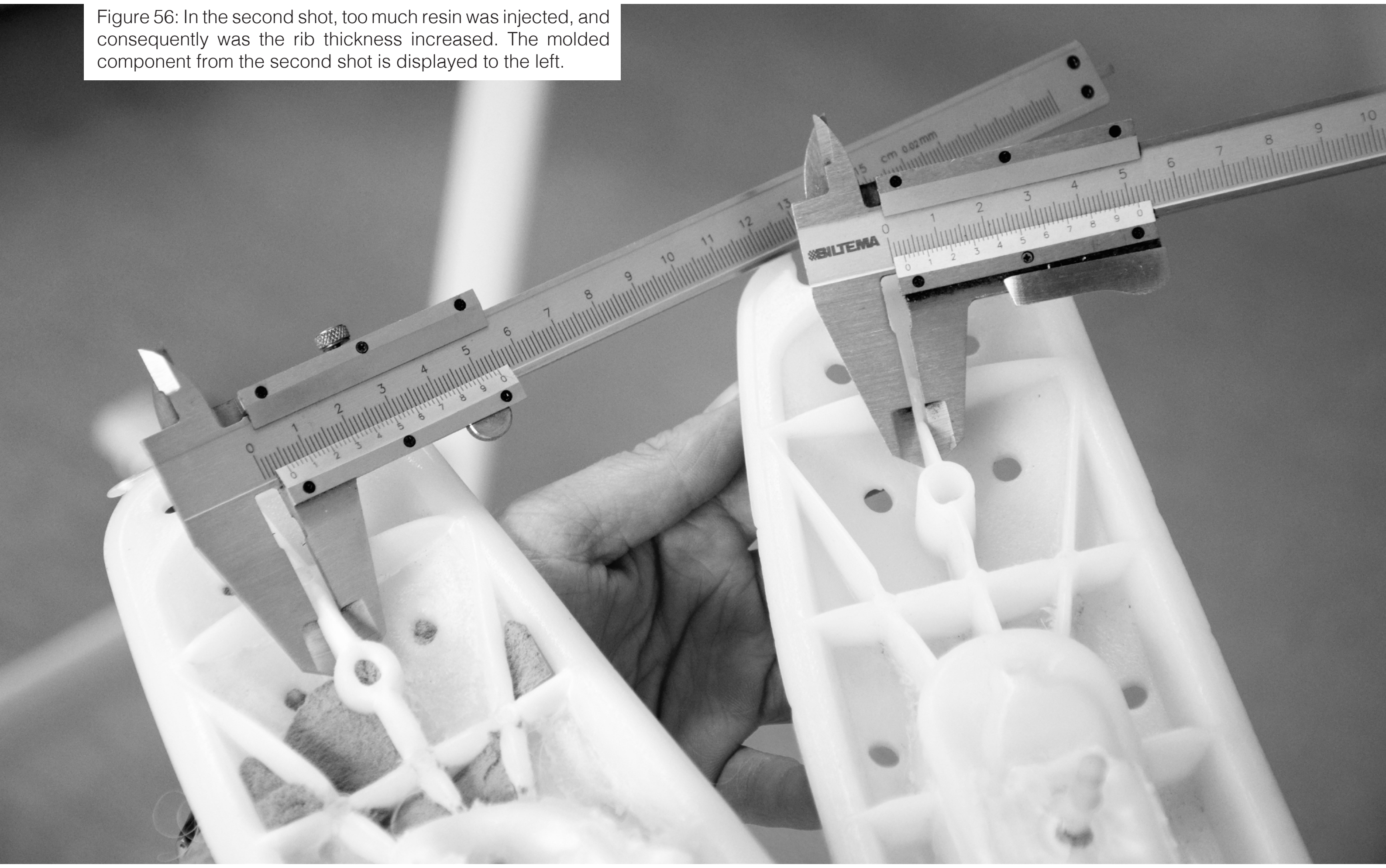

Figure 56: In the second shot, too much resin was injected, and consequently was the rib thickness increased. The molded component from the second shot is displayed to the left.

Learnings

Because the first attempt provided close to good results, it is likely that this method could have provided even better results if all molding parameters were tuned correctly. Head of development at OM BE Plast, Knut Richard Kviserud, explained during the molding that tuning the parameters for a new mold usually requires several attempts (personal communication, June 2016). Furthermore, when testing the HDPU-foam mold with the TrollLabs Rapid Prototyping Injection Molder, the part was not ejected until the mold was cold. If the cooling time had been increased in this case, it is likely that the areas of greater thickness could have frozen. It is also possible that unwanted chemical reactions with the release agent could have prevented the resin from freezing. However, seeing that this was not a problem earlier, this was deemed less likely.

Another learning was that the mechanical integrity of the molds is an issue when using the tool insert method (see figure 57). It is therefore likely that a stronger mold material is better suited for high pressure molding. However, seeing that the geometry of the test component was very complex, it is also likely that mechanical integrity of the mold would have been less of an issue if the geometry was simpler.

Finally, the full scale test confirmed that the porosity in the previous moldings were because of the TrollLabs Rapid Prototyping Injection Molder, and not the mold material itself. This implies that it should be possible to make high quality injection molded components in a near office situation, if improvements, addressing the porosity issues, are made to the TrollLabs Rapid Prototyping Injection Molding machine.

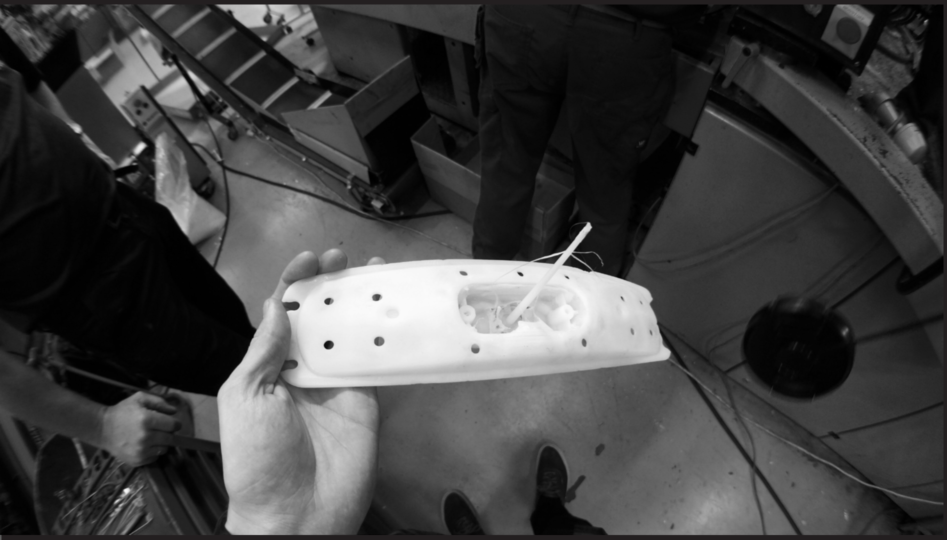

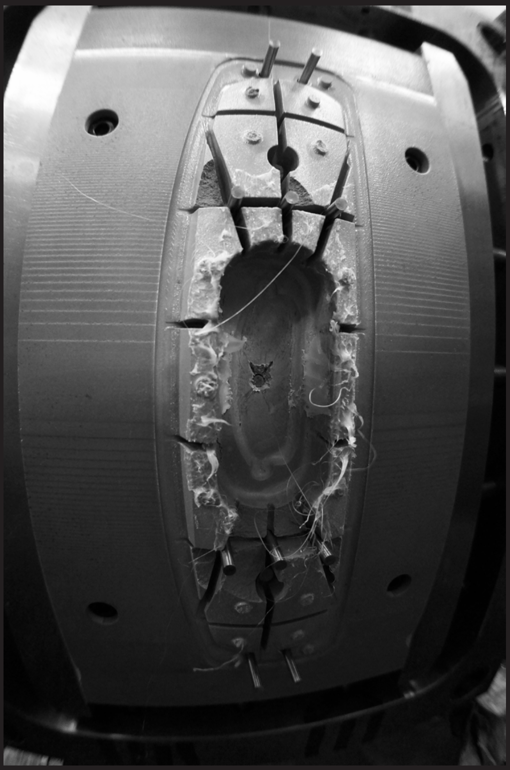

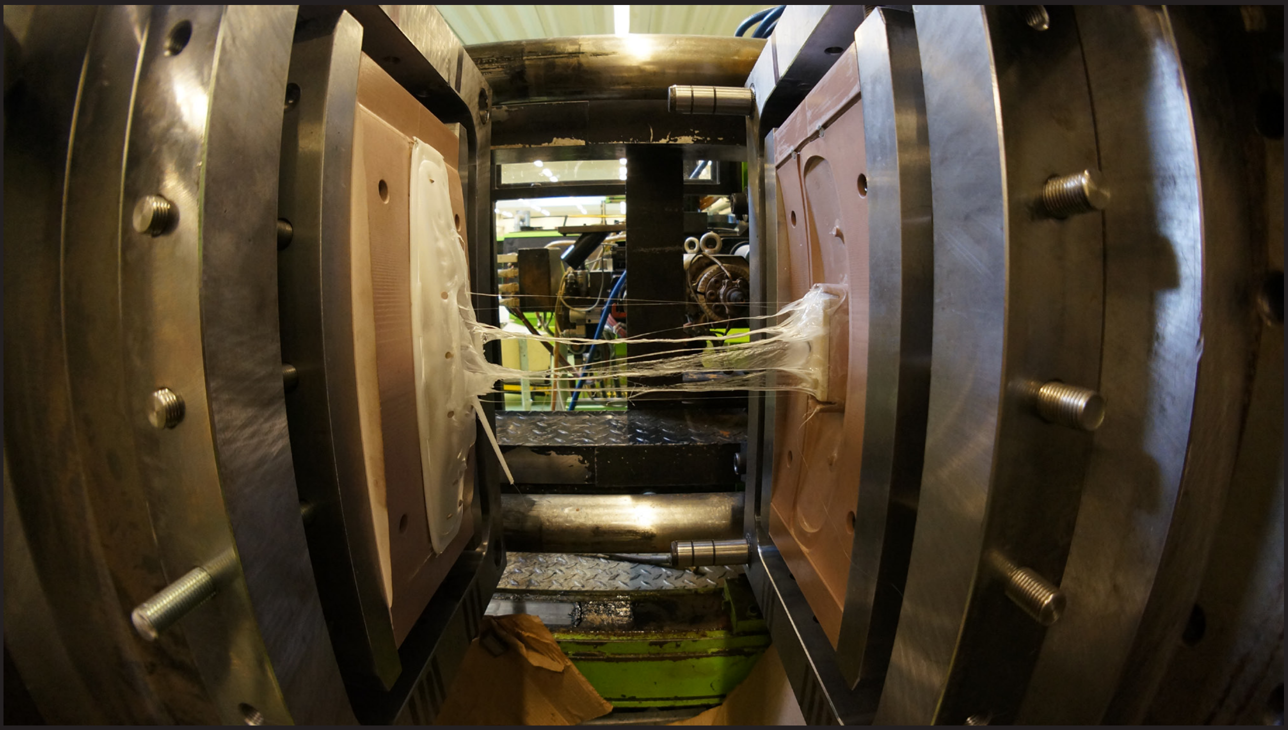

Figure 57:
Top left: Even the shop workers at OM BE were impressed by the first molding. The area around the sprue was affected because of the short cooling time. Top right: The second shot proved to be too much pressure for the mold. Notice the areas that have been ripped out. Middle: The the remains of the second shot. A longer cooling cycle would probably have prevented the separation of the component. However, the pressure was still too high. Bottom right: The first shot captured most of the complex geometry, and provided a very good surface finish in the part.

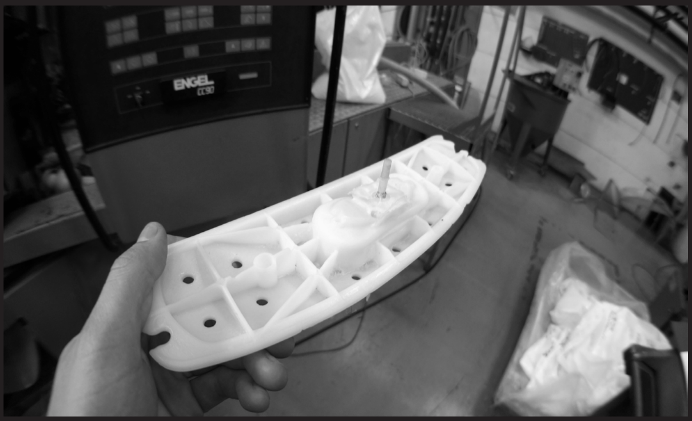

Chapter Eight

Evaluation of the Techniques

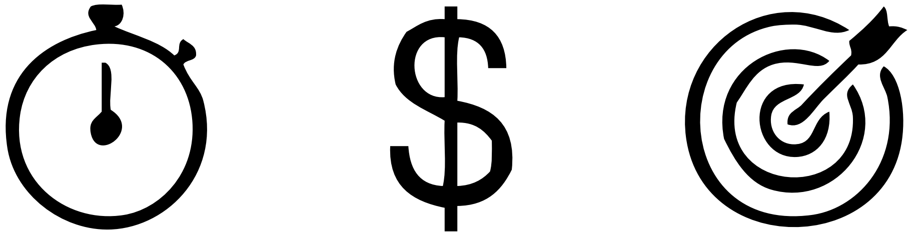

Figure 58: The techniques were measured on efficiency, cost and effectiveness.

Introduction

The ultimate goal of this project was to establish a cheap, efficient and effective way of prototyping injection molded components. Efficiency is measured in time, and consequently is the time spent on creating each prototype an important measure of the direct rapid tooling technique. Furthermore will the amount of manual labour required for the technique have a large impact on cost, together with materials used. Finally will the quality of the injection molded part be a measure of how effective the direct rapid tooling technique can produce a prototype. In the following, a benchmark of time and money spent on making the two mold halves from Chapter Five, using the most promising rapid tooling techniques, is given. The benchmark is compared to the quality of the final prototype.

Technique	Preparing file and setup	Manufacturing	Post processing	Total time
Alloy 910 at Ultimaker 2	10 min	2 x 60 hrs	5 min	120 hrs and 15 min
Epoxy Coated Paper at Mcor Iris	10 min	8 hrs	3 hrs freeing geometry. 15 min epoxy coating + 8 hrs curing	16 hrs 25 min
Epoxy Coated Wood at Roland MDX-540	2 x 30 min	Rough milling: 2 x 30 min. Fine milling: 2 x 90 min	15 min epoxy coating + 8 hrs curing	13 hrs 15 min
Milling HDPU-foam at Roland MDX-540	2 x 30 min	Rough milling: 2 x 1 min. Fine milling: 2 x 60 min.	15 min epoxy coating + 8 hrs curing	11 hrs 17 min
Milling Aluminum at Roland MDX-540	2 x 60 min	Rough milling: 2 x 2 hrs. Fine milling: 2 x 5 hrs	15 min	14 hrs 15 min
VeroBlackPlus at Objet Eden 250	10 min	3 hrs 30 min	10 min	3 hrs 50 min

Table 13: The amount of time spent on making the various molds using corresponding techniques. “2 x” indicates two times, once for each mold half.

Efficiency

The total amount of time included preparing the file in the related software, setting up for rapid prototyping, manufacturing and post processing. For the epoxy coated molds, the curing time is shorter in table 13 than what was given in Chapter Five. This was because there exist epoxy systems that can cure in a much shorter amount of time with similar results, and that the long curing time therefore was unnecessary. Corresponding times are given in table 13.

The total time was given in hours and minutes, and divided into three categories with ordinal ranking. The categories were:

- Short: Tooling can be built in a working day (less than 8 hrs).
- Medium: Tooling can be ready within 24 hrs (8 - 24 hrs).
- Long: Tooling takes longer than 24 hrs.

In addition to time, a measure was given on consistency. Consistency describes how consistent the rapid prototyping machine can produce the tooling, and will have an impact on time spent fabricating the part. The consistency was divided into three categories: poor, good and great. The requirements were the following:

- Poor - two or more attempts are required for successfully producing a part.
- Good - the part is produced on first attempt with acceptable surface finish and dimensions.
- Great - the part is produced on first attempt with great surface finish and dimensions.

Based on the two efficiency measures, the tested techniques were divided into the corresponding categories. The measure for each technique is given in table 15.

Cost

Technique	Materials Cost (minimum quantity)
Alloy 910 at Ultimaker 2	1 spool: 300 NOK
Epoxy Coated Paper at Mcor Iris	Office paper (2500 sheets): 250 NOK. Epoxy (600 g): 399 NOK
Epoxy Coated Wood at Roland MDX-540	Red oak: 500 NOK/m^2. Epoxy (600 g): 399 NOK
Milling HDPU-foam at Roland MDX-540	HDPU foam (250x250x50mm): 200 NOK. Epoxy (600g): 399 NOK
Milling Aluminum at Roland MDX-540	Aluminum bolt (50x50x3000mm): 1200 NOK
VeroBlackPlus at Objet Eden 250	One container: 4000 NOK

Table 14: Materials cost for the tested techniques.

The material cost needed for the two mold halves was measured in NOK, and are given in table 14. The cost was divided into three categories: cheap, less cheap and expensive. The ranking was ordinal, and the cut-off the following:

- Cheap - materials cost less than 500 NOK
- Less cheap - materials cost from 500 to 1000 NOK
- Expensive - materials cost more than 1000 NOK

The amount of manual labour, which also have an impact on cost, was divided into three categories: little, some and much. The categories had an ordinal ranking, and the cut-off between the categories was the following:

- Little - applying release agent, or no manual labour
- Some - manual labor or supervision of less than 4 hrs.
- Much - manual labor or supervision of more than 4 hrs.

The cost measures with rankings are given in table 15.

Technique	Total time	Consistency	Cost	Manual labor
Alloy 910 at Ultimaker 2	Long	Poor	Cheap	Little
Epoxy Coated Paper at Mcor Iris	Medium	Poor	Less cheap	Some
Epoxy Coated Wood at Roland MDX-540	Medium	Good	Less cheap	Much
Milling HDPU-foam at Roland MDX-540	Medium	Great	Less cheap	Some
Milling Aluminum at Roland MDX-540	Medium	Good	Expensive	Much
VeroBlackPlus at Objet Eden 250	Short	Great	Expensive	Little

Table 15: Efficiency and cost measures for the tested techniques.

Figure 59: The measures were mainly based on data from probing and three point bending test.

Effectiveness

A measure of effectiveness of the different techniques was based on qualitative results from the probing, as well as the quantitative results from the three point bending test. The qualitative measures were based on the the surface finish and the dimensions of the part. The qualitative measures were divided into the categories poor, good and excellent, and given ordinal rankings. For surface finish, the criterias for the categories were as follows:

- Poor - a rough surface finish with pores present.
- Good - a rough surface, but no pores present.
- Excellent - a smooth surface without pores.

For dimensions, the the criterias for the categories were:

- Poor - failed to fill cavity completely
- Good - filled cavity, but did not capture all details
- Excellent - captured all details

The quantitative measures were based on maximum applied load from the three point bending test (see table 11) for the polypropylene specimens. The specimens were divided into three categories. These were:

- Low - held less than 800 N
- Medium - held 800 - 1000 N
- High - held more than 1000 N

For the techniques that had more than one specimen tested, an average of the two results is used. The qualitative and quantitative measures of effectiveness are given in table 16.

Technique	Surface finish	Dimensions	Strength
Alloy 910 at Ultimaker 2	Good	Excellent	Medium
Epoxy Coated Paper at Mcor Iris	Poor	Excellent	Low
Epoxy Coated Wood at Roland MDX-540	Good	Good	Medium
Milling HDPU-foam at Roland MDX-540	Good	Good	Low
Milling Aluminum at Roland MDX-540	Good	Good	High
VeroBlackPlus at Objet Eden 250	Excellent	Excellent	Medium

Table 16: Qualitative and quantitative measures of effectiveness.

Benchmark

Based on the measures of efficiency, effectiveness and cost, a benchmark was given. All measures had an ordinal ranking with three internal categories. The categories were given a score from one to three, where one was the lowest score, and three was the highest. An arithmetic average was calculated from the scores, which also forms an overall score (5). The ranking is given in table 17.

Left unaddressed in the evaluation is the mechanical integrity of the mold materials. As shown in Chapter Seven was the pressure in full scale injection molding too much for the complex HDPU-foam mold. It is likely that this pressure could have affected the outcome of full scale testing for other mold materials also. Because these qualities were not tested in the probing, and consequently could not provide a fair comparison, they were left out of the evaluation. Another matter that was left unaddressed was the durability of the molds. The number of shots a mold can take will be decisive for whether or not the technique is suitable for low volume production. This will be discussed more later.

$$\text{Overall Score} = \frac{\text{Time} + \text{Manual Labor} + \text{Consistency} + \text{Cost} + \text{Surface Finish} + \text{Dimensions} + \text{Strength}}{7} \tag{5}$$

Technique	Time	Manual Labor	Consistency	Cost	Surface Finish	Dimensions	Strength	Overall Score
Alloy 910 at Ultimaker 2	1	3	1	3	2	3	2	2.14
Epoxy Coated Paper at Mcor Iris	2	2	1	2	1	3	1	1.71
Epoxy Coated Wood at Roland MDX-540	2	1	2	2	2	2	2	1.86
Milling HDPU-foam at Roland MDX-540	2	2	3	2	2	2	1	2.00
Milling Aluminum at Roland MDX-540	2	1	2	1	2	2	2	1.86
VeroBlackPlus at Objet Eden 250	3	3	3	1	3	3	2	2.57

Table 17: A quantitative comparison of the different techniques.

Chapter Nine

Discussion

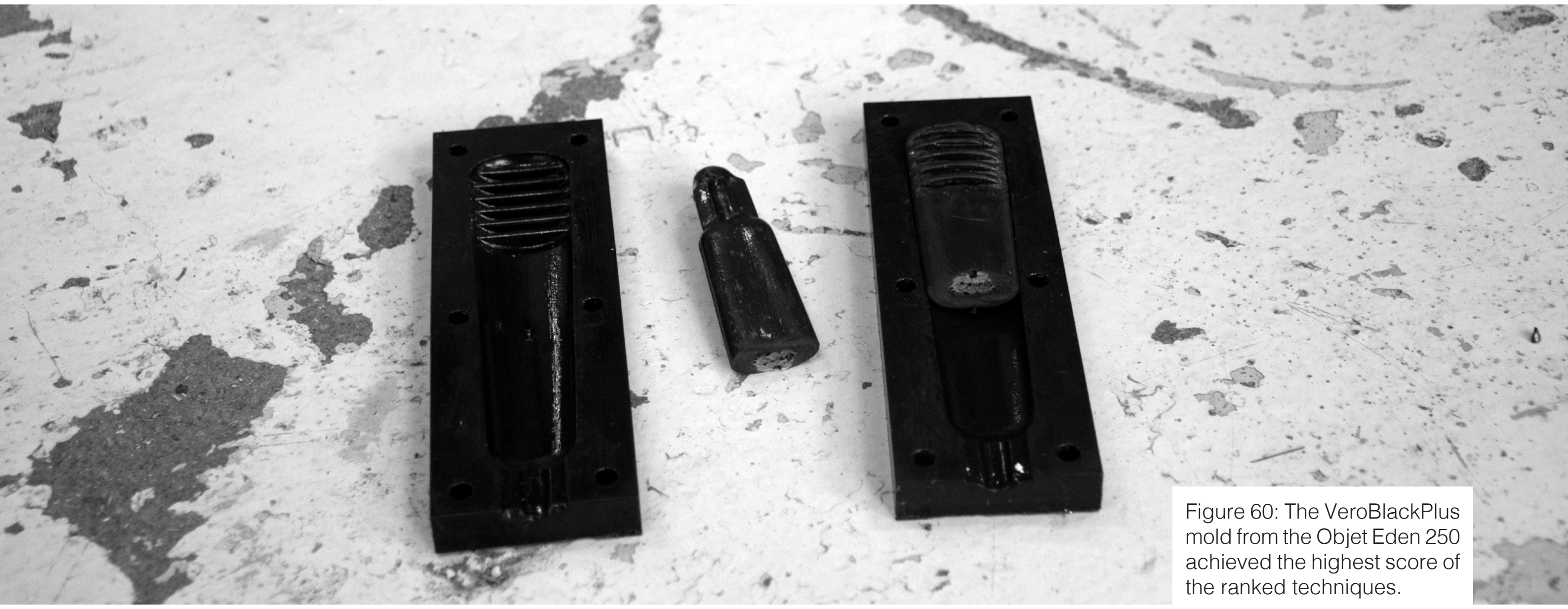

Figure 60: The VeroBlackPlus mold from the Objet Eden 250 achieved the highest score of the ranked techniques.

Findings: Techniques for Direct Rapid Tooling

Several techniques for direct rapid tooling were explored in this report. The techniques tested were based on both additive and subtractive manufacturing technologies. By wayfaring, the techniques were probed, and consequently could the least promising techniques be ruled out, and the most promising techniques pursued. Some of the explored techniques could successfully manufacture prototypes. The strength of the these prototypes were tested using a three point bending machine to give a quantitative measure of their quality, as well as demonstrating how a simple mechanical test can be used in prototyping to evaluate mechanical integrity. Furthermore was a full scale prototype designed, built and tested, to learn more about the scalability of the various techniques. A discussion of the main findings is presented in the following paragraphs.

Which Techniques Worked?

What can be observed from table 17 was that VeroBlackPlus came out with the highest score of the ranked techniques. This was because it provided the absolute best surface finish in the molding, and could be made in a much shorter time than the rest. It is however important to be aware that this technique was also by far the most expensive, and that the maximum possible size of the geometry is limited.

The technique with the second highest score was the Alloy 910. This was most likely because of its very low price, and minimal manual labor required. However, the score does not do justice on the poor consistency and long manufacturing time of this technique. With a manufacturing time of more than 120 hours, the Alloy 910 was 33 times slower than the VeroBlackPlus! Additionally, the operation had to be restarted several times because of poor adhesion to the build plate, poor calibration and a clogged nozzle. It is uncertain if these consistency issues would persist for more expensive FDM systems.

The technique with the third highest score was milling the mold in HDPU foam, and sealing the surface with epoxy. The clear benefit of this technique is that milling HDPU foam is very fast, and that very large build sizes are available. What prevented this technique from scoring higher was that much manual labor is required while milling and applying epoxy. The manufacturing time is also extended due to curing of the epoxy.

The remaining techniques that were evaluated, namely Epoxy Coated Paper, Epoxy-Wood, and Aluminum, achieved a lower score for various reasons. The Epoxy Coated Paper molds simply required too much manual labor and provided too poor quality to be beneficial. The Epoxy-Wood provided overall satisfactory results, but have a major weakness in anisotropy of the material. Because of the highly anisotropic and moisture sensitive behavior, the dimensional stability of the wood molds over time is rather poor. Additionally, it was very difficult to find large block sizes of the suited hardwood materials. That being said, there might exist other types of wood that might be better suited. The Aluminum mold was originally included as a reference, as there already exist empirical evidence that aluminum molds can provide high quality moldings. However, the fact that the aluminum mold did not score any higher sparks an interesting discussion of which attributes are worth most - efficiency, cost or effectiveness?

Weaknesses and Sources of Error

Because none of the measures on efficiency, cost and effectiveness were weighted in the evaluation in Chapter Eight, all measures contributed equally to the score. This may not be correct for all cases. It is for example likely that the amount of manual labor will have a larger impact on price than material cost, especially in a high cost country such as Norway. Furthermore can a small entrepreneurial start-up company, doing their first batch of products, cherish a lower price over speed, while it can be opposite for a large company doing prototyping. The various priorities can be accounted for through weighting, but was left out in this report.

Other important measures not addressed were performance characteristics such as durability and strength of the molds. As shown in Chapter Seven, holds full scale injection molding machinery much higher pressure than the Rapid Prototyping Injection Molder. The test geometry from the probing did not account for the ability to hold geometry details, like in the full scale testing, nor did it provide any information if the structural integrity of the mold was sufficient to withstand the required pressure for providing these details. Furthermore was durability not considered. Although durability can be a less important attribute when the technique is used solely for prototyping, and only a handful of components is required, it is of great importance when considering low volume production. For small start-up companies can the ability of producing a small batch of components, using direct rapid tooling, make a big difference, as the investment cost would be reduced drastically. These measures should be investigated more thoroughly in future studies.

For the evaluation in Chapter Eight, several potential sources of errors might have altered the results in table 17. Most importantly were the strength of the specimens in the three point bending test highly dependent on the Rapid Prototyping Injection Molder, as shown in Chapter Seven. Although all specimens were injection molded using the same machine, the pressure and temperature fluctuated throughout the molding. This resulted in voids and bubbles of different sizes, which again initiated premature crack growth and consequently might have had a great impact on the final strength of the specimen. Moreover, because the voids and bubbles were not the same size, nor placed at the same locations for all specimens, they represent a large contribution on uncertainty in the results. Other sources of error could be misalignment of the specimens, or inaccuracy in the tensile testing machine.

Another weakness of the three point bending test was that the test geometry from the probing did not have the same shape or material as the master model (see figure 61). Because the master model had an internal cavity, as opposed to the test geometry which was solid, no fracture was observed upon testing. If the master model and the test geometry would have had the same shape, it would have been easier to determine to what degree the porous structure of the specimens contributed to strength. Furthermore, it would be easier to decide whether or not the finite element analysis was accurate or not. Finally, it is of essence that only one or two data points were gathered for each technique tested. For achieving a significant result, many more data points should be obtained.

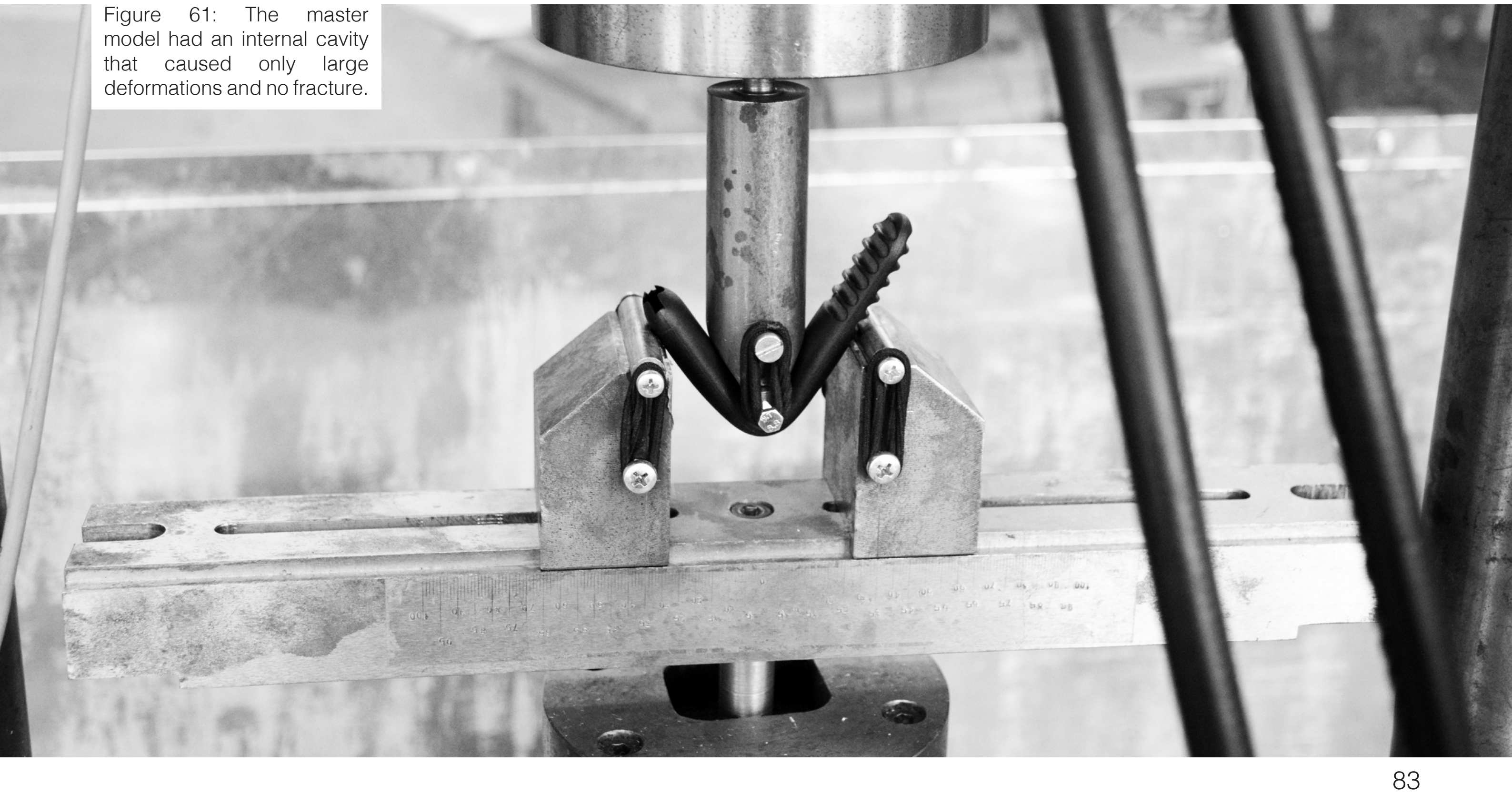

Figure 61: The master model had an internal cavity that caused only large deformations and no fracture.

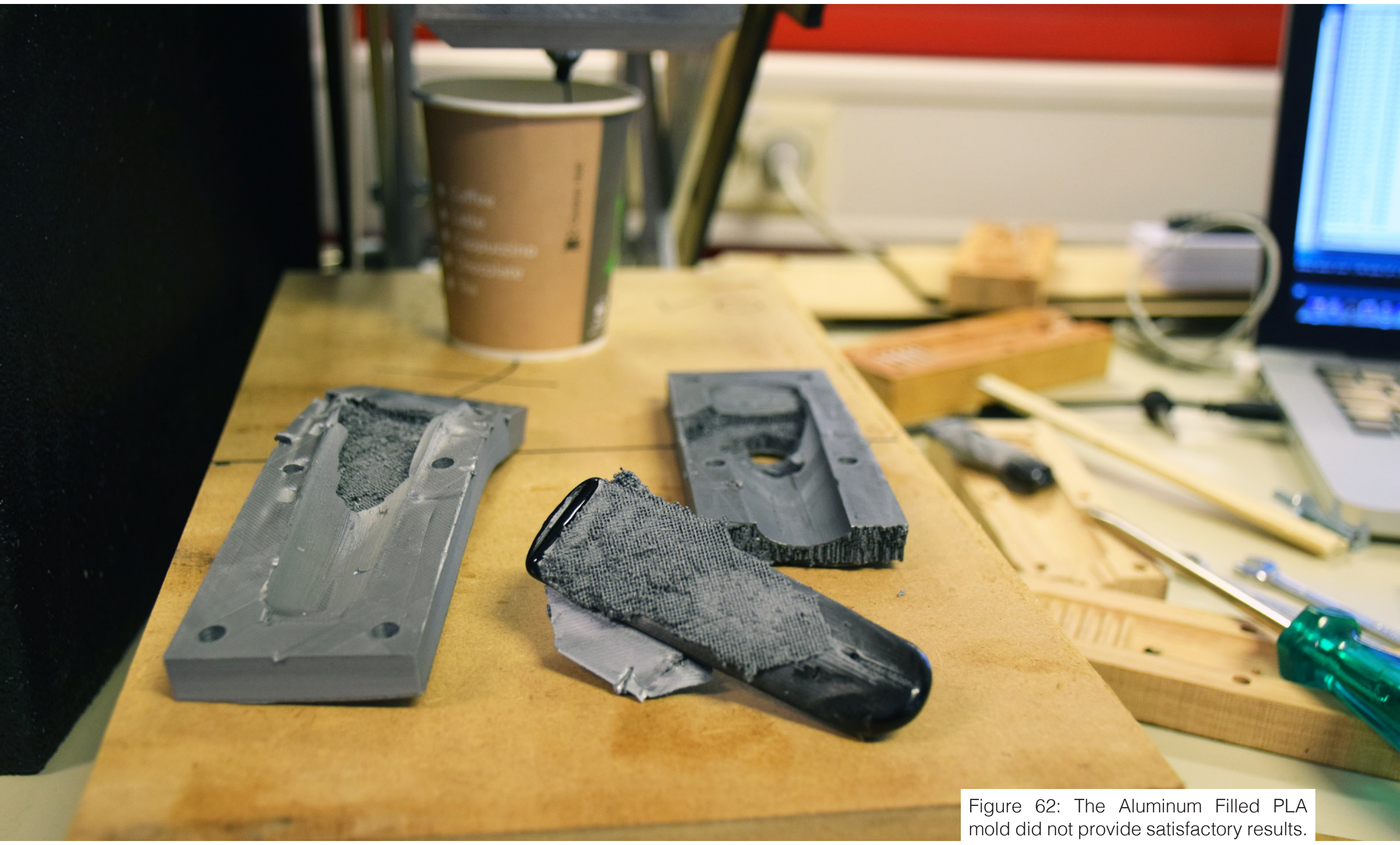

Figure 62: The Aluminum Filled PLA mold did not provide satisfactory results.

Which Techniques Did Not Work?

The techniques that were tested, but did not provide any useful results, and therefore were not included in the ranking, were Aluminum Filled PLA, regular PLA and Monochrome White. What was common for these techniques was that all molds melted upon injection of the resin. For a mold material, this is perhaps the most critical functionality, and consequently were they not pursued any further. One weakness is however that the aluminum filled PLA and regular PLA molds were only tested with PLA as injection material. Because PP has a lower melting temperature than PLA, it is possible that these molds also could have provided a successful molding if they were tested with PP. However, because other materials with higher melting temperatures, such as Alloy 910, exist for FDM 3D-printers, the PLA mold material was deemed less suitable.

The partially electroplated 3D-printed molds should have provided better results. Seeing that electroplating of 3D-printed materials has already been done successfully both by amateurs and companies (Cera, 2014 and Kickstarter, 2015), it is likely that a useful result could have been achieved if more optimization effort was put in. Because chemistry normally requires a high degree of accuracy, it is possible that it would have been easier to identify error sources if the measuring unit of tablespoons had been replaced by grams or millilitres. This could be an example of where more traditional research methods should have been employed. That being said, one reason for why this technique was not pursued any further was because of malfunctioning of the Ultimaker 2 3D-printer, which made it difficult to to produce any new molds to be electroplated.

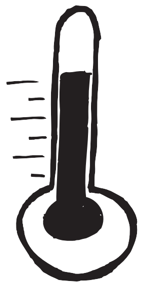

Withstand thermal degradation

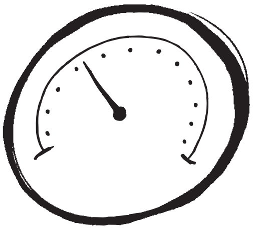

Withstand internal pressure

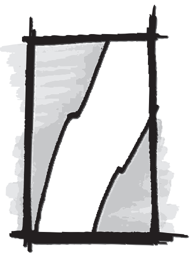

Good surface quality

Figure 63: The three most important qualities for a mold were a high enough melting temperature, sufficient mechanical integrity and good surface quality.

Important Qualities for Molds Used For Direct Rapid Tooling

Based on learnings from the techniques that worked and those that did not work, as well as the full scale prototype from Chapter Seven, it is possible to deduce a handful of important qualities a mold for direct rapid tooling must or should have. Firstly, the mold material must have a high enough melting temperature so that the material does not melt upon injection, as shown with the PLA and Monochrome White molds. Secondly, the structural integrity of the mold must be sufficient to withstand the pressure applied by the injection molding machine, as was shown in Chapter Seven. Depending on the injection molding method utilized and the complexity of the geometry, this pressure can vary from just a few bars, and up to several hundred. Furthermore, the mold must provide a good enough surface finish for the part to be successfully ejected. From the early paper mold in the second round of probing, the part broke upon ejection because the complex part of the geometry adhered to the mold. After applying epoxy and release agents to the mold surfaces, ejection was no longer a problem. The surface of the mold should therefore be hard and smooth, with little friction.

A property that originally was of great concern, but that proved not to be a big issue, was thermal conductivity. For all the tested mold materials, except aluminum, the thermal conductivity was very low. From the aluminum mold in round three of the probing, it was learned that the aluminum mold needed to be pre-heated in advance in order to prevent the resin from freezing as soon as it hit the mold surface. This was not necessary for the other molds. One disadvantage is however that a low thermal conductivity in the mold material also implies longer cooling times, as was shown in the full scale testing in Chapter Seven. Because mold materials with both low and high thermal conductivity provided satisfactory results, no further recommendation is given.

Findings: Prototyping Injection Molded Components

The two methods employed for prototyping injection molded components were the tool insert method and the desktop injection molding method. In the tool insert method, a rapid prototyped tool insert was placed into a family mold, and further placed in a traditional injection molding machine. The benefit of this method was that all parameters could be tuned so that they resemble the parameters used for mass production. More specifically could a high enough injection pressure be utilized to fill all geometry details, and a larger volume of resin could be injected to make larger parts. Moreover, this method allowed for the usage of molds of various sizes. For the desktop injection molding method, a much smaller injection pressure could be utilized than for the tool insert method, as well as there was a restriction on the maximum volume of the prototype. Furthermore, the TrollLabs Rapid Prototyping Injection Molder proved to have insufficient control over temperature and pressure parameters, which caused voids and bubbles in the injection molded components. Yet, this method was perhaps the most innovative finding in this report.

The TrollLabs Rapid Prototyping Injection Molder was originally designed and built to enable probing of direct rapid tooling techniques. Although the design is far from perfect, it was sufficient to test all the direct rapid tooling techniques presented in Chapter Five, quickly and cheaply. As a benchmark was the time spent on probing the ten different molds from Chapter Five roughly the same as the time spent on designing, building and testing the full scale prototype from Chapter Seven. Of course, the full scale prototype was far more complex and at a higher resolution, as well as the time spent included logistics and delays at the external injection molding facility. However, logistics and delays are also part of the reality of most companies.

An example of where a desktop injection molding machine, in combination with a direct rapid tooling technique can be useful for SBS is in the design and prototyping of snap fit connections. Snap fit connections are common plastic design features that poses challenges with respect to injection molding manufacturability, material properties, interaction and geometry - or feasibility, function, fit and form, respectively. By separating the snap fit connection from the larger component it belongs to, can the tooling be manufactured rapidly by a rapid prototyping technique, such as Polymer Jetting, and the part be prototyped quickly using a desktop injection molder. The prototyped snap fit connection can then be attached to the remaining component, and tested with the other components in the assembly.

On the contrary will the tool insert method be much better suited for low volume batches, such as those for pre-production or a limited number of products, as it offers superb control over the process parameters.

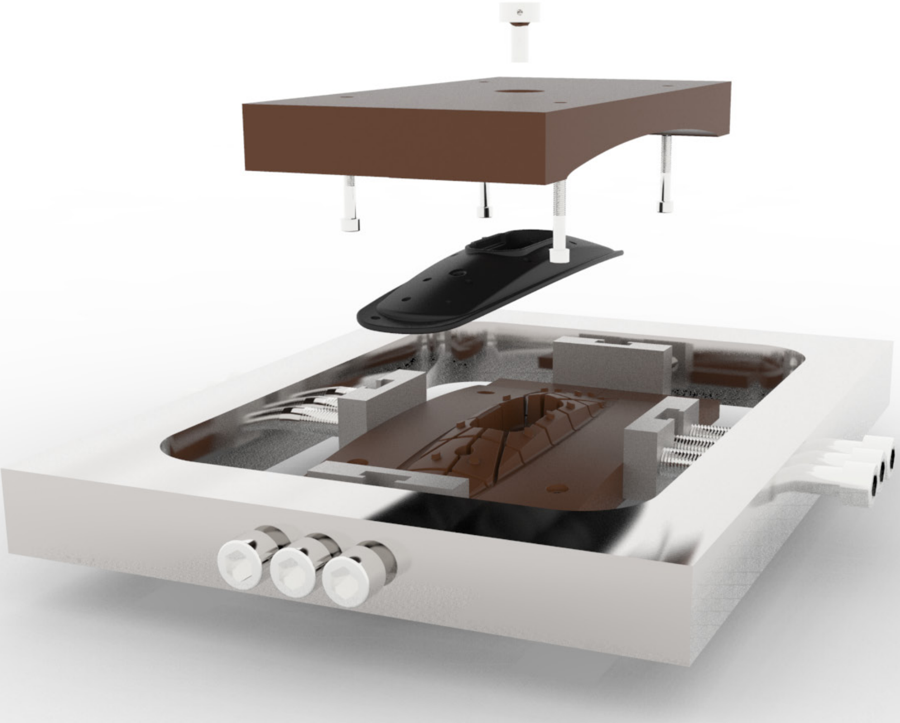

Figure 64: The tool insert method allowed for production level parameter control.

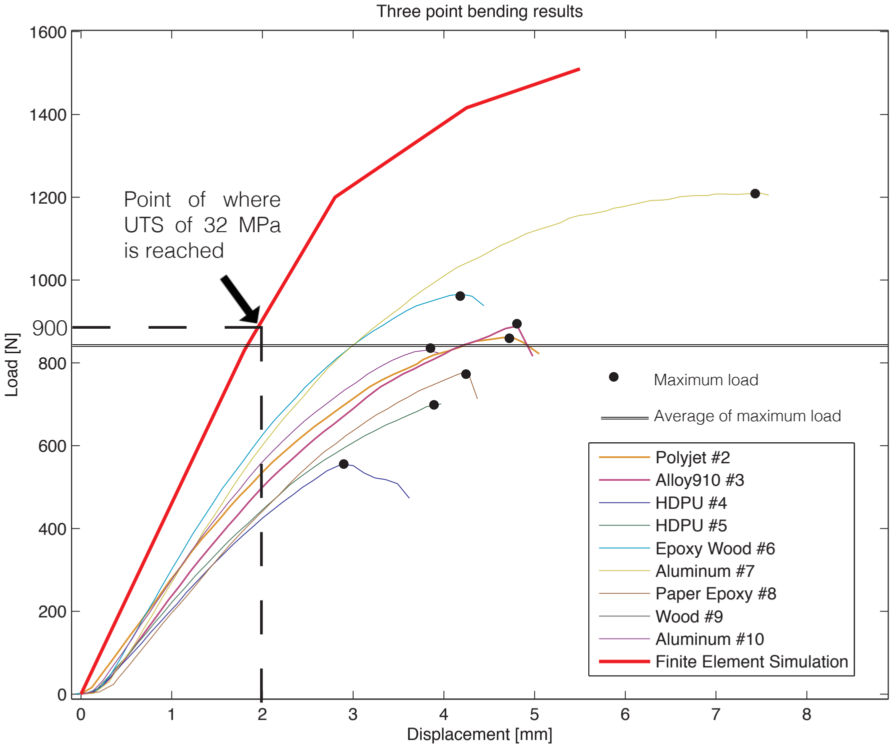

Figure 65:
The plot shows the load-displacement curve for the FEA and polypropylene specimens. The black dots represent the maximum load applied for each specimen. By finding the maximum deformation of 2 mm for the FEA, it can be found that the maximum applied load was 900 N.

Discussion of FEA

Although a structural finite element analysis was not originally within the scope of this report, it was included in Chapter Six to provide a benchmark of theoretical versus real performance. Moreover, because it was a substantial part of the pre-master work, and it is a highly relevant approach to addressing challenges concerning mechanical integrity, some aspects will be discussed briefly here. An introduction to structural finite element analysis of polypropylene is found in appendix B.

The finite element simulation showed that the specimen should have reached the ultimate tensile stress of 32 MPa (see table 1) after approximately 2 mm of deformation. Table 11 showed that the tested polypropylene specimens fractured after 3.80 mm for the lowest, and at 7.58 mm for the highest. This means that the simulation indicated that that the specimens should have fractured before they actually did, and consequently that the finite element simulation provided a conservative estimate. Moreover, by assuming that the maximum displacement from the simulation was 2 mm, it can be seen from figure 65 that the estimated maximum applied force was approximately 900 N. By calculating the arithmetic average of specimens 2, 3, 4, 5, 6, 7, 8 and 10, it can be seen that the average maximum applied load for the polypropylene specimens was 849 N. Therefore, the finite element simulation was conservative, and was only off by 50 N in terms of accuracy, i.e. it was too stiff.

The material model used in this simulation was a linear-elastic, nonlinear-plastic material model, referred to as a metal plasticity approach in appendix B. Essentially, because polypropylene is nonlinear elastic (Sælen, 2012), the metal plasticity approach models the nonlinear elasticity by nonlinear plasticity, as simple nonlinear elasticity is not readily available in ABAQUS. Consequently, this approach is not suited for unloading scenarios. However, it did prove to be conservative in terms of stress-displacement, and somewhat accurate in terms of load. A calibration of the model, with a lower Young's modulus could have provided more accurate results. An effect that was not addressed in the simulation was the time dependent behavior, namely viscoelasticity and viscoplasticity. However, because of the small displacement rate of 3 mm/sec in the testing, it is likely that this would only have caused a very small contribution to the results.

One word of caution: because of the porous structure of the test specimens, the small amount of data points, and because a representative defect-free master specimen was not tested, it is possible that the rather good results will not be consistent for future studies. A recommendation for employing structural finite element analyses in the future is that a reference test should always be included to calibrate the material model.

Figure 66: The Wayfaring Model is intended as a framework for high risk, high innovation projects in the early stages of product development (or the Fuzzy Front End). The outcome from the wayfaring should provide input for traditional product development models such as Ulrich and Eppinger (2012).

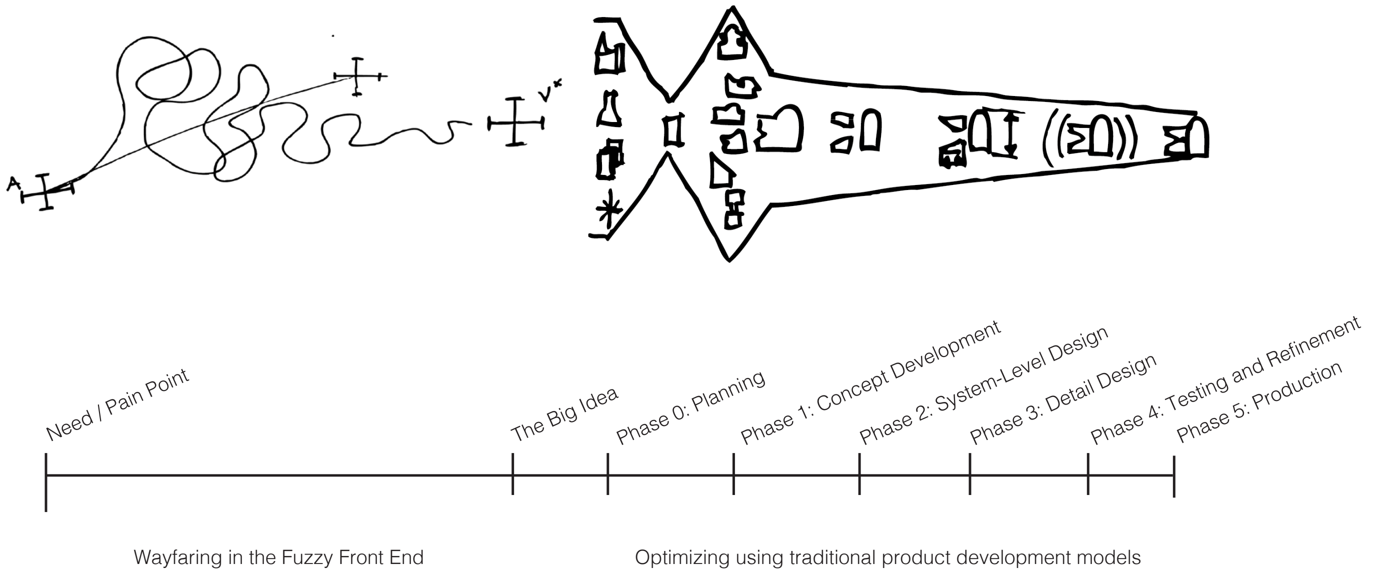
Need / Pain Point
The Big Idea
Phase 0: Planning
Phase 1: Concept Development
Phase 2: System-Level Design
Phase 3: Detail Design
Phase 4: Testing and Refinement
Phase 5: Production
Wayfaring in the Fuzzy Front End
Optimizing using traditional product development models

Discussion of Work Method

The goal of this project was to explore several techniques, and furthermore see which technique could provide the best output. By observing which cause provided what effect, could causes that provided desired effects be brought into the next round - a means of trial and error. The focus was not on optimizing one technique, as other later stage models such as Ulrich and Eppinger (2012) provide better tools for, nor was it on inducing a rule between cause and effect, as is common in traditional research.

Consequently, using the Wayfaring model had a large impact on the outcome of the project. Especially was having short sprints of design-build-test, by using rough prototypes, an enabler for testing many techniques in a short amount of time. This allowed for failing quickly and cheaply at an early stage, before too much time and money had been invested. Moreover, this approach was a tradeoff between accuracy and speed. It is likely that more traditional research approach would have provided more accurate data from each experiment, that might have been beneficial later in the project. However, it would also have been slower, leaving fewer techniques to be explored. In hindsight was this speed crucial for the evolution of the project. Furthermore, by reflecting after each round of probing could the next step be decided from the latest information available. An example of this was when it was decided to apply release agent to the molds. Although one eventually could have found the same information by spending more time of the project on a literature review, one would also have missed other important learnings such as setting the right melting temperature or melting time of the polymer.

Is Direct Rapid Tooling the Way to Go?

Direct rapid tooling enables prototyping the form, fit, function and feasibility of a plastic product in a relative short amount of time. In the case of SBS, the size of most injection molded components fit well within the size limitations of direct rapid tooling, although there are limitations on complexity of the geometry. It is therefore important to acknowledge the strengths and weaknesses of each direct rapid tooling technique. For smaller parts, some additive manufacturing techniques can be beneficial, while for larger parts, subtractive techniques might be the only option. Furthermore can less complex geometry be injection molded with lower pressure. In which case, a cheaper and less strong mold material can be utilized.

Moreover, direct rapid tooling is not intended as a direct replacement for neither rapid prototyping nor structural finite element analysis. Rather, the prototyping resolution should be increased gradually throughout the project (see figure 67). In the early phases of product development, where prototypes are used for learning, and product meanings can be dominant probing markers, the fit, function and feasibility can be perhaps the least relevant attributes to the product. For this purpose, rapid prototyping, or even lower resolution prototyping is better suited. Likewise will a structural FEA contribute to awareness of the loading situation. By identifying areas of high stress and stress concentrations under certain loading conditions, can design improvements be implemented in a short amount of time.

One final matter to address is the inevitable question of will additive manufacturing technology replace traditional manufacturing methods such as injection molding? The answer can be yes, maybe or no. Perhaps, one day, additive manufacturing will become so rapid that it will take over all plastic production. Until this day, will advances in additive manufacturing contribute to the progression of direct rapid tooling.

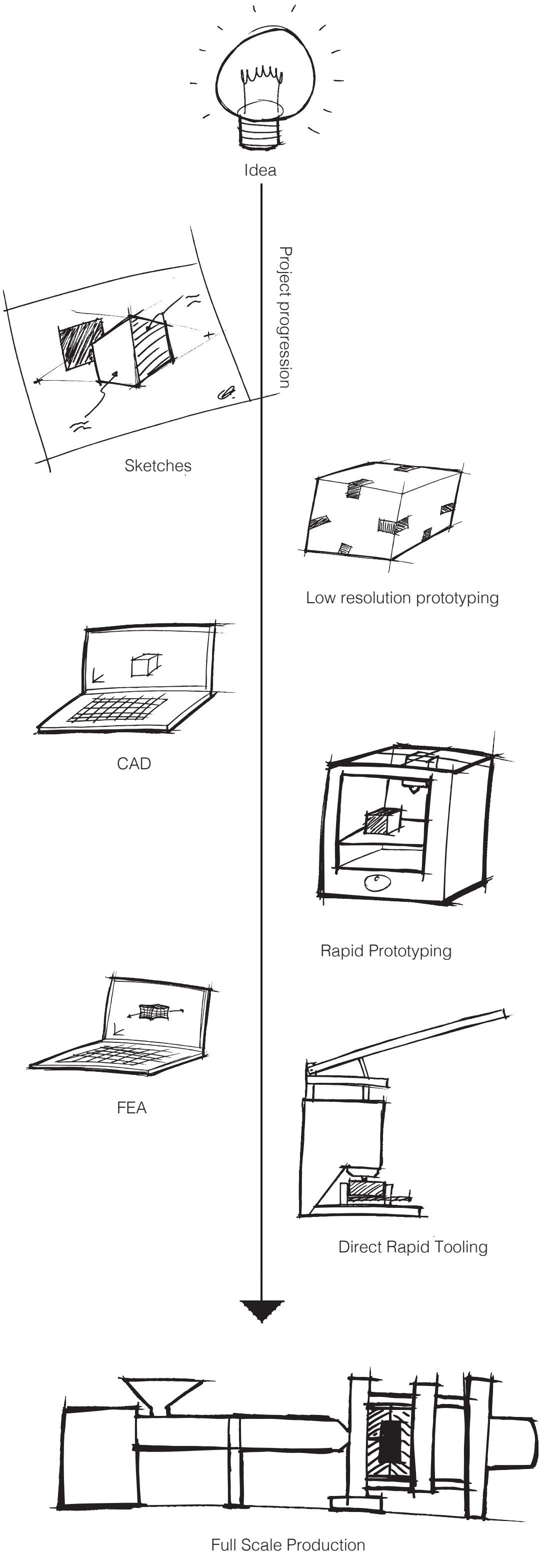

Figure 67: The prototyping resolution should be adapted to the progress of the project. In the early stages, the prototypes should be kept rough and rapid to enable quick learning and explore possibilities. Later, the resolution should be increased in order to converge (Standford Bootcamp Bootleg, 2015).

Chapter Ten

Concluding Remarks and Further Work

Concluding Remarks

The most common way of producing thermoplastic products is through injection molding. However, due to expensive tooling, it is hard to justify building prototypes. Deciding on a design without empirical evidence can lead to costly and time consuming design re-loops, in which can harm the competitive advantage of companies. Consequently, it was desirable to find a cheap, efficient and effective way of prototyping injection molded components.

This thesis investigated direct rapid tooling techniques for low volume injection molding production. By Wayfaring, and using prototypes for learning, several direct rapid tooling techniques were explored. Molds were fabricated using rapid prototyping techniques such as fused deposition modeling, selective heat sintering, laminated object manufacturing, polymer jetting and CNC-milling. The molds were tested using a self-built desktop injection molding machine, and the molded components were tested using three point bending. Furthermore, a more complex mold was CNC-milled and tested in a full scale injection molding machine. The tested techniques were evaluated with respect to cost, efficiency and effectiveness.

From the study, it was found that polymer jetting VeroBlackPlus-material could fabricate molds quickest, and with best quality of the tested techniques. Although fused deposition modeling a nylon-based polymer, named alloy 910, and CNC-milling high density polyurethane foam were cheaper, they had limitations in terms of speed, quality and consistency. Furthermore, it was demonstrated how evaluating the form, fit, function and feasibility of a plastic product by direct rapid tooling, could be performed by desktop injection molding (for smaller components) or by utilizing tool inserts in production injection molding machinery.

A concluding remark is that employing direct rapid tooling techniques can be a good way of prototyping various dimensions of a plastic component. Moreover, the question of whether or not to invest in a prototype, or which direct tooling- or rapid prototyping technique should be employed, highly depend on the situation. For SBS can utilizing direct rapid tooling of structural design features contribute to rapid learning, and furthermore reducing the time-to-market. For the small entrepreneurial company about to sell their first 200 products, can employing direct rapid tooling for these low volumes remove an enormous barrier to enter the market. Conversely, for the artist evaluating his or her design with respect to aesthetics, would direct rapid tooling be a long detour, and consequently should additive manufacturing be employed instead.

Further Work

Although several techniques for direct rapid tooling were tested in a short period of time, many remains. Some techniques were left unaddressed due to availability of rapid prototyping machinery and materials. Others were left unaddressed simply because of time constraints. Nonetheless, if more time and resources were available, the following techniques would have been explored.

CNC-milling MDF

Medium density fiber boards (MDF) is a cheap wood material made from soft wood. The wood is broken down to wood fibers, which in turn is combined with glue and wax to form MDF-panels. The benefit of utilizing MDF over wood is that MDF is an isotropic material that does not warp, and is easier to machine. In "Requirements Exploration Through Iteratively Emerging Critical Functionality From Prototyping" (see appendix A), we explain an approach for using MDF-molds in the prototyping of a high-end carbon fiber bike saddle. More specifically is the rough milling performed in the soft MDF-material. The roughed surface is then coated with epoxy, which soaks several millimeters into the surface. The fine milling can then be performed in a hard material, leaving a hard and smooth finish with good dimensional stability. Unfortunately, because of load capacity issues with the Roland MDX-540 CNC mill, this approach was left untested for direct rapid tooling.

CNC-milling Tooling Boards

In "Alternative Materials for Rapid Tooling", King and Tansey (2001) discusses the use of novel tooling boards, such as the Cibatool 2000, for rapid tooling. From the product datasheet, it can be seen that the Cibatool 2000 is an aluminum reinforced composite material, consisting of fine aluminum particles in an epoxy matrix (Vantico, 2000). King and Tansey further explain that the milling can be performed in one step, leaving a good surface finish. They also claim that the milling can be more than five times faster than milling aluminum, and that it is capable of producing several hundred parts. The price is not mentioned.

Selective Laser Sintering of Alumide

Selective laser sintering (SLS) is a high-end additive manufacturing technique similar to SHS. This technique allows for using composite powders, such as alumide, for additive manufacturing. According to Materialise (2016), alumide is a blend of aluminum and polyamide powders that create a metal-esque, non porous material. Senior researcher at Sintef Materials and Chemistry, and contributor to the AddForm project, Erik Andreassen, explained in an interview that they had good results with using alumide for direct rapid tooling (personal communication, September 2015). Because an SLS-machine was not available, this technique was not tested.

Polymer Jetting Digital ABS2

3D-printing giant Stratasys claim on their web site that they achieved good results with utilizing their DigitalABS2 material, in combination with polymer jetting, for direct rapid tooling. In contrast to alumide is DigitalABS2 not reinforced with any metal. Because this material is only compatible with selected Stratasys 3D-printers, which were not accessible, this technique was not tested.

Surface Treatment with Seram Coatings

The NTNU-based start up company, Seram Coatings, claim to have made the hardest thermal spray coating in the world. Their technology revolves around thermal spraying of silicon carbide (SiC) onto surfaces to reduce abrasion. According to research engineer in Seram Coatings, Emil Valaker, is it possible to utilize this coating on plastics. However, he also explain that the coating is very brittle, so that little or no deformations are allowed in the coated surface (personal communication, May 2016).

References

Beaudoin-Lafon, M., Mackay, W.. (2003). Prototyping Tools and Techniques. In: Sears, A., Jacko, J.A. (Eds.). *The Human-Computer Interaction Handbook*. Mahwah: Lawrence Erlbaum Associates.

Bogue, R.. (2013). 3D Printing: The Dawn of a New Era in Manufacturing?. *Assembly Automation, 33 (4)*, 307 - 311.

Boparai, K.S., Singh, R., Singh, H.. (2016). Development of rapid tooling using fused deposition modeling: a review. *Rapid Prototyping Journal, 22,* 281-299.

Cards PLM Solutions. (2016). CAM. Retrieved June 9th from https://www.cardsplmsolutions.nl/en/plm-software/nxa/cam-3/screenshots

Cera, B. (2014). Copper Electroplating/forming 3D Prints. Retrieved Jan 22nd 2016 from http://bryancera.blogspot.no/2014/09/copper-electroplatingforming-3d-prints.html

Cleveland, B.. (2008). When Low-Volume Injection Molding Makes Cents. Retrieved Mar 30th 2016 from: http://www.makepartsfast.com/2008/06/527/when-low-volume-injection-molding-makes-cents/

Colton, J.S., Crawford, J., Pham, G., Rodet, V.. (2001). Failure of Rapid Prototype Molds during Injection Molding. *CIRP Annals - Manufacturing Technology, 50 (1),* 129 - 132.

Dang, V.Q.. (2013). *The Design, Manufacturing and Testing of an Undertray for Formula SAE* (Bachelor Thesis, OSU). Oregon: OSU.

Design Guidelines: Injection Molding. (2016). Retrieved May 31st 2016 from https://www.stratasysdirect.com/resources/injection-molding/

Ekelund, D.I.. (2015). *3D Printet Paper as Structural Material* (Master's Thesis, NTNU). Trondheim: NTNU.

Elverum, C.W., Welo, T.. (2015). On The Use of Directional and Incremental Prototyping in the Development High Novelty Products: Two Case Studies In the Automotive Industry. *Journal of Engineering and Technology Management, 38*, 71 - 88.

Fitchmun, D.R., Mencik, Z.. (1973). Morphology of Injection-Molded Polypropylene. *Journal of Polymer Science, 11*, 951 - 971.

Fujiyama, M., & Awaya, H.. (1977). Mechanical Anisotropy in Injection-Molded Polypropylene. *Journal of Applied Polymer Science, 21*, 3291-3309.

Gate types. (2016). Retrieved March 25th 2016 from https://en.wikipedia.org/wiki/Injection_mold_construction#Gate_types

Gerstenberg A., Sjöman, H., Reime T., Abrahamsson, P., & Steinert, M.. (2015). A Simultaneous, Multidisciplinary Development and Design Journey - Reflections on Prototyping, *Entertainment Computing - ICEC*, Trondheim: Researchgate.

Groover, M.P.. (2011) *Principles of Modern Manufacturing, SI Version*. John Wiley & Sons Ltd.

Hammond, J.S., Keeney, R.L., Raiffa, H. (1998). The Hidden Traps in Decision Making. *Best of Harvard Business Review*.

Hartmann, B., Klemmer, S.R., Bernstein, M., Abdulla, L., Burr, B., Robinson-Mosher, A., Gee, J.. (2016). Reflective physical prototyping through integrated design, test and analysis. *Proceedings of the 19th annual ACM symposium on User Interface software and technology*, New York: ACM. 299 - 308.

Injection-molded Part Radiusing and Draft Guidelines. (2008). Retrieved March 23rd 2016 from https://www.protolabs.com/injection-molding/fundamentals-of-molding/draft

Karapatis N.P., van Griethuysen J.-P.S., Glardon R.. (1998). Direct Rapid Tooling: a review of current research. *Rapid Prototyping Journal, 4 (2)*, 77 - 89.

King, D., Tansey, T.. (2012). Alternative materials for rapid tooling. *Journal of Materials Processing Technology, 121*, 313-317.

Kucklick, T.R.. (2013). *The Medical Device R&D Handbook*, 2nd edition. CRC Press.

Kickstarter. (2015). Orbit1: A Tabletop Electroplater Turns Your Ideas into Gold. Retrieved Nov 5th 2015 from https://www.kickstarter.com/projects/1499748748/orbit1-a-tabletop-electroplater-turns-your-ideas-i?ref=discovery

Kittilsen, K., Balters, S., Steinert, M.. (2016). Introducing the Wayfaring Approach for the Development of Human Experiments in Interaction Design and Engineering Design Science, *International Design Conference - Design 2016*. Dubrovnik: the Design Society.

King, D., Tansey, T.. (2003). Rapid tooling: selective laser sintering injection molding. *Journal of Materials Processing Technology, 132*, 42 - 48.

Lacey, R.M. (1964). *U.S. Patent no. US 3305460 A*. Method of electroplating plastic articles: Google Patents.

Lim. Y.-K., Stolterman, E., Tenenberg, J.. (2008). The Anatomy of Prototypes: Prototypes as Filters, Prototypes as Manifestations of Design Ideas. *ACM Transactions on Computer-Human Interaction (TOCHI), 15 (2)*, 1-27.

Malloy, R.A.. (2011). *Plastic Part Design for Injection Molding, an Introduction, 2nd edition*. Hanser Publications. chapter 5: Prototyping and Experimental Stress Analysis

Masood, S.H., Song, W.Q.. (2004). Development of new metal/polymer materials for rapid tooling using Fused deposition modelling. *Materials and Design, 25*, 587-594.

Materialise. (2016). Laser Sintering: Materials and Datasheets. Retrieved May 5th 2016 from http://manufacturing.materialise.com/laser-sintering-materials-datasheets-0

McCurdy, M., Connors, C., Pyrzak, G., Kanefsky, B., Vera, A.. (2006). Breaking the Fidelity Barrier: An Examination of our current characterization of prototypes and an example of a mixed-fidelity success. In: *Proceedings of the SIGCHI Conference on Human Factors in Computing Systems.*

OM BE Plast. (2016). Addform. Retrieved May 3rd 2016 from http://www.ombe.no/index.php/utvikling/item/118-addform

Pahl, G., Beitz, W.. (1988). *Engineering Design: A systematic approach*. Springer.

Polanco-Loria, M., Clausen, A. H., Berstad, T., & Hopperstad, O. S.. (2010). Constitutive Model for Thermoplastics with Structural Applications. *International Journal of Impact Engineering, 37*, 1207-1219.

Proto-pasta. (2016). Conductive PLA. Retrieved April 21st 2016 from https://www.proto-pasta.com/pages/conductive-pla

Rogers, T. (2015). Five Things You Need To Know About Injection Molding. Retrieved June 9th 2016 from https://www.creativemechanisms.com/blog/five-things-you-need-to-know-about-injection-molding

Rosochowski, A., Matuszak, A.. (2000). Rapid tooling: state of the art. *Journal of Materials Processing Technology, 106*, 191-198.

Røstum, H. H.. (2014). *Behaviour and modeling of Injection Molded PP* (Master thesis, NTNU). Trondheim: NTNU.

Steinert, M., Leifer, L.J., (2012) ‘Finding One’s Way’: Re-Discovering a Hunter-Gatherer Model based on Wayfaring*. *International Journal of Engineering Education, 28 (2)*, 251-252.

Sælen, K.. (2012). *Validation of Material Model for Polypropylene (PP)* (Master thesis, NTNU). Trondheim: NTNU.

Ullman, D.G.. (2010). *The Mechanical Design Process, 4th ed*. New York: McGraw/Hill.

Ulrich, K.T., Eppinger, S.D.. (2012). *Product Design and Development, 5th ed*.. New York: McGraw/Hill.

Vantico. (2000). Cibatool Board Material Datasheet. Retrieved Feb 6th 2016 from http://www.lindberg-lund.com/files/Tekniske%20datablad/VAN-EXPR2000-TD.pdf

Viswanathan, V., Linsey J.. (2011). Design Fixation in Physical Modeling: An Investigation on The Role of Sunk Cost, *Computer and Information in Engineering Conference*, Washington DC: ASME.

Wikipedia. (2016). Electroplating. Retrieved June 5th 2016 from https://en.wikipedia.org/wiki/Electroplating

Wu, C. H.., & Liang, W. J.. (2005). Effects of Geometry and Injection-Molding Parameters on Weld-Line Strength. *Polymer Engineering & Science, 45 (7)*, 1021-1030.

Youmans, R.J.. (2011). The effects of physical prototyping and group work on the reduction of design fixation. *Design Studies, 32 (2)*, 115 - 138.

Young, M.K. et al. (1997). *U.S. Patent no. US 5641448 A*. Method of producing plastic injection molds for prototype parts: Google Patents.

Appendix A

Publication to the 26th CIRP Design Conference

Available online at www.sciencedirect.com

ScienceDirect

Procedia CIRP 00 (2016) 000–000

www.elsevier.com/locate/procedia

26th CIRP Design Conference

Creating Dynamic Requirements Through Iteratively Prototyping Critical Functionalities

Carlo Kriesi[a]*, Jørgen Blindheim[a], Øystein Bjelland[a], Martin Steinert[a]

[a] *NTNU Trondheim, Richard Birkelandsvei 2b, Trondheim 7491, Norway*

* Corresponding author. Tel.: +47 469 41 893; *E-mail address:* carlo.kriesi@ntnu.no

---

Abstract

This paper introduces the wayfaring model for requirement generation. Rather than pre-fixing requirements, we propose exploring unknown unknowns, and suggest finding and adapting the emerging set-based requirements while exploring. Fundamentally, as primary navigation tool towards final requirements, we propose to find and use critical functionalities iteratively, within interlaced knowledge domains. The model argument is based on two cases: The developments of a conceptual desktop plastic injection molder incl. control system, and the iterative prototyping of molds for a lightweight carbon fiber composite bike saddle. In both projects, the critical functionalities dominate the direction of the next prototype and consequently proven design specifications emerge.

© 2016 The Authors. Published by Elsevier B.V.

Selection and peer-review under responsibility of Professor Lihui Wang.

Keywords: Critical Functionality; Prototyping; Case Study; Manufacturing; Abductive Learning; Emerging Requirements

---

1. Requirement exploration

Prototypes are a powerful tool in product development and can be interpreted in a variety of ways. While some industries might see a prototype as the last few stages before being ready for serial production, we present two case studies where we used *'prototypes to learn'*, as Leifer and Steinert [1] put it. In the early product development phase where the final specifications are not yet known, some 'future' problems are not yet on the radar, and are hence lacking a valid solution ('unknown unknowns') [2]. This pre-lean product development phase is crucial, as later changes to the design and to the requirements will create enormous costs [3]. In this paper we propose a method that helps finding these unknown unknowns when tackling the challenge of developing a completely new product where the problem definition and requirement specifications still contain many degrees of freedom. Once these requirements are established, one can rely on other methods, such as systems engineering and lean, where this proposed method could provide viable requirement inputs, as described in Haskins et al. [4].

1.1. Build to learn

Ulrich and Eppinger [5] give a broad definition of what a prototype is: *'An approximation of the product along one or more dimensions of interest'*. Along the lines of the d.school philosophy we see prototypes as *'anything that takes a physical form'* [6]. Elverum and Welo [7] point out that even for complex physical products where the costs of a prototype are high, it is even more important to understand how to prototype in an efficient manner in order to save money and still have highly valuable learning outcomes. Even quickly built, low-resolution prototypes can give the development team crucial information about potential shortcomings of their design early on in the design process [8,9]. Furthermore, different kinds of prototypes provoke different discussions within design teams [10]. However, they should be *'designed to answer questions'* [11]. We propose to use wayfaring in order to find the right questions and use the answers in the best way possible, namely to iteratively find and further refine requirements for the following development steps.

2212-8271 © 2016 The Authors. Published by Elsevier B.V.
Selection and peer-review under responsibility of Professor Lihui Wang.

1.2. Wayfaring and probing a vision

Schrage [11] describes product development cultures in organizations as *'Spec-driven'* and *'Prototype-Driven'*, where in the first case the prototypes are designed according to predefined specifications, and in the latter case the specifications are constant subject to change under the influence of the various learnings from the prototypes. We see the prototype-driven development culture as a crucial element of the wayfaring model [12]. Similar to an explorer in the age of Columbus that sets sail in order to find new lands, a product development team departs to find the really big idea, and follows a vision and some vague and often imprecise or even wrong information (wayfaring). The opposing manufacturing analogy would be today´s cargo ship that create a steady just in time supply route over the oceans by following a pre-defined, optimized route to specific GPS locations (navigation). By prototyping and testing quickly and early on in the journey, the 'explorer' team can learn and consciously reflect on the outcome [13] and, unlike in pure 'trial and error', find new 'tracks' that nudges them in a promising direction towards the vision. Gerstenberg et al. [14] describe the process as follows: The journey consists of many probes, where each '*probe is a circle of designing, building and testing of an idea or prototype'*. In addition, they propose to prototype simultaneously in interlaced knowledge domains, creating multi-level probe-circles where each level represents one discipline involved in the development process. Fig. 1 and Fig. 2 graphically represent this process. Such iterative probing circles also increase the designers' confidence in their solution [8,9].

1.3. Critical functionality and functional requirements

Developing and refining a completely new product is – unlike in incremental product development – a long exploration of unknown unknowns and subsequent specifications. However, how can one find and create these requirements? During the wayfaring journey described above, one will deduct certain critical functionalities from the prototypes that need to be fulfilled in order to arrive at the really big idea. Especially in complex systems, these critical functionalities are often not foreseen since the solution is discovered along the way. By probing solutions for these critical functionalities we discover dynamic functional requirements, or evolving set-based requirements. Studies have emphasized the importance of the latter, as they do not constrain the future development, unlike when working with point-requirements [3,15]. The next prototyping iteration can then build onto the newly discovered functional requirement, until a satisfying solution is found.

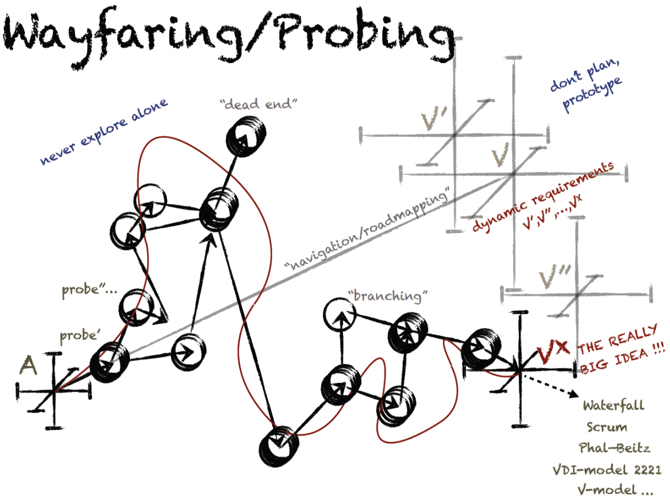
Wayfaring/Probing
"dead end"
never explore alone
dont plan, prototype
V'
V
dynamic requirements V',V'',..,V^x
"navigation/roadmapping"
probe''...
probe'
A
"branching"
V''
Vx
THE REALLY BIG IDEA !!!
Waterfall
Scrum
Phal–Beitz
VDI-model 2221
V-model ...

Fig. 1. The Wayfaring Process (From [14]).

Since it is not possible to map out all possible solutions to a complicated problem beforehand, there is no guarantee to arrive at the global optimum. However, through multiple probing cycles one can be confident that one will arrive at the best local optimum within the explored solution-space.

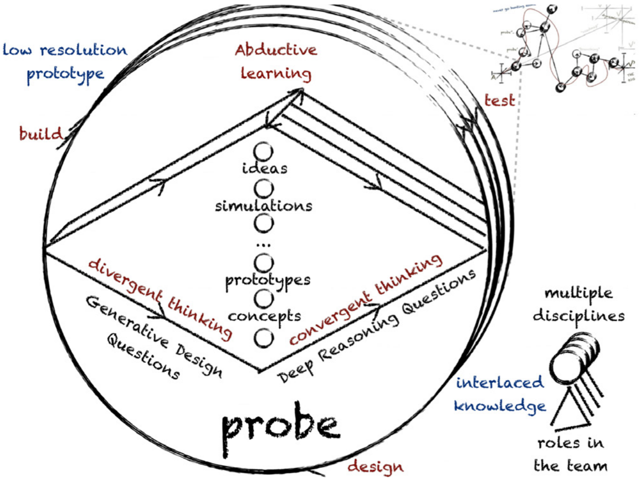
low resolution prototype
Abductive learning
build
test
ideas
simulations
...
prototypes
concepts
divergent thinking
Generative Design Questions
convergent thinking
Deep Reasoning Questions
multiple disciplines
interlaced knowledge
roles in the team
probe
design

Fig. 2. Multi-Layer Probing Circle (From [14]).

1.4 Case studies

To support our proposition of using the wayfaring as a tool to discover critical functionalities and creating dynamic requirements, which in turn become dominant probing markers and design features, we analyze the following two case studies of development journeys: The development of a desktop injection molder, and the path to the first prototypes for a high-end carbon fiber bike saddle. In both projects, the direction shifted multiple times during the wayfaring process and critical functionalities that emerged along the way became the focus of intensive probing.

2. Case study: desktop plastic injection molder

2.1. Finding a need through wayfaring

Our first example is the development of a desktop sized plastic injection molder. The project started with a vision to improve the handover from CAD-models to injection-molded components in a major Scandinavian company. Because of expensive tooling, the design phase of injection molded plastic parts is critical. Moreover, if a component is designed poorly, and the tooling is manufactured accordingly, significant re-work is required on the tooling. This is both costly and can delay the product launch significantly.

The starting point for the project was initially to do finite element analysis (FEA) of plastic components to obtain knowledge of their structural integrity. However, after doing several rounds of probing, by testing both linear- and nonlinear approaches to FEA, as well as looking into the manufacturing process of injection molding, it became clear that FEA was too time consuming within the boundaries of the project. Therefore, we decided to shift our focus into prototyping.

The idea was now to explore different ways of prototyping injection molded components. We explored several techniques, such as additive manufacturing, indirect- and direct rapid tooling. Several of these techniques seemed very promising. However, a critical obstacle to overcome was to provide realistic mechanical properties in the prototype. From the prototyping techniques listed above, direct rapid tooling was the only technique that would provide these properties. In order to get a first feeling for whether or not we should proceed with this approach, we did a quick round of probing. By making polymer molds using a fused deposition modeling 3D-printer, and using a glue gun to simulate an injection molder. The question was to see if such a simple approach created any useful results.

After seeing that prototyping injection molded components using direct rapid tooling was within reach, we continued pursuing this path. However, a reoccurring problem was that there was no good way to test the various prototyping techniques, as this required full-scale injection molding machinery. Neither the company nor we had direct access to such infrastructure. Thus, we set off to build a simple injection-molding machine that could be used in a near-office situation. The according wayfaring journey is illustrated in Fig. 3.

2.2. Using critical functionality as navigation tools

The basic principles of injection molding are to melt a polymer, and then inject it into a cavity. We therefore continued our wayfaring journey by isolating the *critical functionalities*, namely heat and pressure, and probing them separately.

For pressure, we looked for inspiration in existing solutions, such as hydraulic clamps, full-scale injection molding machinery, and sealant guns. After probing several of these concepts, we learned that a purely mechanical solution would be suitable. The first requirement that emerged was therefore that the injection molder should be hand operated.

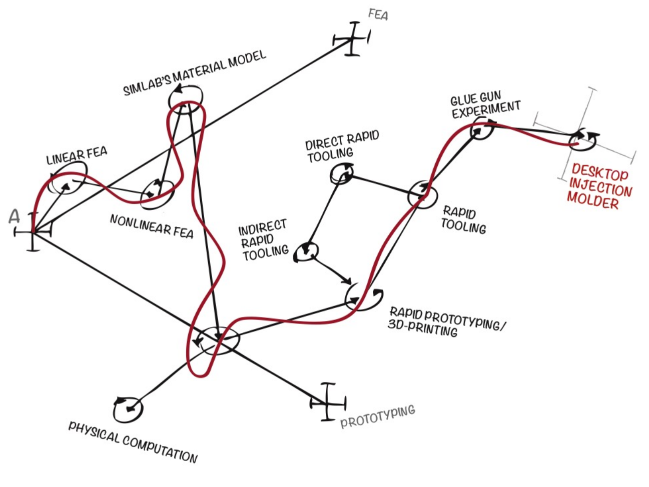

Fig. 3. The wayfaring journey leading up to the injection molder.

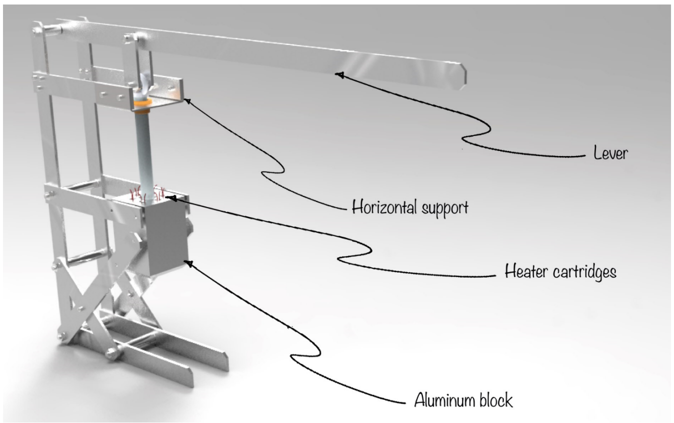

Fig. 4. CAD model of the mechanical structure.

The next round of probing consisted of sketching a cantilever-based design, and building a low-resolution cardboard prototype. Although at this point we only had one requirement, several more would emerge along the way. Because the injection molder had to be able to inject a minimum amount of volume, the height of the injection chamber, and consequently the minimum stroke, emerged. The prototype also showed the need for a horizontal support and a free link connected to the cantilever. Another advantage of the cardboard prototype was that it was easy to move around the pivot points in order to test various cantilever setups. Therefore, a smoothly working mechanism quickly emerged. A rough hand calculation of the theoretical maximum pressure provided by the current design gave a thumbs-up for moving on.

For heat, we considered stovetops, autoclaves and heater cartridges. However, seeing that some additive manufacturing technologies, such as fused deposition modeling, utilize heater cartridges to heat a nozzle, we identified that the same concept could be applied for the injection molder. Essentially, this meant heating a block of metal (in this case aluminum) by the means of heater cartridges. The requirements were therefore that the aluminum block had to fit multiple heater cartridges, serve as a heat medium, an injection chamber, and a nozzle.

2.3. Designing the details

Having found requirements for the critical functionalities, the remaining requirements and subsequent design emerged from what was available in terms of materials in the workshop and as well a few off-the-shelf components.

While physically building the structure, the CAD-model would serve as an interim reference (see Fig. 4). Consequently, if unknown unknowns were discovered while building, and changes had to be made to the design at this point, we would update the CAD-model accordingly.

2.4. Developing the heating system

Critical functionalities were also the main drivers for designing the heating system. This mechatronic system requires prototyping in three interlaced knowledge domains simultaneously, namely the software, electronic, and mechanical domains.

The three different sub-sections of critical functionalities are: Powering the heater cartridges; measuring the temperature; controlling the temperature. All sections were first prototyped independently and then combined with the other sections, in order to form a complete heating system.

For powering the heater cartridges, we used an Arduino Uno microcontroller and a breadboard. This combination allowed for probing several different circuit designs in a short period of time. The idea of our circuit design was to use a low voltage to control a transistor, which in turn controls a higher voltage. It took multiple probing circles of trying various bipolar junction transistors, metal-oxide-semiconductor field effect transistors and solid-state relays (SSR) before experiencing that an SSR was more robust and easier to use.

For measuring and subsequently controlling the temperature in the heater block, we used a k-type thermocouple. The code and circuit for the thermocouple was tested independently, before it was implemented together with the cartridge system. Finally, based on an open source proportional integral differential (PID) algorithm, the different software sections were combined to form a functioning controller.

2.5. Testing

The desktop sized injection molder was finally tested. Although the design had shortcomings, we managed to successfully injection mold simple test geometries. Some of the requirements that emerged along the journey and were tested are:

- The injection molder must be hand operated.
- The lever system must provide enough pressure to inject the polymer melt into the cavity.
- The heater cartridges must heat the aluminum block to at least 200°C.

The developed injection molder is currently being used in a research project investigating how to improve the handover between CAD-models, 3D printed prototypes and injection molded components.

3. Case study: carbon fiber bike saddle

3.1. Introduction

Our second example of employing the wayfaring model is the development of a novel solution for lightweight carbon fiber bicycle saddles. Traditional bike saddles are connected to seat posts in a way that requires a complex design, giving high stress concentration in the connection interfaces. This complex design makes the saddle heavy, and also more prone to failures. The project started with an idea of a new way of joining the saddle to the seat post, to overcome these shortcomings. For patentability reasons, the details of the actual design will not be disclosed here.

The critical obstacle to overcome in this project was to establish a good manufacturing method. Because of the critical functionalities, namely being light and strong, carbon fiber was an obvious material choice for the saddle. However, in order to reduce tooling cost while prototyping, low-resolution manufacturing methods were employed, namely using medium density fiber (MDF) molds for as long as possible. Along the journey, critical functionalities were used as the main navigation tool to allow dynamic functional requirements to emerge.

3.2. Building a proof-of-concept prototype

For obvious reasons, the joint between the saddle and the seat post had to be strong enough to support the weight of a human being. This was our first critical functionality. Before our initial design with respect to this critical functionality, we built a low-resolution prototype out of wood. From this prototype we could decide most requirements for the geometric shape of the joint. However, the prototype provided no information on how the design performed with respect to real life loads. We therefore decided to build a proof-of-concept prototype.

The aim of the next round of probing was to see how the design would perform when made from carbon fiber. We aimed at making the parts in the easiest and cheapest way possible to maintain pace, and have rapid learning cycles. Carbon fiber composite is the preferred material due to the ability to build lightweight structures. The unique thing about carbon fiber is the ability of tuning the material properties by adjusting the fiber orientation within each individual ply. Furthermore, carbon fiber pre-impregnated with epoxy (prepreg) was preferred because it is easier to handle in the manufacturing process when compared to dry fibers. The basic principle of manufacturing laminates is to cut and stack prepreg plies in a mold, and then apply heat and pressure to consolidate the laminate. The molds are usually made from metal, which provides a good surface finish. However, this also makes them expensive. Therefore, we decided to make the molds from a cheaper material.

Using CAD/ tools for modeling the geometry enabled us to CNC-mill the molds from MDF blank. After milling, we sealed the surface of the mold with epoxy, and then sanded it to a smooth finish, as this allowed for easier demolding of the saddle, as well as creating a good surface finish. The finished mold with the prepreg panels was then put in a sealed bag and a vacuum pump was used to pull vacuum, thus compressing the laminate. Finally, an oven was used to add heat during the curing cycle.

The seat post was made using a different approach: We rolled plies of prepreg on a mandrel and firmly wrapped the layup with PET film. When heat was added the film shrank, thus compressing the laminate. The other parts required to assemble the saddle and seat tube were similarly made by compressing prepreg around 3D-printed ABS male molds, which were left within the finished part.

Testing the saddle revealed a lack of strength in the joint, and geometric requirements were further refined and implemented in the CAD model. However, we could clearly see that we were heading in the right direction to realize this product as a lightweight solution.

3.3. Improving the design

For the next iterations of prototyping the focus was to get user feedback on the saddle geometry and joint strength.

To keep the prototyping costs at a low level, we decided to stick to MDF molds. To eliminate the need for sanding thereof we further improved the tooling process by sealing the surface with epoxy before doing the fine milling. This way we could do the rough milling in a soft material, and get a hard surface to do the fine milling afterwards, leaving a high tolerance machined surface with limited need for sanding and polishing. This new approach to making molds successfully enabled for rapid testing of multiple geometries of the saddle in order to increase the rider's comfort.

However, at this point it became apparent that MDF releases fumes at the elevated temperatures during the curing cycle. Unfortunately, these fumes enter the vacuum pump where they condense and gradually damage the pump. Furthermore, heating of the mold is time consuming and inaccurate, as the heat has to be transferred by convection or radiation. Also, the porous nature of MDF, even when coated with epoxy, made it necessary to put the whole mold in a vacuum bag in order to compress it. Another drawback is the exothermal reaction that takes place in laminates due to the low thermal conductivity of MDF.

Despite these disadvantages, using MDF enabled us to test and optimize the saddle design in a cheap and fast way to a point where it satisfied our expectations.

3.4. *Transitioning to aluminum molds and heat control*

The focus for the next iterations was on the critical functionalities of the curing process, namely: Heat, pressure, and debulking of the prepreg. Now that the design of the saddle itself was according to the original vision, it made sense to invest in a high-end mold made of aluminum.

The high conductive heat transfer coefficient of aluminum allows for direct heating of the mold, by the means of heat cartridges, and subsequent precise temperature control. The curing cycle consists of three phases: Ramp up, curing, and ramp down of the temperature, and each phase has to be specifically set according to the prepreg used. An emerging requirement was therefore precise temperature control.

Although there are commercial temperature controllers available, making our own was faster and cheaper. Similar to the heating system for the injection molder described above, we used the Arduino platform to run a PID-controller in combination with an SSR. Adding a touch display allowed for easy tailoring of the curing cycle. Fig. 5 shows the heat controller connected to the aluminum saddle mold.

Also, the upgrade to the aluminum mold enabled us to simplify the vacuum process by using the flange of the molds as sealing points. From struggling with regular vacuum bagging material, we learned that silicone bladders provide a superior solution, since they allow for higher curing temperatures, and are reusable.

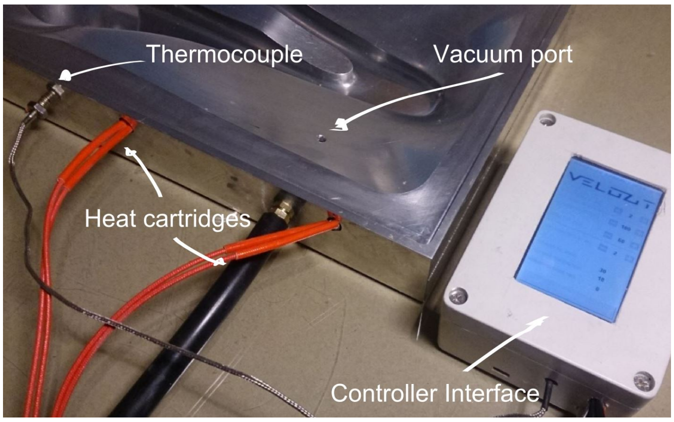

Fig. 5. Detailed view of heating system in the saddle mold.

While the overall quality of the parts increased as expected, it became clear that increased curing pressure was the next critical functionality that needed probing.

3.5. *Increasing curing pressure*

Prepregs are usually cured at high pressure assisted by an autoclave or by internal bladder inflation in order to reduce voids in the material.

For the first iterations of molding the seat post, we inflated a bicycle tube to achieve the internal pressure required to compress the laminate towards a female mold. From probing different bladder types, the functional requirements thereof emerged. It had to be flexible, and it had to be able to withstand up to 185°C. Silicone is a suitable material for this task. Using additive manufacturing and casting techniques, we were able to make the bladders according to the newly found requirements. Fig. 6 shows an illustration of the design and layup in a seat tube mold.

We realized that the same process can be utilized for the saddles: By clamping a lid on top of the mold, the silicone bladder, originally used to obtain vacuum, is supported by adding external pressure between the lid and the bladder (see Fig. 7).

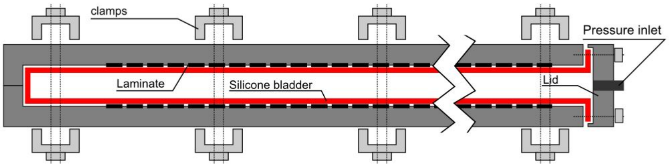

Fig. 6. Design and layup within the seat post mold.

3.6. *Summary*

This journey of prototyping critical functionalities has taken us from the initial concept idea to arrive at a final product that is adapted to a manufacturing process allowing for low tooling costs and low production costs compared to that of autoclave processed parts. Through iteratively prototyping critical functionalities, ever more specific requirements describing both the product itself and its manufacturing process have been continuously improved. Some of these were:

- The shape of both, the joint and the saddle itself.
- A high-end surface finish.
- Adjustable curing cycles for different prepreg configurations.

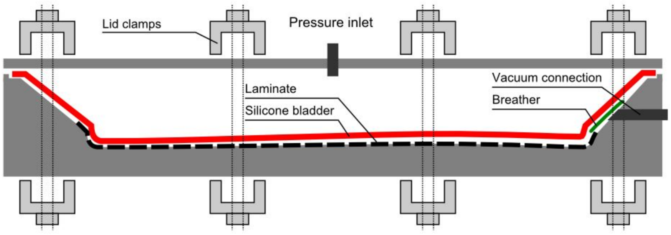

Fig. 7. Design and layup within the seat mold.

4. Closing remarks

We presented and analyzed two case studies of early stage product development processes that used the wayfaring method as a tool to discover critical functionalities and subsequent requirements. This approach helped in two fundamentally different projects: The desktop injection molder, where the external design was driven by the critical functionalities and the fulfillment thereof, and the bike saddle where the critical functionality had to fit in the external design that was predefined by standard dimensions for saddle and seat-post.

A benefit of employing the wayfaring model was the opportunity to discover *unknown unknowns,* for example the damaging nature of MDF molds, and adjust accordingly. This opportunity was primarily enabled by the probing loops of design-build-test. Of course intense simulation and external information gathering may have provided similar insights, but at significant higher costs esp. in terms of time and access/availability of expert information/services.

Furthermore, the iterative, repeating probing cycles allow for the emergence of prototype driven specifications, rather than specification driven prototypes. As pointed out by Schrage [11], are cultures in which prototypes determine specifications, such as in small entrepreneurial companies, more effective when information is scarce, and the outcome ambiguous. E.g. in the case of designing the electrical circuit with transistors instead of relays, testing was absolutely crucial for having a functional circuit. If the circuit had been designed without testing, a major design re-loop would have been inevitable.

Left unaddressed is the viability of this method within an industrial context, as this is part of ongoing research. However, empirical evidence, based on own experiences (e.g. Gerstenberg et al. [14]), and the engineering class ME310 that evolved into a hub for highly visionary industry projects [16], suggest that the iterative prototyping approach have a great potential within projects with high degrees of freedom.

One word of caution: It is unlikely that the wayfaring model as we applied it here provides similarly successful results when it comes to incremental later stage product-development, such as improving a certain product along the same critical functionalities, or when it comes to optimizing e.g. a production process. In these cases there are analysis and improvement tools available, such as lean, which fit a pre-defined solution space significantly better.

Acknowledgements

This research is supported by the Research Council of Norway (RCN) through its user-driven research (BIA) funding scheme, project number 236739/O30.

References

[1] Leifer LJ, Steinert M. Dancing with ambiguity: Causality behavior, design thinking, and triple-loop-learning. Information Knowledge Systems Management 2011:151–73.
[2] Sutcliffe A, Sawyer P. Requirements elicitation: Towards the unknown unknowns. Requirements Engineering Conference (RE), 2013 21st IEEE International, IEEE; 2013, p. 92–104.
[3] Kennedy BM, Sobek DK, Kennedy MN. Reducing Rework by Applying Set-Based Practices Early in the Systems Engineering Process. Systems Engineering 2014;17:278–96.
[4] Haskins C, Forsberg K, Krueger M, Walden D, Hamelin D. Systems engineering handbook. Int. Council on Systems Engineering; 2006.
[5] Eppinger S, Ulrich K. Product Design and Development. 5th Edition. New York: McGraw/Hill; 2012.
[6] Plattner H. Bootcamp bootleg. Design School Stanford, Palo Alto 2010.
[7] Elverum CW, Welo T. On the use of directional and incremental prototyping in the development of high novelty products: Two case studies in the automotive industry. Journal of Engineering and Technology Management 2015;38:71–88.
[8] Dow SP, Heddleston K, Klemmer SR. The Efficacy of Prototyping Under Time Constraints. Proceedings of the Seventh ACM Conference on Creativity and Cognition, New York: ACM; 2009, p. 165–74.
[9] Kriesi C, Steinert M, Meboldt M, Balters S. Physiological Data Acquisition for Deeper Insights into Prototyping. Proceedings of NordDesign 2014:580–9.
[10] Edelman JA, Leifer L, Banerjee B, Sonalkar N, Jung M, Lande M. Hidden in plain sight: affordances of shared models in team based design. Proceedings of ICED 09, the 17th International Conference on Engineering Design, vol. Vol. 2, Design Theory and Research Methodology, Palo Alto, CA, USA: The Design Society; 2009, p. 395–406.
[11] Schrage M. The Culture(s) of PROTOTYPING. Design Management Journal (Former Series) 2010;4:55–65.
[12] Steinert M, Leifer LJ. “Finding One”s Way': Re-Discovering a Hunter-Gatherer Model based on Wayfaring. International Journal of Engineering Education 2012;28:251.
[13] Schön DA. The reflective practitioner: How professionals think in action. vol. 5126. Basic books; 1983.
[14] Gerstenberg A, Sjöman H, Reime T, Abrahamsson P, Steinert M. A Simultaneous, Multidisciplinary Development and Design Journey – Reflections on Prototyping. In: Chorianopoulos K, Divitini M, Baalsrud Hauge J, Jaccheri L, Malaka R, editors. Entertainment Computing - ICEC 2015, vol. 9353, Cham: Springer; 2015, p. 409–16.
[15] Ward A, Liker JK, Cristiano JJ, Sobek DK. The second Toyota paradox: How delaying decisions can make better cars faster. Sloan Management Review 1995;36:43–61.
[16] Carleton T, Leifer L. Stanford’s ME310 course as an evolution of engineering design. Proceedings of the 19th CIRP Design Conference– Competitive Design, Cranfield University Press; 2009.

Appendix B

Excerpt from pre-master: Finite Element Analysis of Polypropylene

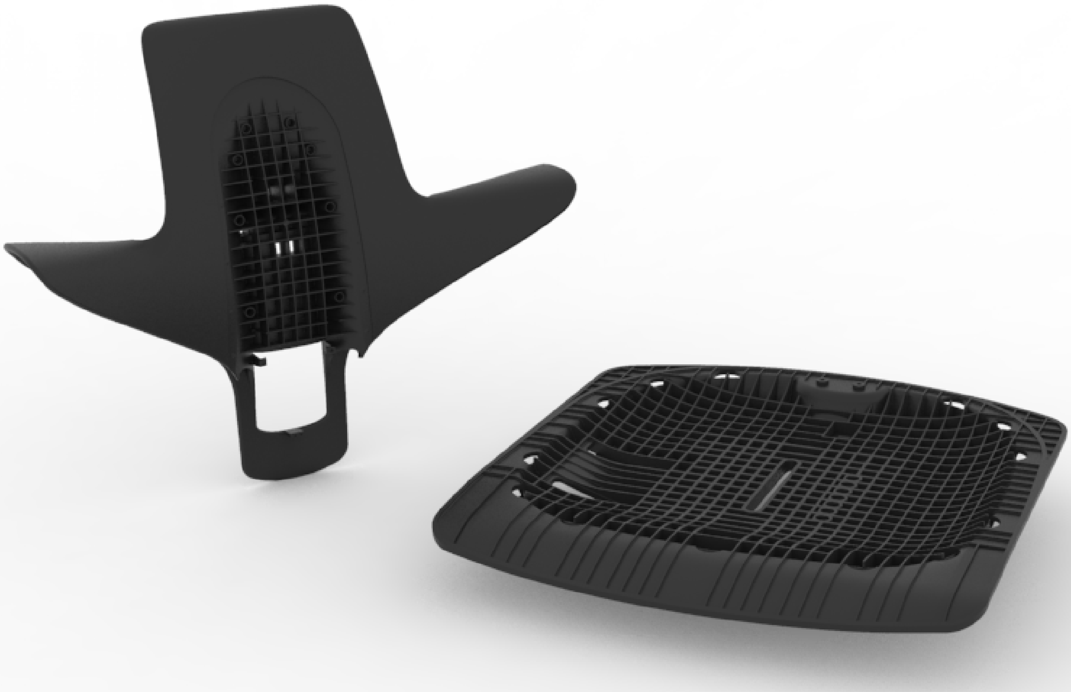

Figure B1: The HÅG Capisco Pulse backrest (left) and HÅG H09 seat (right).

Introduction

A very common way to obtain knowledge on the mechanical behavior of components is to perform a structural finite element analysis (FEA). The finite element method is a numerical technique of solving differential equations. An FEA analysis is always an approximation, and good results are thus achieved by minimizing error.

When performing FEA, geometry, normally created in a CAD-software, is divided into a finite number of elements. At the boundary of each element there are several nodes. For each node, an equation is solved, and data such as load, deformation, stresses and strains can be obtained. The governing equation being solved depends on what type of problem is addressed, and will be touched upon later.

Significant efforts on modeling the mechanical behavior of polypropylene have been done at NTNU SimLab by Arild Clausen (Mario Polanco-Loria et al., 2009) and his master students Kristin Sælen (2012) and Heine H. Røstum (2014). Some of their work will be restated here to give the reader an introduction to the topic. For in-depth studies, the master theses of Sælen and Røstum are recommended for further reading.

The realm of finite element simulations goes far beyond plastics. Therefore, a few selected SBS components, made from injection-molded polypropylene are studied. The components are displayed in figure B1.

Polypropylene

Polypropylene (PP) is a semi crystalline thermoplastic polymer, which is made from the monomer propene. A thermoplastic polymer consists of long molecular chains that sometimes can be covalently cross-linked. A semi crystalline thermoplastic polymer has a mix of crystalline and amorphous regions, depending on the orientation and packing of the molecular chains (Røstum, 2014). When subjected to loading, the amorphous regions are first uncoiled, and then crystalline areas are rotated and separated. Because the molecular chains can slide relative to each other, polymers can take large plastic deformations (Sælen, 2012). In the following paragraphs, it is assumed that PP is a homogeneous, isotropic material.

PP can exhibit linear elastic, hyperelastic, viscoelastic and viscoplastic behavior. In addition to this, PP has a higher yield stress in compression than in tension. A large amount of material models for simulating PP are available. However, leading experts on the field, Erik Andreassen at SINTEF Materials and Chemistry, and Arild Clausen at SimLab, NTNU, both agree that although there are many models available, the real challenge is to find a material model that provide good enough results, but is still easy to use. In the subsequent paragraphs, some approaches on simulating PP using FEA are presented.

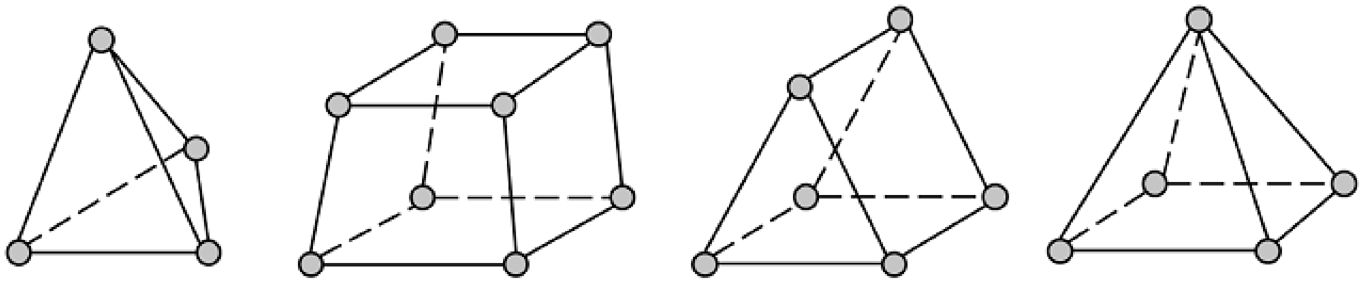

Figure B2: Four types of volume elements. From left to right: pyramid, hexahedral, triangular prism and tetrahedral.

Meshing

Common for all approaches is meshing. There are a number of different mesh types available in different finite element software. Generally, mesh types can be volume elements (3D) or shell elements (2D). Furthermore, volume elements can be divided into hexahedral (brick), triangular prism, pyramid and tetrahedral mesh (see figure B2). Shell elements can be divided into triangle and quadrilateral mesh.

Using shell elements is a common way of simplifying geometry, especially when working with thin structures such as composite materials. Because the computational power is a major concern when doing numerical simulations, these simplifications are often very useful. However, because of draft angles needed for manufacturability, shell elements will not be a realistic approach for injection-molded geometries, and volume elements should be used instead. Also, because of the complex geometry of the case components, tetrahedral meshing is the only mesh that will fully capture the geometry (see figure B3).

It is important to capture geometry properly to provide accuracy. The finer the mesh, the more accurate the solution will be. However, refining the mesh globally will significantly increase the number of equations needed to be solved, and thus also simulation time. Therefore, it is good practice to refine the mesh where stress gradients are high. Typical areas can be areas of stress concentrations such as corners and holes.

In addition to providing accuracy, the mesh quality will significantly influence convergence, or rate of convergence. For instance, if the mesh is too skewed, convergence issues will arise. This especially concerns nonlinear simulations. In many cases, if the mesh quality is poor, it is likely that the simulation will not converge at all, thus providing no result. Most finite element software's have a tool that allows for checking the mesh before commencing the simulation. These tools should be used.

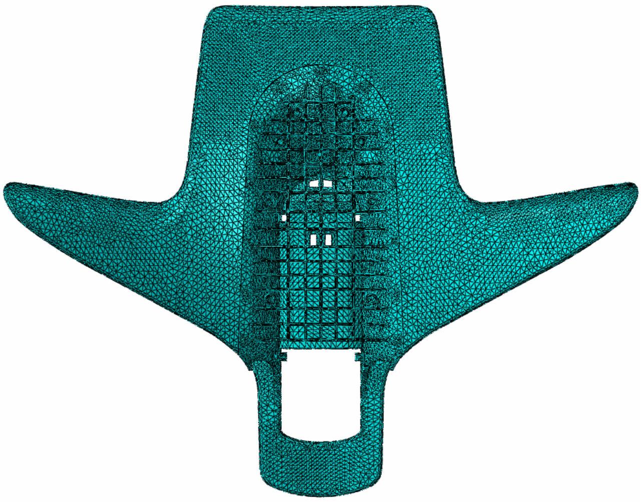

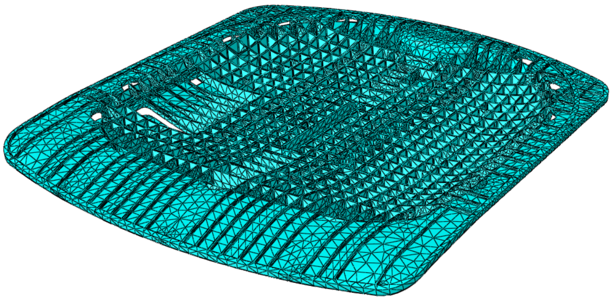

Figure B3: Meshing of the selected components. Both geometries are meshed using a tetrahedral mesh.

Linear Elastic Approach

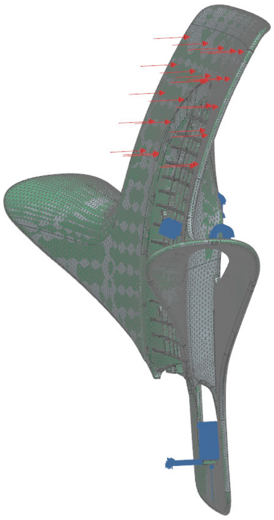

Most metals, and some polymers, exhibit linear elastic behavior. This means that when subjected to loading that does not exceed the yield stress, the material will return to its initial state. The relation between stress and strain in this area is linear, and is governed by Hooke's law (1):

$$\sigma = E \cdot \varepsilon \qquad (1)$$

The linear elastic approach is by far the most common FEA method applied in industry today. Often, solvers with good linear elastic capabilities are embedded in commercial CAD software such as Solidworks and Siemens NX. By assuming that the elastic part of the stress-strain curve is linear-elastic, conservative results can be achieved (see figure B7). This is often sufficient for structural purposes.

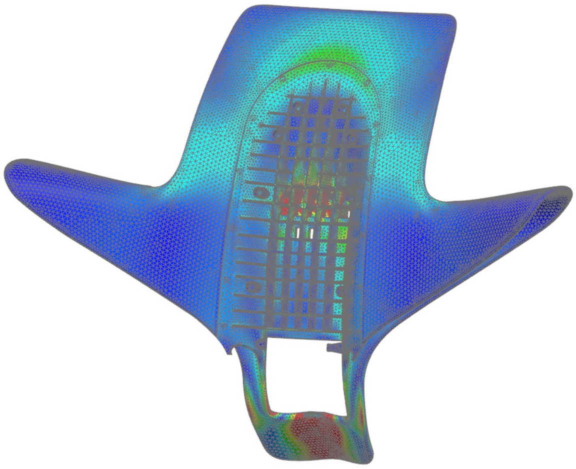

An example of a linear-elastic simulation performed of the HÅG Capisco Pulse backrest in NX Nastran is shown in figure B4. Here, a linear elastic material with Young's modulus 1600 MPa and Poisson's ratio ν = 0.45 was used. The load was an evenly distributed F = 1334 N, to simulate BIFMA loads, and boundary conditions as shown in figure B4. The material has a yield stress of approximately 30 MPa.

Because the load case should represent a realistic BIFMA test the chair has already passed, it is clear that the linear elastic approach gives somewhat conservative results. However, it is still possible to obtain critical areas of stress concentrations from the simulation.

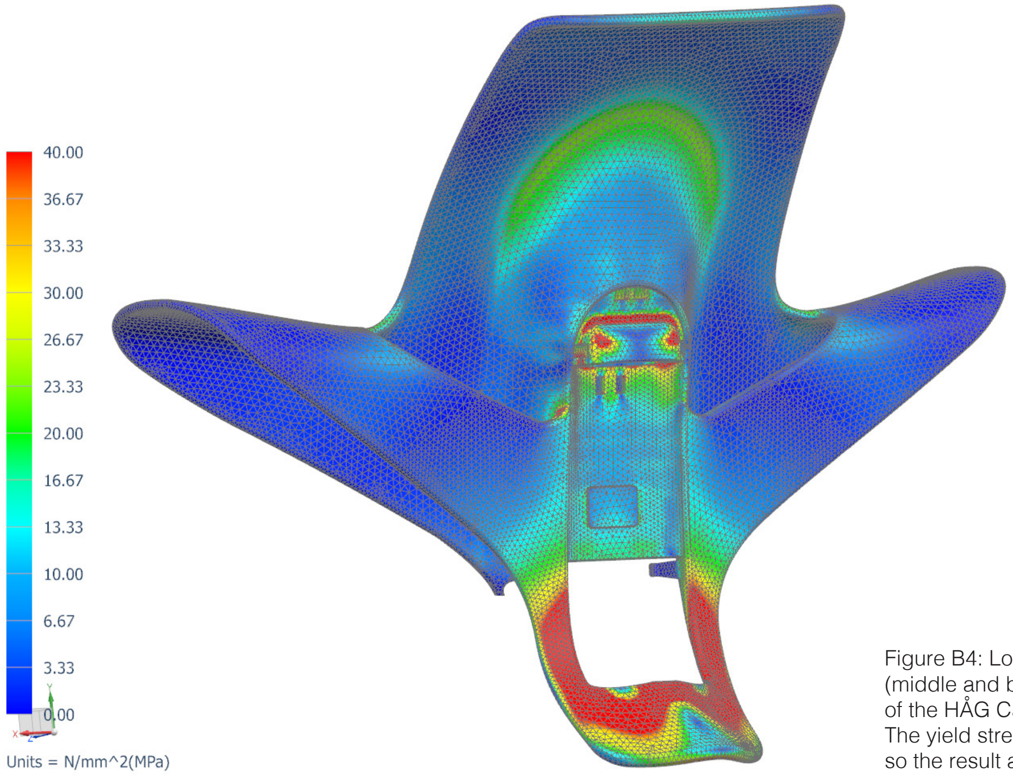

Figure B4: Load case (top) and results (middle and bottom) from a linear FEA of the HÅG Capisco Pulse backrest. The yield stress of PP is about 30 MPa, so the result are conservative.

Metal Plasticity Curve Approach

In contrast to most metals, PP is not fully linear-elastic. This means that the relation between stresses and strains in the elastic region do not follow Hooke's law entirely. Even at small deformations, there is a nonlinear relation between stresses and strains. By looking at nominal stress-strain curves supplied by SBS material supplier Rondo Plast, for recycled PP (see figure B7), this becomes evident. This is also shown in the work of Sælen (2012). Although conservative, a regular linear finite element analysis, solely based on Hooke's law will not provide the complete truth.

Governing Equations

One approach to address this issue is to use metal plasticity curves as an approximation. Valberg and Thaulow (2014) suggest four different models to capture the nonlinear behavior of metals. These are Ludwik's Law (1), the Swift relation (2), the Voces relation (3) and expanded Voces relation (4). For all relations, constants are determined through evaluation of experimental data.

$$\sigma = K\varepsilon^{n} \tag{2}$$

$$\sigma = A + K\varepsilon^{n} \tag{3}$$

$$\sigma = A - Be^{-C\varepsilon} \tag{4}$$

$$\sigma = A + D\varepsilon - Be^{-C\varepsilon} \tag{5}$$

Simulation Considerations

In order to perform nonlinear simulations, more advanced finite element software should be used. Although both NX Nastran and Solidworks have nonlinear capabilities, more documentation is available for advanced simulation software such as ABAQUS and ANSYS. In the following, the CAE software ABAQUS v 6.14 has been used.

An example of performing a nonlinear simulation of the Håg Futu seat, using a metal plasticity curve approach, can be seen in figures B5 and B6. The material is recycled polypropylene, using the data supplied by Rondo Plast. In ABAQUS, a new material with plastic properties can be defined. The material data supplied by Rondo Plast is then entered into ABAQUS through a table, in combination with a Young's modulus and Poisson's ratio. Here, a fixed boundary condition is used in combination with a forced displacement. When doing nonlinear simulations, it can be beneficial to enforce displacement, instead of applying a load, to reduce simulation time. The reaction forces can be collected in the post-processor.

Yield Criterion

As mentioned previously, PP exhibits significantly larger yield stress in compression than in tension (Sælen, 2012). In ABAQUS, this can be implemented using the Drucker-Prager yield criterion (2015), which is described by the following relation:

$$\sqrt{\frac{1}{6}\left[(\sigma_1-\sigma_2)^2+(\sigma_2-\sigma_3)^2+(\sigma_3-\sigma_1)^2\right]} = A + B(\sigma_1+\sigma_2+\sigma_3) \tag{6}$$

The constants A and B can be found using the following expressions:

$$A = \frac{2}{\sqrt{3}}\left(\frac{\sigma_c\sigma_t}{\sigma_c+\sigma_t}\right) \qquad B = \frac{1}{\sqrt{3}}\left(\frac{\sigma_t-\sigma_c}{\sigma_c+\sigma_t}\right) \tag{7}$$

Where σ_T is the yield stress in uniaxial tension, and σ_C is the yield stress in uniaxial compression.

For normal, static loading, using a metal plasticity curve, in combination with the Drucker-Prager yield criterion should give sufficient results. However, this approach is not suited for unloading conditions.

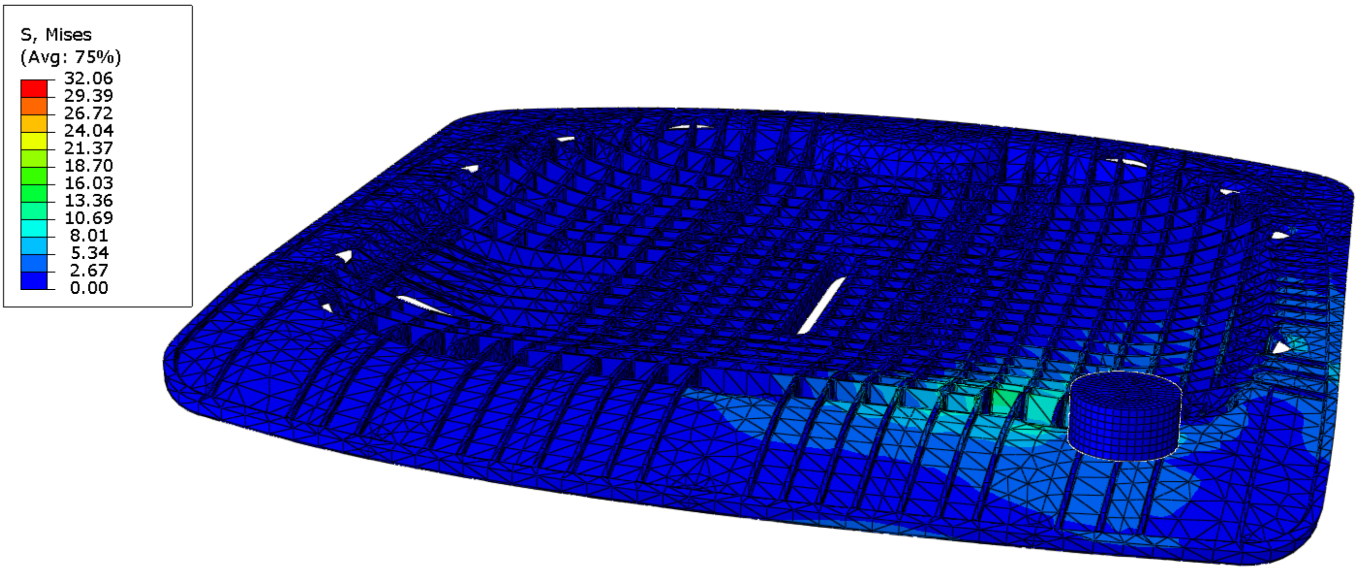

Figure B5: A nonlinear FEA of the HÅG H09 seat using a metal plasticity approach.

Hyperelastic, viscoelastic and viscoplastic approach

Strain Rate Dependent Behavior

PP exhibit both viscoelastic (Plazek & Plazek, 1983) and viscoplastic behavior (Sælen, 2012). Viscoelasticity means strain rate dependence in the elastic region, whereas viscoplasticity implies strain rate dependence in the plastic region. The rate of which a load is applied will therefore affect the deformation. In ABAQUS documentation, a viscoelastic material model is described as "(...) isotropic rate-dependent material behavior for materials in which dissipative losses primarily caused by "viscous" (internal damping) effects (...)".

In ABAQUS, viscoelastic behavior can be implemented through test data. Therefore, creep data, or stress relaxation data must be provided. Moreover, Creep is when a component deforms over time, subjected to a constant load. On the contrary, stress relaxation is when a loaded component exhibits a decrease in load under no change in deformation. Alternatively, viscoelastic data can be provided through Prony series (8). The Prony series describes the relaxation in the tensile-compression modulus, *E*, shear modulus, *G* and bulk modulus, *K*. ("Prony Series", 2015). The shear modulus relaxation can be expressed as:

$$G(t)=G_{\infty}+\sum_{i=1}^{N}G_{i}e^{\frac{-t}{\tau_i}} \tag{8}$$

Where t is time and τ_i are the relaxation times.

Similarly, viscoplastic data is supplied by adding creep data, or by providing constants for simple creep relations.

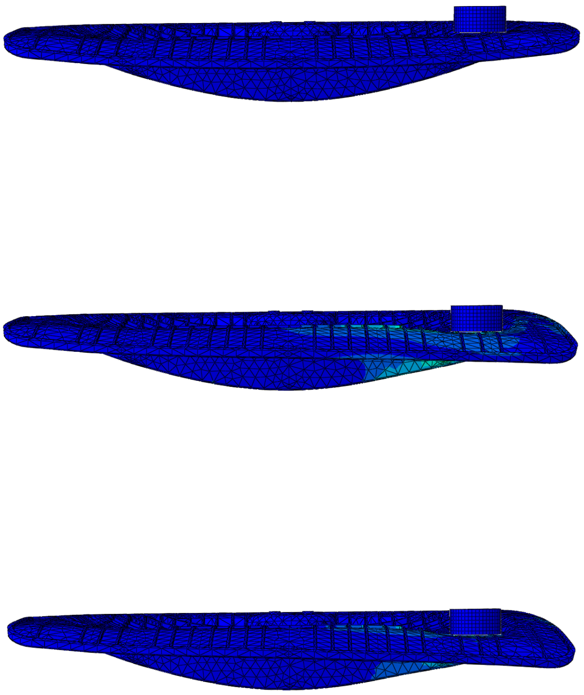

Figure B6: Deformation of the H09 seat from the metal plasticity approach.

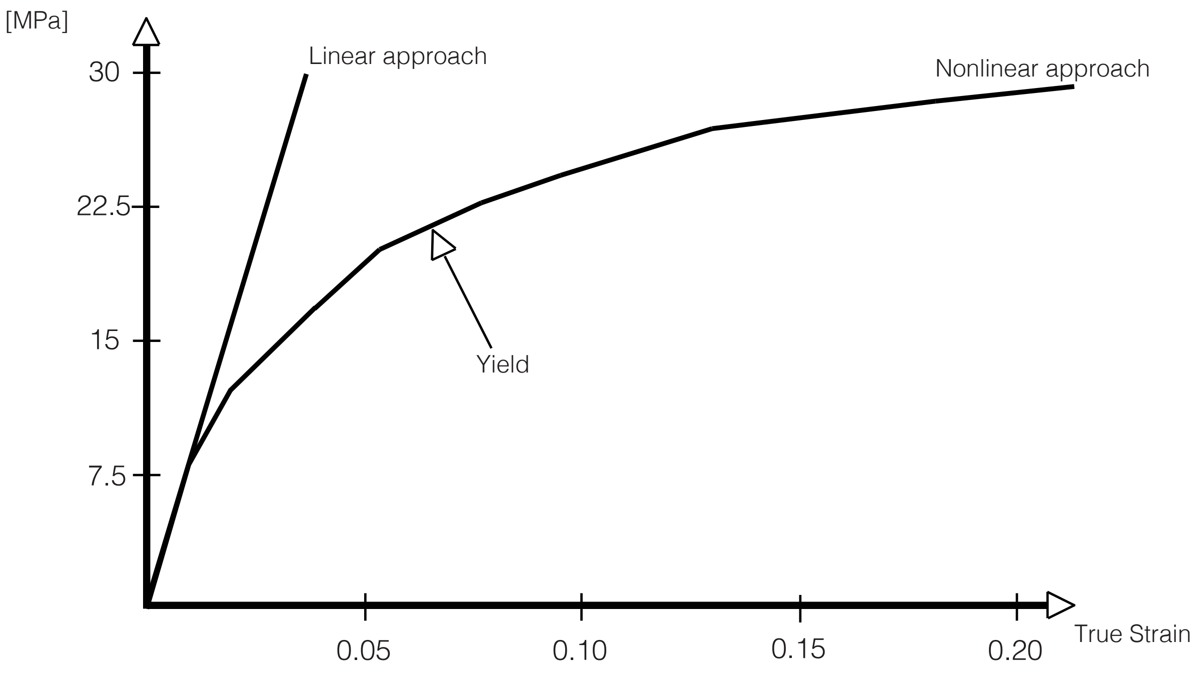

Figure B7: True uniaxial stress-strain curve for Recycled PP. Data provided by Rondo Plast.

Hyperelasticity

In order to capture the nonlinear elastic behavior of PP, a hyperelastic material model can be used. A hyperelastic model is derived from strain energy density functions, and assumes that the material is nearly incompressible. This results in path independent stress states (Polanco-Loria et al., 2010). Many hyperelasticity models are available in ABAQUS, including Neo-Hookean, Ogden, Marlow, Mooney-Rivlin, Polynomial form, Reduced polynomial form and Van der Waals form ("Abaqus documentation", 2015).

Analogous to a spring storing an amount of potential elastic energy, a material can also store elastic energy when subjected to deformation. For a Neo-Hookean material, which is the simplest of the hyperelastic models, this energy is given by the following expression:

$$U = C_{10}\left(\bar{I}_1 - 3\right) + \frac{1}{D_1}\left(J^{el} - 1\right)^2 \tag{9}$$

Where U is the strain energy per unit of reference volume. $\bar{I}_1$ is the first deviatoric strain invariant defined as

$$\bar{I}_1 = \bar{\lambda}_1^{\,2} + \bar{\lambda}_2^{\,2} + \bar{\lambda}_3^{\,2} \tag{10}$$

C_{10} and D_1 are temperature dependent parameters, which are calculated from the initial shear and bulk moduli:

$$\mu_0 = 2C_{10} \qquad K_0 = \frac{2}{D_1} \qquad \text{(11) and (12)}$$

Because we assume that we are dealing with an isotropic material, there are only two independent variables needed, namely the Young's Modulus *E*, and Poisson's ratio, ν. The initial shear and bulk moduli can be derived from these variables:

$$\mu_0 = G = \frac{E}{2\left(1+\nu\right)} \tag{13}$$

and

$$K_0 = K = \frac{E}{3\left(1-2\nu\right)} \tag{14}$$

Using the Neo-Hookean material model in ABAQUS, the parameters C_{10} and D_1 are entered. For virgin PP, these values could typically be

$C_{10} = 276.5$ and $D_1 = 0.00041$

When applying hyperelasticity to a material with a Poisson's ratio greater than 0.495, it is important to use hybrid elements to avoid convergence issues.

Testing

When trying to apply hyperelastic properties to the case examples, convergence was not achieved. However, good results were achieved on simple cubic geometries (see figure B8). The reason for these convergence issues is likely to be poor mesh quality. When performing nonlinear simulations in ABAQUS, the NLGEOM option must be enabled. This implies that the geometry is updated incrementally throughout the simulation. On the contrary, a linear simulation would have been based on the original geometry, and not been updated. Because the geometry is updated, and large deformations are imposed, this requires a good initial mesh. If the mesh becomes too skewed during the simulation, convergence will not be achieved.

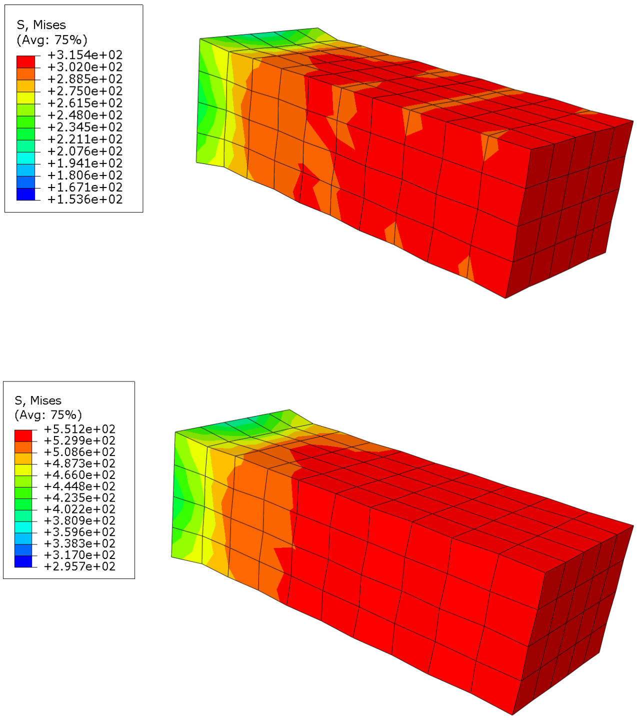

Figure B8: Linear elastic (top) and hyperelastic (bottom) simulations. Both cubes had the same boundary conditions, including the same forced displacement. As can be seen, the distribution of stresses are very similar.

SIMLab’s material model - a hyperelastic-viscoplastic model

NTNU SIMLab has developed a far more advanced material model with their hyperelastic-viscoplastic polymer model (Polanco-Loria et al., 2010). In figure B10, a rheological model that illustrates the major features of SIMLab’s polymer model is shown.

Røstum explain that the material model consist of two parts, an elastic and a plastic part. The elastic part takes into account the intramolecular resistance of the material, whereas the plastic part considers the stretching and breaking of molecular chains. The total strain deformation of the system can be written as

$$\varepsilon = \varepsilon^{e} + \varepsilon^{p} \tag{15}$$

Intramolecular resistance

The hyperelastic stresses, which represent the intramolecular resistance, can be expressed in terms of the following expression

$$\sigma_B = \frac{1}{J_B}\frac{C_R}{3}\frac{\bar{\lambda}_L}{\bar{\lambda}}L^{-1}\left(\frac{\bar{\lambda}}{\bar{\lambda}_L}\right)\left[B^{\bullet}{}_B - \bar{\lambda}_L{}^2 I\right] \tag{16}$$

Where L^{-1} is the inverse of the Langevin function defined as

$$L(x) = \coth(x) - \frac{1}{x} \tag{17}$$

The effective distortional stretch, $\bar{\lambda}$, is defined as

$$\bar{\lambda} = \sqrt{\frac{tr(B^{\bullet}{}_B)}{3}} \tag{18}$$

Where $B^{\bullet}{}_B$ is the distortional left Cauchy-Green deformation defined as

$$B_B^{\bullet} = F_B^{\bullet}(B_B^{\bullet})^T \tag{19}$$

and F_B is the distortional part of the deformation gradient expressed as

$$F_B^{\bullet} = J^{-\frac{1}{3}}F_B \tag{20}$$

The Jacobian determinant is defined as

$$J_B = J = \det(F) \tag{21}$$

Intermolecular resistance

To account for the difference in yield strength in tension and compression, Polanco-Loria et al. suggest using the Raghava yield criterion (Raghava & Caddell, 1973). This can be expressed as:

$$(\sigma_1-\sigma_2)^2+(\sigma_2-\sigma_3)^2+(\sigma_3-\sigma_1)^2+2\left(|\sigma_C|-|\sigma_T|\right)(\sigma_1+\sigma_2+\sigma_3)=2|\sigma_T\sigma_C| \tag{22}$$

Furthermore, by introducing the total stress invariant I_1 and the deviatoric stress invariant, J_2 , as well as the parameter alpha

$$\alpha = \left|\frac{\sigma_C}{\sigma_T}\right| \tag{23}$$

the Raghava yield criterion can be rewritten in terms of equivalent stress:

$$\bar{\sigma}_A = \frac{(\alpha-1)I_1 + \sqrt{(\alpha-1)^2 I_1^2 + 12\alpha J_2}}{2\alpha} \tag{24}$$

By introducing the Raghava yield criterion, the plastic flow, f_A , can be described:

$$f_A = \bar{\sigma}_A - \sigma_T - R = 0 \tag{25}$$

Where σ_T is the yield stress in uniaxial tension. The variable, *R*, is the hardening (or softening) parameter and is described by

$$R(\varepsilon^P) = (\sigma_S - \sigma_T)\left[1 - e^{-H\varepsilon^P}\right] \tag{26}$$

Where, σ_S is the saturation stress, *H* is the hardening parameter and ε is the plastic strain. To account for the viscoplastic behavior, Polanco-Loria et al. suggest the following relation:

$$\bar{\sigma}_A = \sigma_T\left(1 + C\cdot\ln\left(\frac{\dot{\varepsilon}_A^P}{\dot{\varepsilon}_{0A}} + 1\right)\right) \tag{27}$$

Where, *C* and $\dot{\varepsilon}_{0A}$ are strain rate sensitivity parameters.

Coefficients Required			
Poisson’s ratio	ν	Shear modulus	G
Pressure sensitivity coefficient	α	Saturation stress	σ_T
Reference strain rate	$\dot{\varepsilon}_{0A}$	Hardening parameter	H
Strain rate sensitivity coefficient	C	Locking stretch	$\bar{\lambda}_L$
Young’s modulus	E	Initial elastic modulus	C_R
		Bulk modulus	K

Table B1: Coefficients required for SIMLab’s material model.

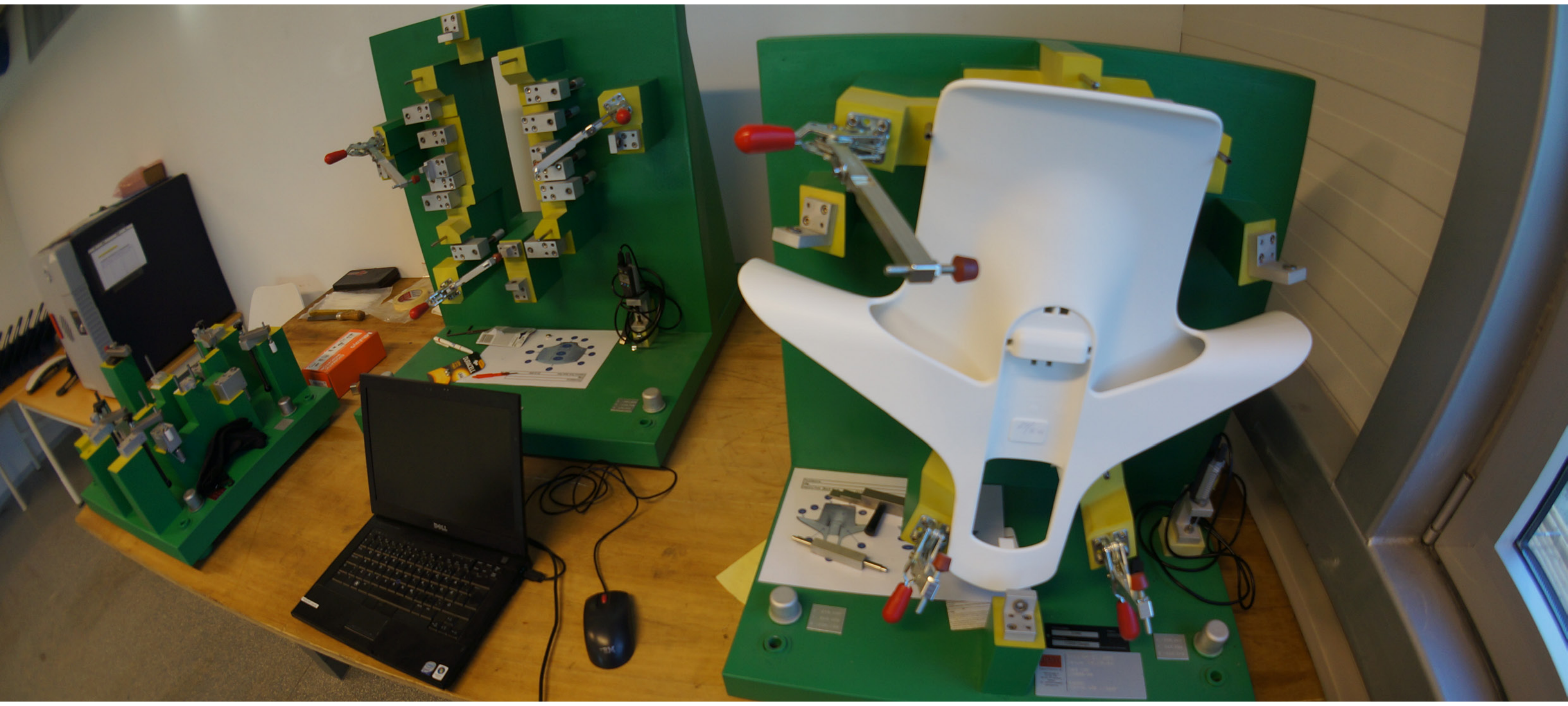

Figure B9: Controlling dimensions at Lycro.

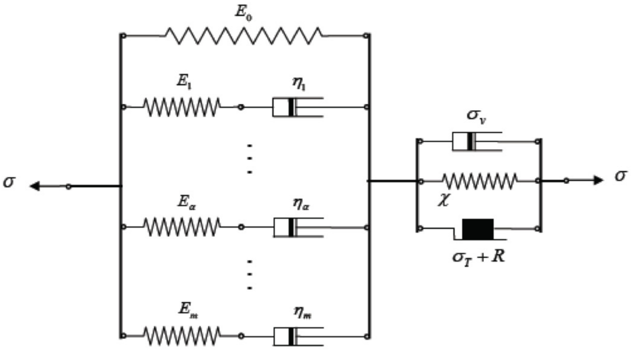

Figure B10: Rheological model of material model. Figure adapted from Røstum (2014).

References

Abaqus 6.14 Documentation, Analysis User's Guide (6.14). (2015) Retrieved Sep. 1st 2015 from http://50.16.225.63/v6.14/books/usb/default.htm

Drucker-Prager Yield Criterion. (2015). Retrieved Dec. 1st 2015 from https://en.wikipedia.org/wiki/Drucker–Prager_yield_criterion

Plazek, D., & Plazek, D.. (1983). Viscoelastic Behaviour of Atactic Polypropylene. *Macromolecules*, 16, 1469-1475.

Polanco-Loria, M., Clausen, A. H., Berstad, T., & Hopperstad, O. S.. (2010). Constitutive Model for Thermoplastics with Structural Applications. *International Journal of Impact Engineering, 37,* 1207-1219.

Prony Series. (2015) Retrieved Dec. 1st 2015 from https://en.wikipedia.org/wiki/Viscoelasticity#Prony_series

Raghava, R., & Caddell R. M. Yeh, (1973). The Macroscopic Yield Behaviour of Polymers. *Journal of Materials Science, 8*, 225-232.

Røstum, H. H.. (2014). *Behaviour and modeling of Injection Molded PP* (Master thesis, NTNU). Trondheim: NTNU.

Sælen, K.. (2012). *Validation of Material Model for Polypropylene (PP)* (Master thesis, NTNU). Trondheim: NTNU.

Thaulow, C., & Valberg, H. (2014). *Plastic Deformation and Fracture.* Trondheim: NTNU

Appendix C

Technical Drawings of TrollLabs Rapid Prototyping Injection Molder

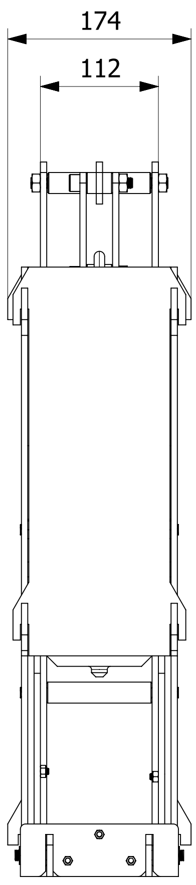

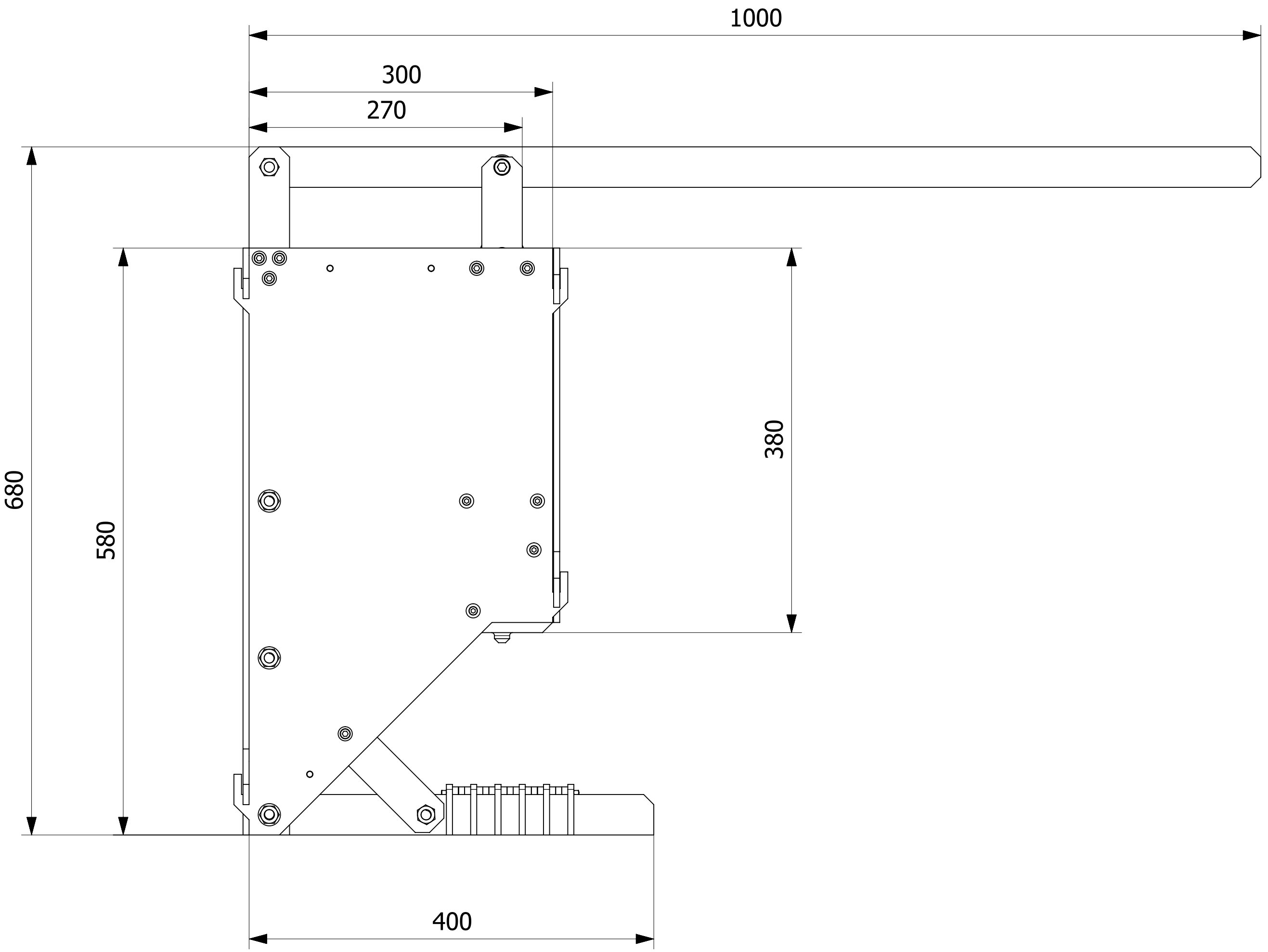
1000
300
270
680
580
380
400

Dato	Konstr./Tegnet	Godkjent	Maalestokk	NTNU - IPM
12/12-15	ØB	Projeksjonsmetode	1:5	
Project no. 10436600			TrollLabs	Erstatning for: / Erstattet av:
DIY INJECTION MOLDER				General tolerance: NS ISO 2786-MEDIUM
Henvisning:		Beregning:		

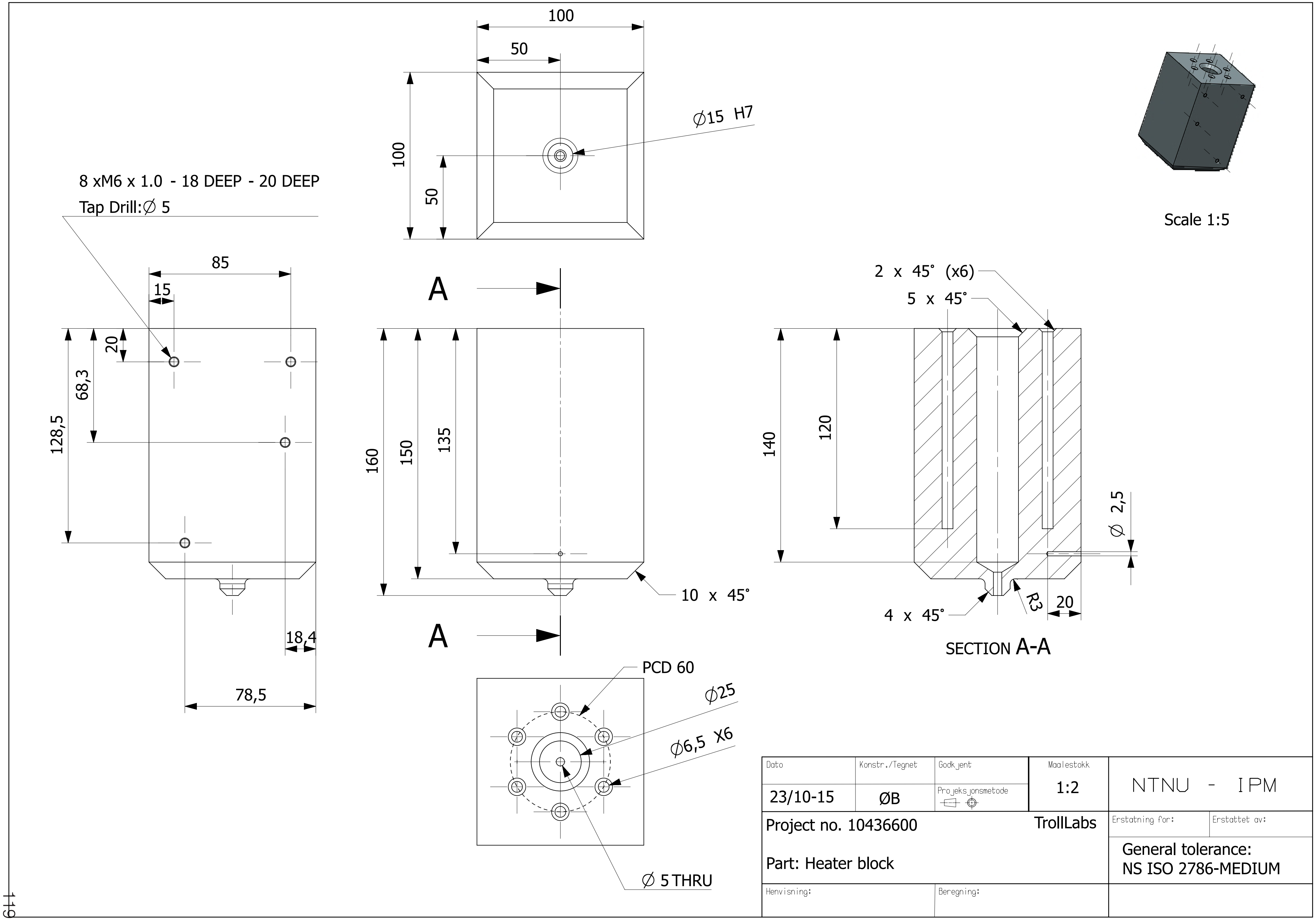
8 xM6 x 1.0 - 18 DEEP - 20 DEEP
Tap Drill:∅ 5
100
50
100
50
∅15 H7
Scale 1:5
85
15
20
68,3
128,5
18,4
78,5
A
A
160
150
135
10 x 45°
2 x 45° (x6)
5 x 45°
140
120
∅ 2,5
4 x 45°
R3
20
SECTION A-A
PCD 60
∅25
∅6,5 X6
∅ 5 THRU

Dato: 23/10-15
Konstr./Tegnet: ØB
Godkjent:
Projeksjonsmetode:
Maalestokk: 1:2
NTNU - IPM
Project no. 10436600
TrollLabs
Part: Heater block
Erstatning for:
Erstattet av:
General tolerance:
NS ISO 2786-MEDIUM
Henvisning:
Beregning:

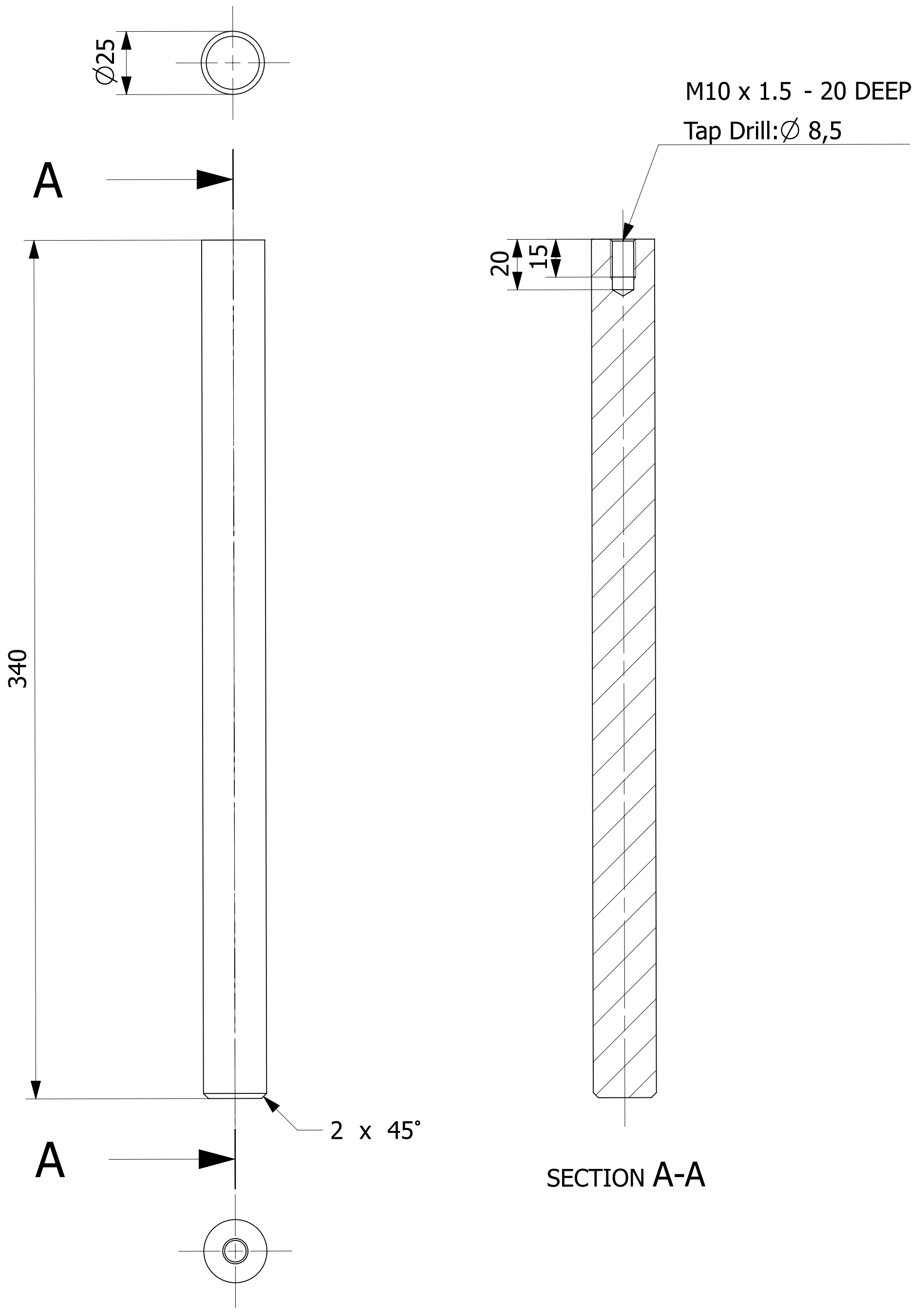
Ø25
A
340
2 x 45˚
A
M10 x 1.5 - 20 DEEP
Tap Drill:Ø 8,5
20
15

SECTION A-A

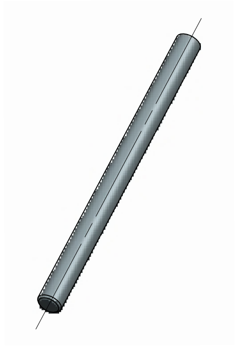

Scale 1:5

Dato	Konstr./Tegnet	Godkjent	Maalestokk	NTNU - IPM
2/11-15	ØB	Projeksjonsmetode	1:2	

Project no. 10436600

TrollLabs

Part: Piston

Erstatning for:

Erstattet av:

General tolerance:
NS ISO 2786-MEDIUM

Henvisning:

Beregning:

Appendix D

Arduino Code for PID-Controller

```
/********************************************************
 * Code for running cartridge heaters and regulating them through PID controller
 * with thermocouple measurement as input.
 * To be used for TROLLLABS Rapid Prototyping Injection Molder
 * A part of premaster work fall 2015.
 * Code put together by Oystein Bjelland (much is borrowed)
 ********************************************************/

//Thermocouple
#include <SPI.h>
#include “Adafruit_MAX31855.h”

//PID
#include <PID_v1.h>

//random variables-----------------------------------------------------------------
int i = 0;
long previousMillis = 0;
long interval = 1000;

// Thermocouple start---------------------------------------------------------------
#define DO  3
#define CS  4
#define CLK 5
Adafruit_MAX31855 thermocouple(CLK, CS, DO);

double Tin;
double iTin;

//Controller start------------------------------------------------------------------
//double Setpoint, Input, Output;

#define RELAY_PIN 10
double targetT;
//int power = 0; // power ranging from 0 - 255
//double dpower = 0;
double Output;

//Specify the links and initial tuning parameters
//double Kp=0.1, Ki=150, Kd=0.45;
double Kp=0.1, Ki=150, Kd=0.45;

PID myPID(&Tin, &Output, &targetT, Kp, Ki, Kd, DIRECT);

int WindowSize = 5000;
unsigned long windowStartTime;

// controller end-------------------------------------------------------------------

void setup()
{
  Serial.begin(9600);

  // setup controller start---------------------------------------------------------

  windowStartTime = millis();

  targetT = 190; //degrees celcius

  pinMode(RELAY_PIN, OUTPUT); //digitalWrite(RELAY_PIN, LOW);
  //pinMode(INPUT_PIN, OUTPUT); digitalWrite(RELAY_PIN, LOW);

 //tell the PID to range between 0 and the full window size
 myPID.SetOutputLimits(0, WindowSize);
 //tun the PID on
 myPID.SetMode(AUTOMATIC);

  // setup controller end------------------------------------------------------------
  // setup thermocouple-------------------------------------------------------------
  Serial.println(“MAX31855 test”);
  // wait for MAX chip to stabilize
  delay(500);
  // end thermocouple -----------------------------------------------------------------

Serial.println(“Ready”);

}

void loop()
{

  i = i + 1;

  //thermocouple loop start-------------------------------------------------------------

  //Check that thermocouple is working
  Tin = thermocouple.readCelsius();
  iTin = thermocouple.readInternal();

  if (isnan(Tin)) {
    Serial.println(“Something wrong with thermocouple!”);
    abort();

  }
  else {
   // Serial.print(“Tin = “);
   // Serial.println(Tin);
  }
  // thermocouple loop end--------------------------------------------------------------

  if (i == 1){
  Serial.println(“OUTPUT, TEMPERATURE, DESIRED TEMEPERATURE”);
  }

  //PID controller start-----------------------------------------------------------------

 unsigned long currentMillis = millis();

    //if(currentMillis - previousMillis > interval) {
     // previousMillis = currentMillis;

  myPID.Compute();
  //power = dpower;
  //analogWrite(RELAY_PIN, power);

  /************************************************
   * turn the output pin on/off based on pid output
   ************************************************/
  if (millis() - windowStartTime > WindowSize){
 // time to shift the Relay Window
   windowStartTime += WindowSize;
 }
  if (Output < millis() - windowStartTime) digitalWrite(RELAY_PIN, LOW);
  else digitalWrite(RELAY_PIN, HIGH);
    //else {
   // digitalWrite(RELAY_PIN, LOW);
  //}


 //PID controller end---------------------------------------------------------------------

 //Print variables to serial monitor------------------------------------------------------
    Serial.print(Output);
    Serial.print(“\t”);
    Serial.print(“”);
    Serial.print(Tin);
    Serial.print(“\t”);
    Serial.print(“”);
    Serial.print(targetT);
    Serial.println(“\t”);


}
```

Appendix E

Data from Three Point Bending

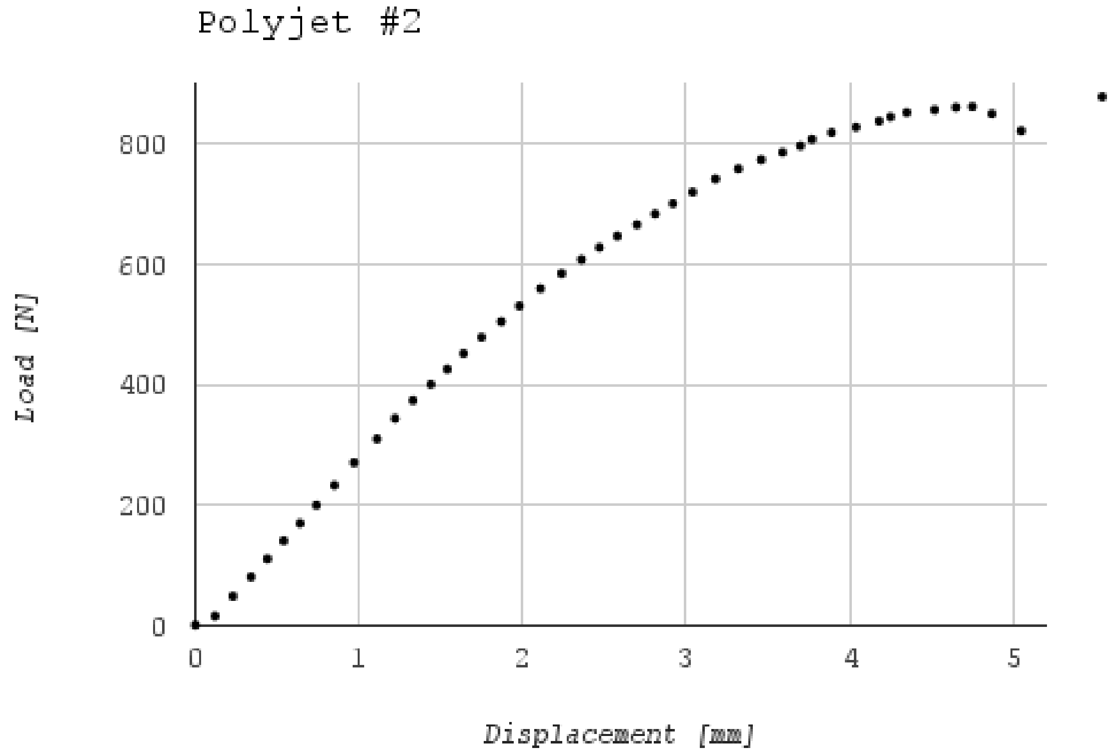

Polyjet #2

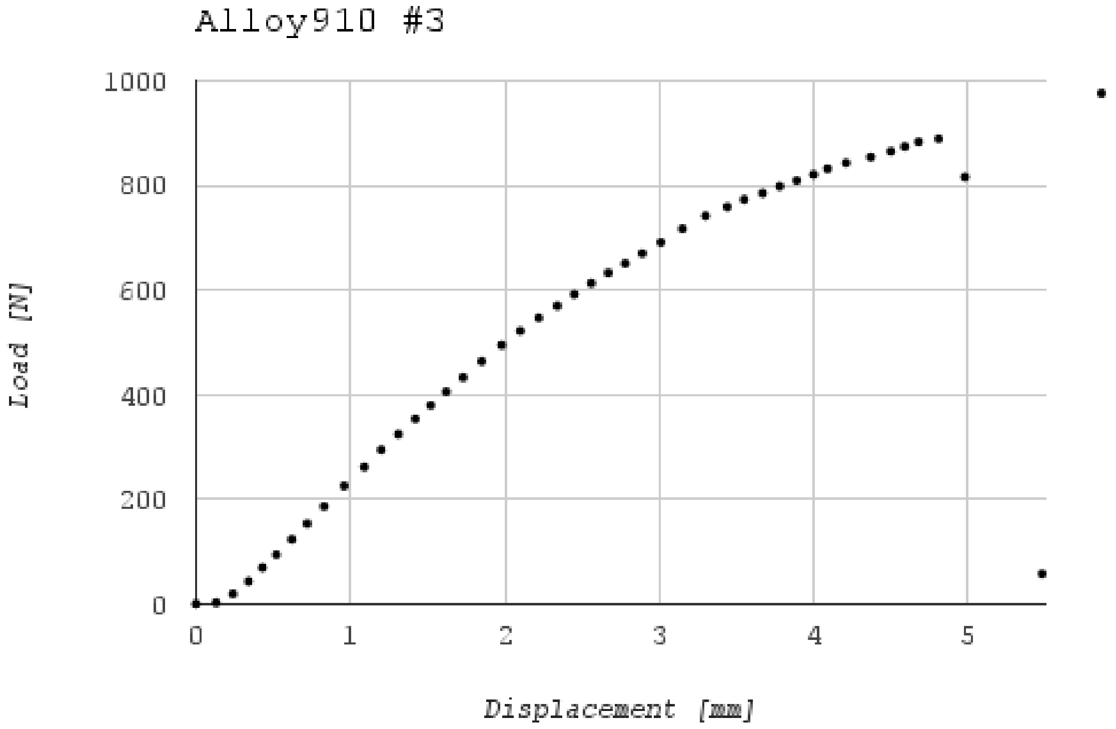

Alloy910 #3

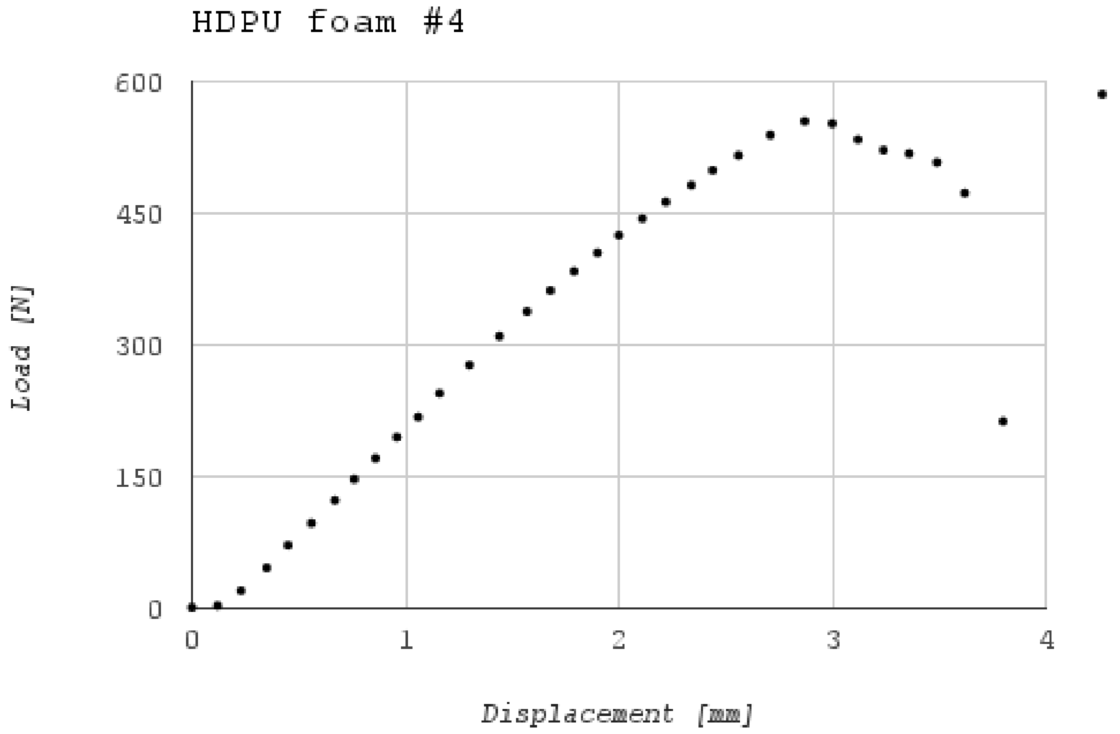
HDPU foam #4
Load [N]
600
450
300
150
0
0
1
2
3
4
Displacement [mm]

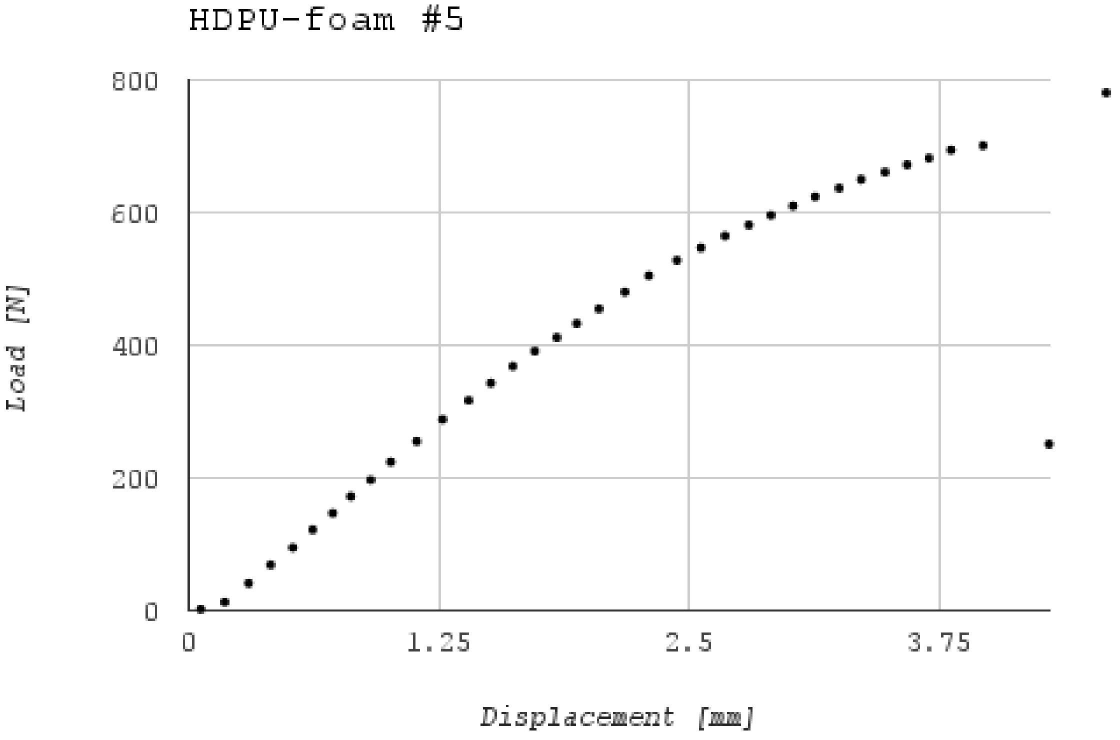
HDPU-foam #5
Load [N]
800
600
400
200
0
0
1.25
2.5
3.75
Displacement [mm]

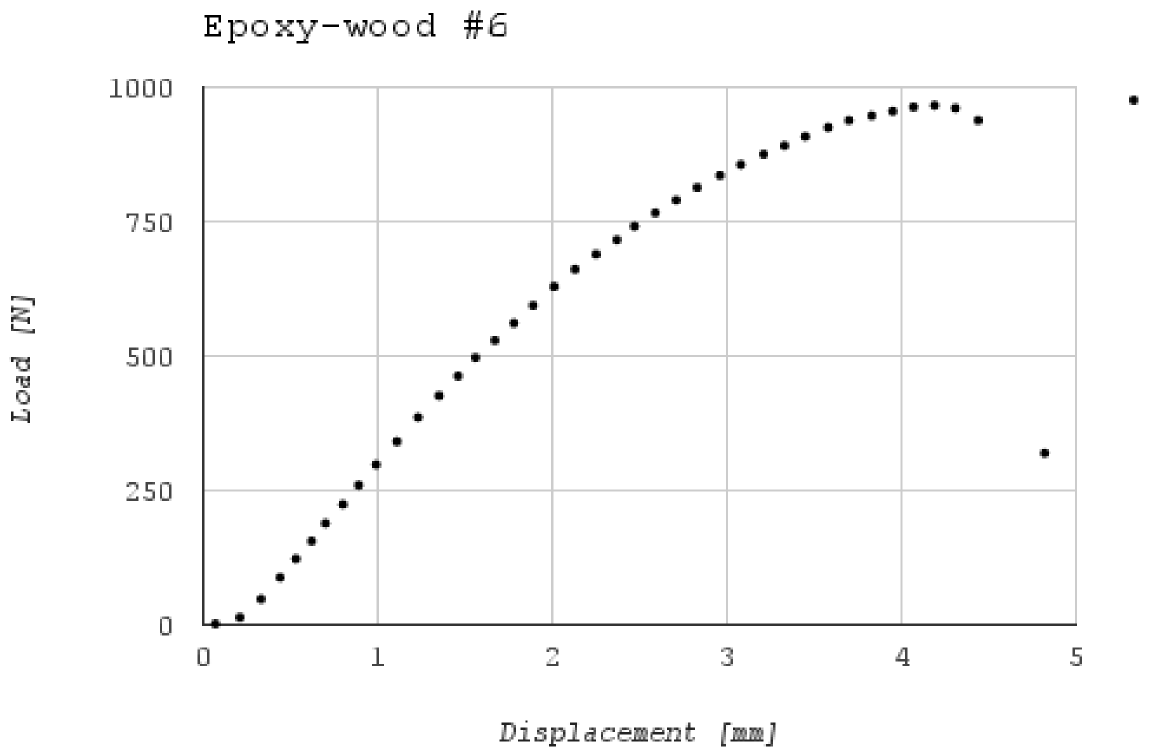
Epoxy-wood #6
1000
750
500
250
0
Load [N]
0
1
2
3
4
5
Displacement [mm]

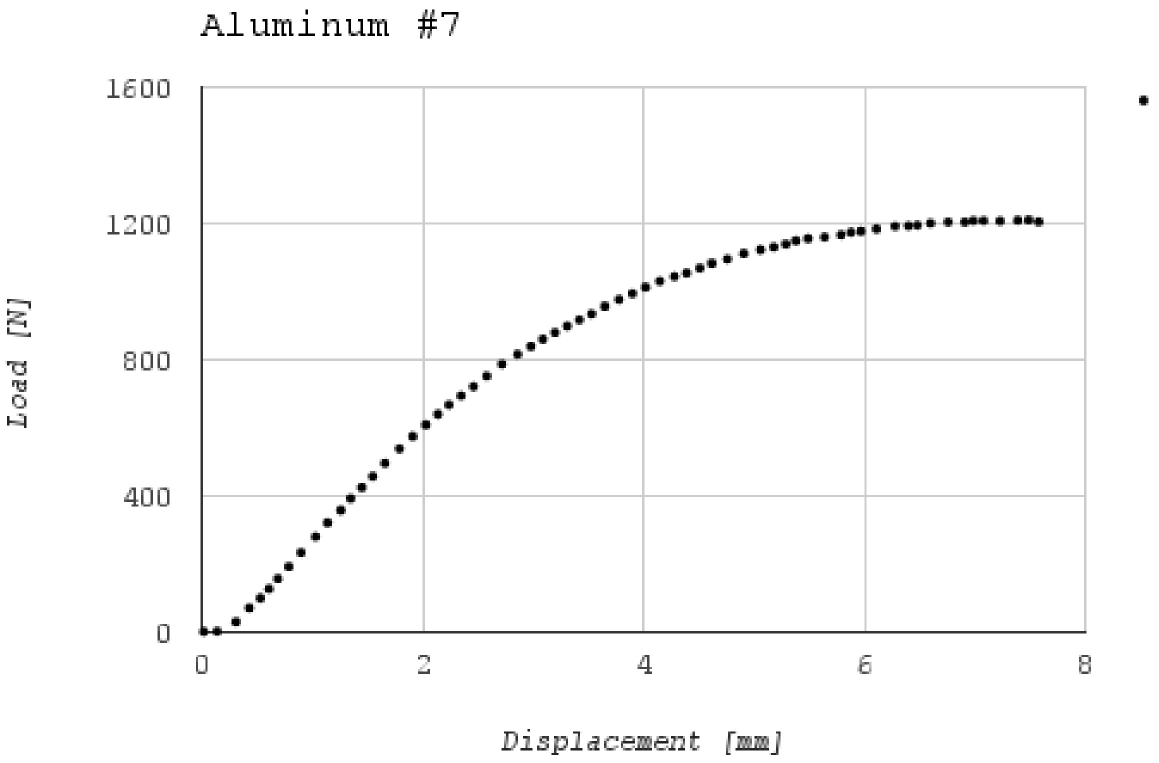
Aluminum #7
1600
1200
800
400
0
Load [N]
0
2
4
6
8
Displacement [mm]

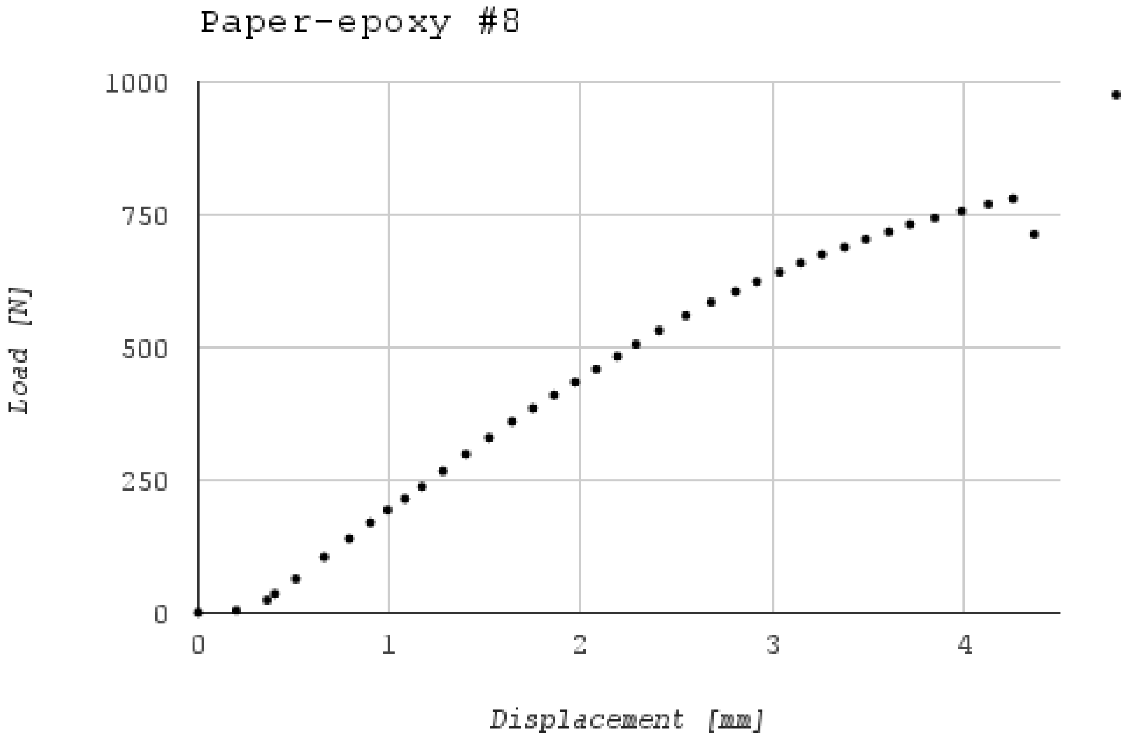
Paper-epoxy #8
1000
750
500
250
0
Load [N]
0
1
2
3
4
Displacement [mm]

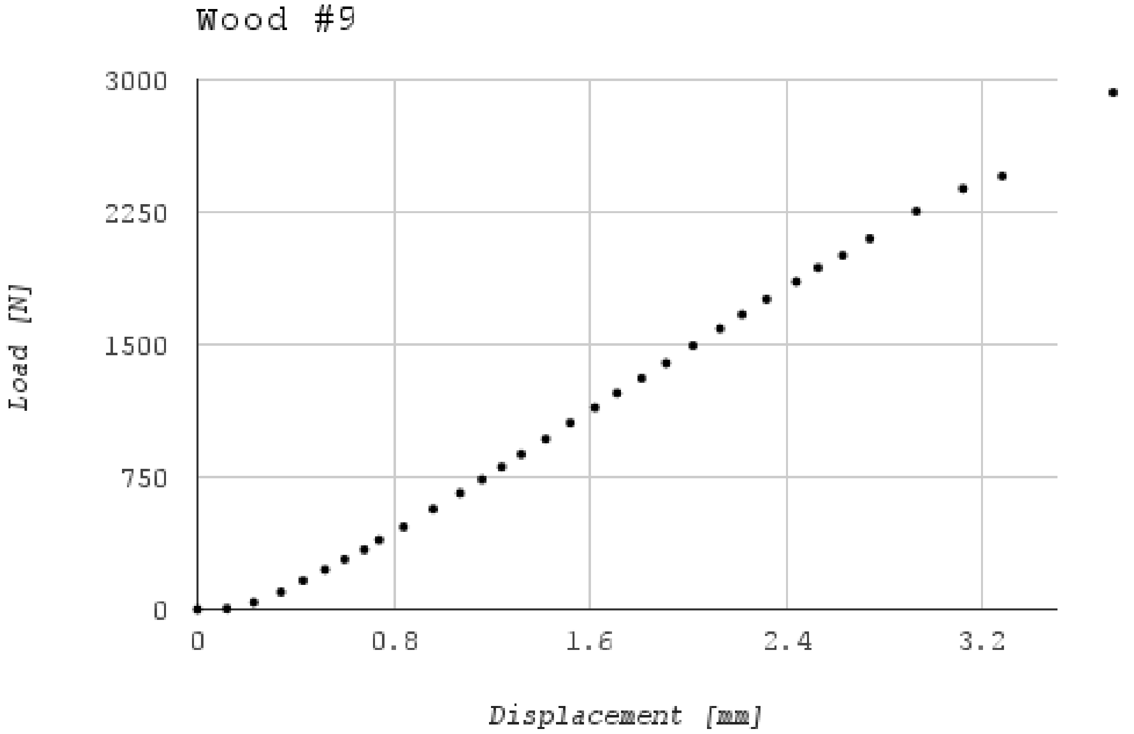
Wood #9
3000
2250
1500
750
0
Load [N]
0
0.8
1.6
2.4
3.2
Displacement [mm]

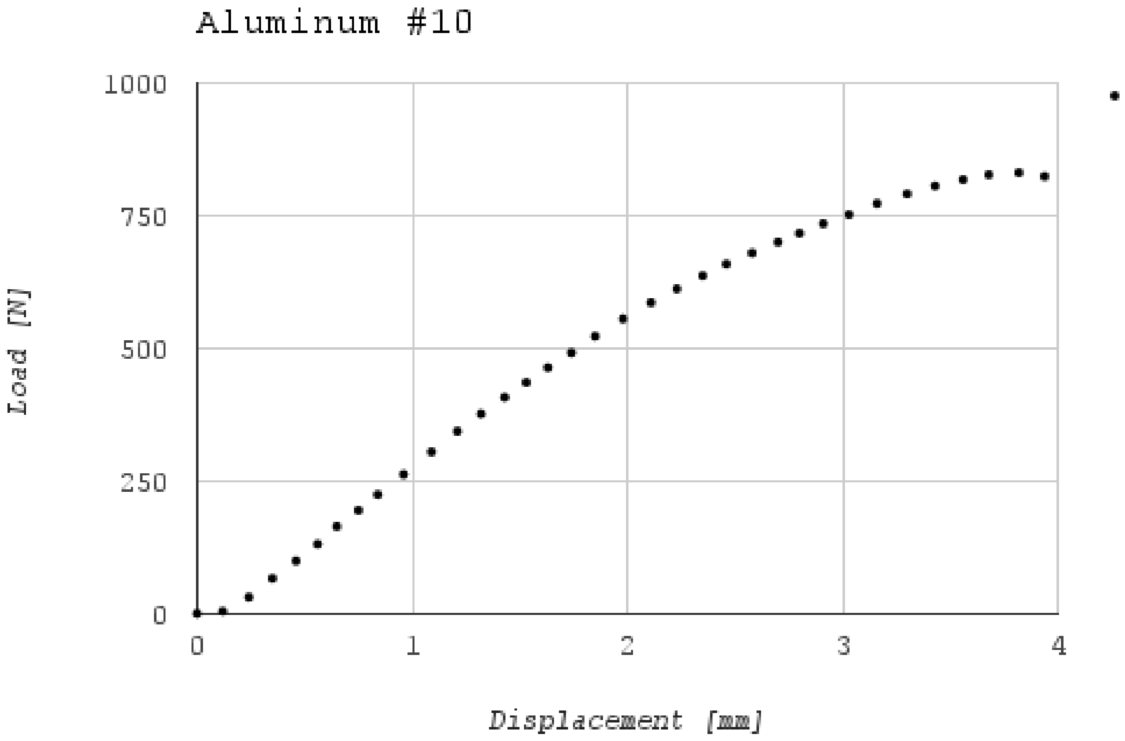
Aluminum #10
1000
750
500
250
0
Load [N]
0
1
2
3
4
Displacement [mm]

Appendix F

Material Data For Finite Element Analysis

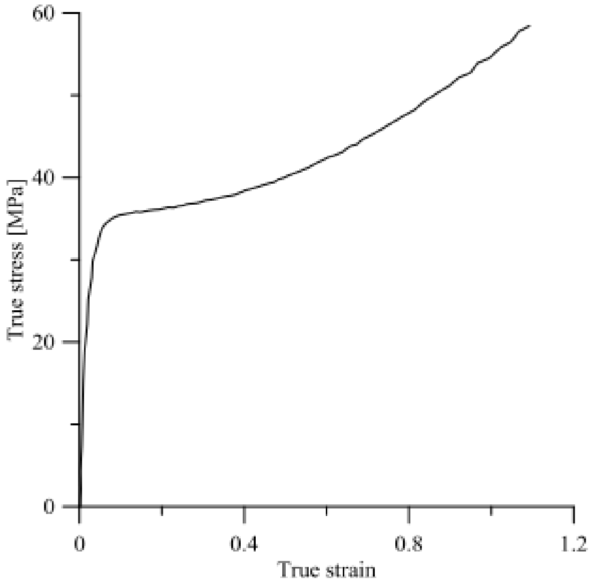

Figure F1: The material data in the ABAQUS simulation were based on specimen PP-T6 in Appendix A - "Tension tests" in Sælen (2012).

Yield Stress	Poisson's ratio	Young's Modulus
34.9 MPa	0.38	1600 MPa

Table F1: Independent variables for isotropic polypropylene. Collected from Appendix A - Tension tests in Sælen (2012)

True Yield Stress [MPa]	True Yield Strain	True Plastic Strain
35	0.02	0
36	0.2	0.18
38	0.4	0.38
42	0.6	0.58
47	0.8	0.78
54	1.0	0.98

Table F2: Stress-strain data for the nonlinear region of isotropic polypropylene. In ABAQUS, the true yield stress and true plastic stress were entered. Collected from Appendix A - Tension tests in Sælen (2012)

Appendix G

Risk Assessment of Planned Activites

NTNU	Kartlegging av risikofylt aktivitet	Utarbeidet av	Nummer	Dato
		HMS-avd.	HMSRV2601	22.03.2011
		Godkjent av		Erstatter
HMS		Rektor		01.12.2006

Enhet: **IPM, NTNU** **Dato: 1/2-16**

Linjeleder: Torgeir Welo

Deltakere ved kartleggingen (m/ funksjon)**: Øystein Bjelland (student), Martin Steinert (veileder), Carlo Kriesi (medveileder)**
(Ansv. veileder, student, evt. medveiledere, evt. andre m. kompetanse)

Kort beskrivelse av hovedaktivitet/hovedprosess: Masteroppgave student Øystein Bjelland. ”Investigate Techniques for Low-Volume Injection Molding Production”

Er oppgaven rent teoretisk? (JA/NEI)**: Nei** *«JA» betyr at veileder innestår for at oppgaven ikke inneholder noen aktiviteter som krever risikovurdering. Dersom «JA»: Beskriv kort aktiviteteten i kartleggingskjemaet under. Risikovurdering trenger ikke å fylles ut.*

Signaturer: *Ansvarlig veileder:* *Student:*

ID nr.	Aktivitet/prosess	Ansvarlig	Eksisterende dokumentasjon	Eksisterende sikringstiltak	Lov, forskrift o.l.	Kommentar
1	Bruk av Trolllabs workshop.	ØB	Romkort	Romkort		
1a	Bruk av roterende maskineri	ØB	Maskinens brukermanual	Ukjent	Ukjent	
1b	Bruk av laserkutter	ØB	Maskinens brukermanual	Ukjent	Ukjent	
1c	Bruk av 3D printer	ØB	Maskinens brukermanual	Ukjent	Ukjent	
1d	Bruk av skjæreverktøy	ØB	Ukjent			
1e	Bruk av samenføynigsmidler (lim og lignende.)	ØB	Produktets brukermanual og datablad	Datablad	Ukjent	
2	Tilstedeværelse ved arbeid utført av andre.	Andre	Andres HMSRV2601	Andres HMSRV2601	Prosessavhengig	
3	Eksperimentelt arbeid	ØB	Egen risikovurdering- må gjøres for hvert enkelt eksperiment		Prosessavhengig	
4	Bruk av egenprodusert sprøytestøpingsmaskin.	ØB	Øystein Bjellands prosjektoppgave, høst 2015.	Beskyttelsesplate r	Ingen	

Enhet: IPM, NTNU **Dato: 1/2 - 16**

Linjeleder: Torgeir Welo

Deltakere ved kartleggingen (m/ funksjon): Øystein Bjelland (student), Martin Steinert (veileder), Carlo Kriesi (medveileder)
(Ansv. Veileder, student, evt. medveiledere, evt. andre m. kompetanse)

Risikovurderingen gjelder hovedaktivitet: Masteroppgave student Øystein Bjelland. " Investigate Techniques for Low-Volume Injection Molding Production"

Signaturer: *Ansvarlig veileder:* *Student:*

ID nr	Aktivitet fra kartleggings-skjemaet	Mulig uønsket hendelse/ belastning	Vurdering av sannsyn-lighet	Vurdering av konsekvens:				Risiko-Verdi (menn-eske)	Kommentarer/status Forslag til tiltak
			(1-5)	Menneske (A-E)	Ytre miljø (A-E)	Øk/ materiell (A-E)	Om-dømme (A-E)		
1	Bruk av Trolllabs workshop.								
1a-i	Bruk av roterende maskineri	Stor kuttskade	2	D	A	A	D	2D	Sørg for at roterende deler tilstrekkelig sikret/dekket. Vær nøye med opplæring i bruk av maskineri.
1a-ii		Liten kuttskade	3	B	A	A	A	3B	Vær nøye med opplæring i bruk av maskineri. Ikke ha løse klær/tilbehør på kroppen.
1a-iii		Klemskade	2	D	A	A	C	2D	Vær nøye med opplæring i bruk av maskineri. Ikke ha løse klær/tilbehør på kroppen.
1a-iv		Flygende spon/gjenstander	3	C	A	A	B	3C	Bruk øyevern og tildekk hurtig roterende deler (Fres og lignende.)
1a-v		Feil bruk-> ødelagt utstyr	3	A	A	C	A	3C	Vær nøye med opplæring i bruk av maskineri

1b-i	Bruk av laserkutter	Klemskade	2	D	A	A	C	2D	Vær nøye med opplæring i bruk av maskineri. Ikke ha løse klær/tilbehør på kroppen.
1b-ii		Brannskade	3	B	A	A	A	3B	Vær nøye med opplæring i bruk av maskineri. Bruk hansker ved håndtering av varme materialer.
1b-iii		Øyeskade-laser	2	D	A	A	C	2D	Bruk øyevern! Skru av laser når maskinen ved oppsett.
1b-iv		Brann	2	B	A	D	C	2B	Vær nøye med opplæring i bruk av maskin. Ha slukkeutstur tilgjengelig
1c-i	Bruk av 3D-printer	Brannskade	3	B	A	A	A	3B	Vær nøye med opplæring i bruk av maskin.
1c-ii		Innhalering av plast/ printemateriale	5	A	A	A	A	5A	Bruk åndedretsvern/ vernebriller
1c-iii		Feil bruk-> ødelagt maskineri	3	A	A	C	A	3A	Vær nøye med opplæring i bruk av maskin.
1d-i	Bruk av skjæreverktøy	Stor kuttskade	2	D	A	A	D	2D	Bruk skapre verktøy og riktig skjæreunderlag
1d-ii		Liten kuttskade	3	B	A	A	A	3B	Bruk skapre verktøy og riktig skjæreunderlag
1e-i	Bruk av samenføynigsmidler (lim og lignende.)	Eksponering på øyet	2	D	A	A	B	2D	Bruk øyevern, ha datablad tilgjengelig

1e-ii		Eksponering hud	4	A	A	A	A	4A	Bruk hansker, ha datablad tilgjengelig
1e-iii		Eksponering åndedrett	4	A	A	A	A	4A	Bruk åndedretsvern/ god ventilasjon. Ha datablad tilgjengelig.
1e-iv		Søl	4	A	B	A	A	4A	Ha papir/ rengjøringsmateriell tilgjengelig. Ha datablad tilgjengelig.
2	Tilstedeværelse ved arbeid utført av andre.	Se andres risikovurdering om sikkerhet betviles.	3	C	C	C	C	3C	Hold et øye med hva som foregår rundt deg.
3-i	Eksperimentelt arbeid	Elektrisitet- strøm	3	B	A	A	A	3B	Typisk lite energi involvert. Bruk isolerte verktøy
4	Bruk av egenprodusert sprøytestøpingsmaskin.	Brannskade	3	A	A	A	A	3A	Beskyttelsesplater mot brannskade er installert. Det anbefales å bruke hansker.

Sannsynlighet vurderes etter følgende kriterier:

Svært liten **1**	**Liten** **2**	**Middels** **3**	**Stor** **4**	**Svært stor** **5**
1 gang pr 50 år eller sjeldnere	1 gang pr 10 år eller sjeldnere	1 gang pr år eller sjeldnere	1 gang pr måned eller sjeldnere	Skjer ukentlig

Konsekvens vurderes etter følgende kriterier:

Gradering	**Menneske**	**Ytre miljø Vann, jord og luft**	**Øk/materiell**	**Omdømme**
E **Svært Alvorlig**	Død	Svært langvarig og ikke reversibel skade	Drifts- eller aktivitetsstans >1 år.	Troverdighet og respekt betydelig og varig svekket
D **Alvorlig**	Alvorlig personskade. Mulig uførhet.	Langvarig skade. Lang restitusjonstid	Driftsstans > ½ år Aktivitetsstans i opp til 1 år	Troverdighet og respekt betydelig svekket
C **Moderat**	Alvorlig personskade.	Mindre skade og lang restitusjonstid	Drifts- eller aktivitetsstans < 1 mnd	Troverdighet og respekt svekket
B **Liten**	Skade som krever medisinsk behandling	Mindre skade og kort restitusjonstid	Drifts- eller aktivitetsstans < 1uke	Negativ påvirkning på troverdighet og respekt
A **Svært liten**	Skade som krever førstehjelp	Ubetydelig skade og kort restitusjonstid	Drifts- eller aktivitetsstans < 1dag	Liten påvirkning på troverdighet og respekt

Risikoverdi = Sannsynlighet x Konsekvens
Beregn risikoverdi for Menneske. Enheten vurderer selv om de i tillegg vil beregne risikoverdi for Ytre miljø, Økonomi/materiell og Omdømme. I så fall beregnes disse hver for seg.

Til kolonnen "Kommentarer/status, forslag til forebyggende og korrigerende tiltak":
Tiltak kan påvirke både sannsynlighet og konsekvens. Prioriter tiltak som kan forhindre at hendelsen inntreffer, dvs. sannsynlighetsreduserende tiltak foran skjerpet beredskap, dvs. konsekvensreduserende tiltak.

NTNU	Risikomatrise	utarbeidet av	Nummer	Dato
HMS/KS		HMS-avd.	HMSRV2604	08.03.2010
		godkjent av		Erstatter
		Rektor		09.02.2010

MATRISE FOR RISIKOVURDERINGER ved NTNU

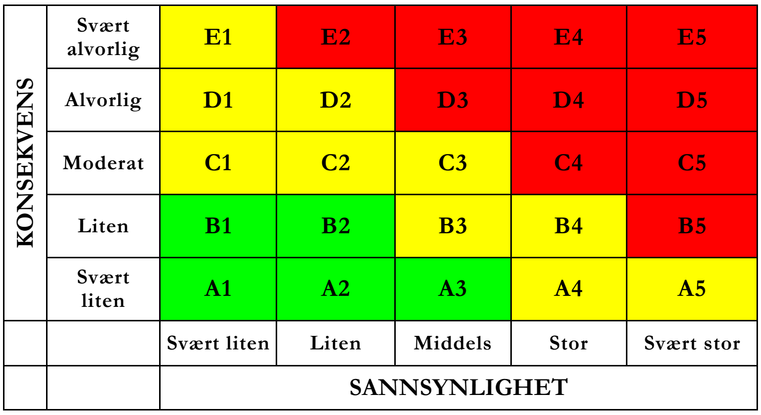

KONSEKVENS	Svært alvorlig	E1	E2	E3	E4	E5
	Alvorlig	D1	D2	D3	D4	D5
	Moderat	C1	C2	C3	C4	C5
	Liten	B1	B2	B3	B4	B5
	Svært liten	A1	A2	A3	A4	A5
		Svært liten	Liten	Middels	Stor	Svært stor
		SANNSYNLIGHET				

Prinsipp over akseptkriterium. Forklaring av fargene som er brukt i risikomatrisen.

Farge		Beskrivelse
Rød	🟥	Uakseptabel risiko. Tiltak skal gjennomføres for å redusere risikoen.
Gul	🟨	Vurderingsområde. Tiltak skal vurderes.
Grønn	🟩	Akseptabel risiko. Tiltak kan vurderes ut fra andre hensyn.